



Experimental characterization and testing of vehicle-to-grid charging technologies



Author:

Rasmus Meier Knudsen

DTU Wind-M-0783

July 2024

Author:

Rasmus Meier Knudsen

Title:

Experimental characterization and testing
of vehicle-to-grid charging technologies

DTU Wind-M-0783

July 2024

ECTS: 35

Education: Master of Science

Supervisors:

Mattia Marinelli

Kristian Sevdari

Kristoffer Laust Pedersen

DTU Wind & Energy Systems

Remarks:

This report is submitted as partial fulfillment of the requirements for graduation in the above education at the Technical University of Denmark.

DTU Wind & Energy Systems is a department of the Technical University of Denmark with a unique integration of research, education, innovation and public/private sector consulting in the field of wind energy. Our activities develop new opportunities and technology for the global and Danish exploitation of wind energy. Research focuses on key technical-scientific fields, which are central for the development, innovation and use of wind energy and provides the basis for advanced education at the education.

Technical University of Denmark
Department of Wind and Energy Systems
Frederiksborgvej 399
4000 Roskilde
Denmark
www.vindenergi.dtu.dk

Abstract

This thesis explores the feasibility of Bidirectional Power Transfer (BPT) using the ISO 15118-20 standard with the Watt&Well V2X Electric Vehicle Supply Equipment (EVSE) as an experimental platform. The research involved setting up an experimental environment to assess the BPT capabilities by gaining control of the EVSE and performing measurements.

The results showed successful vehicle compatibility and characterization of the system efficiency, response times, and other electrical metrics. ISO 15118-20 facilitated seamless communication and interoperability between the EVSE and a prototype vehicle as well as vehicle emulators, validating it as a promising standard for the European adoption of BPT.

The research suggests that ISO 15118-20 BPT performs similarly or better than the previous generation CHAdeMO-based technology on metrics such as efficiency and response time. It could transform modern electric vehicles into versatile energy storage units, enhancing grid stability and facilitating the integration of renewable energy. Although there are challenges such as ensuring widespread adoption and grid integration, the Watt&Well V2X EVSE has proven effective in advancing grid-following bidirectional technologies. The experimental control and measurement environment adequately supported the research work, despite some limitations in controllability and measurement quality.

Using ISO 15118-20 for BPT is practical and beneficial for both the automotive and energy sectors. Future work should focus on addressing remaining challenges and enabling support among existing and new vehicles, to enable large-scale implementations and fully realize the advantages of BPT on modern vehicles.

Acknowledgements

The author would like to thank:

Mattia Marinelli, Main supervisor, DTU

Kristian Sevdari, Co-supervisor, DTU

Kristoffer Laust Pedersen, Co-supervisor, DTU

Gabriel Fabbri, MSc Sustainable Energy, DTU

For good cooperation in the lab and his immense effort in the data processing of the shared data included in this thesis, as well as many good conversations on our very related thesis projects and the e-mobility world in general.

European Union, Horizon Europe

The work in this thesis has been supported by the research projects EV4EU (Horizon Europe grant no. 101056765) and by the research project FLOW (Horizon Europe grant no. 101056730).

Magnus Fich Rabjerg and **Adam Juel Madsen**, Research Technicians, DTU

For all the help in the lab, and for putting up with the noise of the EVSE.

Monta, CPI team

A big thanks to Monta ApS and especially the CPI team for their day-to-day support, the unique industry access provided, and many good conversations and advice regarding this thesis.

ElaadNL, Testlab

Thank you to the ElaadNL foundation and especially the staff of the ElaadNL Testlab for the unique opportunity to test at their facilities, and the support provided during our visit.

Steffen Høj, Business Development Manager, Polestar

For the access to a press car for testing.

Unnamed Automotive OEM

For the unique opportunity to test DC BPT with their prototype vehicle.

Contents

Abstract	iii
Terms & Abbreviations	vii
List of Figures	x
List of Tables	xii
1 Introduction	1
1.1 Background	1
1.2 Overview of Bidirectional Power Transfer Technologies	2
1.3 Research Questions	3
2 State of the Art	5
2.1 Categorization of BPT technologies	6
2.2 Overview	7
2.3 EV-EVSE communication	8
2.4 EV-CSMS communication	20
2.5 CSMS-Secondary Actor communication	25
3 Experimental Design	27
3.1 Overview of Watt&Well V2X EVSE	27
3.2 Network setup	32
3.3 Measurement setup	34
3.4 Vehicle emulation and sniffing	38
3.5 Control setup	41
3.6 Selection of test cases	49
4 Results	53
4.1 Vehicle compatibility	53
4.2 Efficiency	58
4.3 System characteristics	60
4.4 Additional findings	65
5 Discussion	67
5.1 Electrical performance	69
5.2 Experimental setup	71
6 Conclusion	75
Bibliography	77
A Appendix	83
A.1 Watt&Well documentation	83
A.2 ISO 15118 material	87
A.3 EV emulators and sniffers	92
A.4 Code	93
A.5 Miscellaneous	102

Terms & Abbreviations

Term/Abbreviation	Explanation
AC	Alternating Current
API	Applications Programming Interface
BPT	Bidirectional Power Transfer
CP	Control Pilot, see IEC 61851 Annex A
CAN	Controller Area Network
CPO	Charge Point Operator
CSMS	Charging Station Management System
DC	Direct Current
DER	Distributed Energy Resource
DSO	Distribution System Operator
DTU	Technical University of Denmark
EV	Electric Vehicle
EVCC	Electric Vehicle Communication Controller
EVSE	Electric Vehicle Supply Equipment
FPT	Forward Power Transfer (charging)
FPT	High Level Communication
HPGP	HomePlug Green PHY. OSI model layer 2 communication specification
IEC	International Electrotechnical Commission
ISO	International Standards Organisation
OBC	On-Board Charger
OCPP	Open Charge Point Protocol
OEM	Original Equipment Manufacturer
PFC	Power Factor Correction
PLC	Power Line Communication
PWM	Pulse Width Modulation
RFID	Radio-Frequency Identification. Typically implemented in charging cards and keys for starting charging sessions.
RPT	Reverse Power Transfer (discharging)
SECC	Supply Equipment Communication Controller
TSO	Transmission System Operator
V2G	Vehicle-to-grid. Covers both Grid-following BPT AND General EV-EVSE communication within ISO 15118

List of Figures

- 2.1 Service catalog from the Parker Project providing an overview of possible use cases for bidirectional power transfer capabilities. Image source: Parker Project[2]. 6
- 2.2 Overview of the interoperability mechanisms in the electric mobility ecosystem covered by this thesis. Secondary Actor refers to grid actors beyond the CSMS. 8
- 2.3 CHAdeMO connector. Image source: Wikimedia Commons [20]. 9
- 2.4 CCS2 connector, also known as configuration FF. Image source: Wikimedia Commons [24] 10
- 2.5 Difference between DIN SPEC 70121 and ISO 15118-2. Image adapted from CharIN [26]. 10
- 2.6 Scope of the ISO 15118 standards. Image source: [16]. 11
- 2.7 Diagram of the ISO 15118 standards and how they fit in the OSI model. Image source: *What is ISO 15118?* 11
- 2.8 Diagram illustrating how SLAC crosstalk. Image source: [29]. 13
- 2.9 ISO 15118-20 Schema diagram 188, showing message elements for a DC BPT Dynamic ChargeLoopReq message. Image source: [16]. 21
- 2.10 Graphic representation of the WebSocket protocol. 22
- 2.11 Illustration of the utility-CSMS-EVSE-EV interoperability ecosystem. Image source: [44]. 25

- 3.1 Front view of the Watt&Well V2X EVSE with components labeled. 28
- 3.2 Watt&Well EVI board. 28
- 3.3 Block diagram of the EVI board. The dashed lines indicate isolation. Image source: Watt&Well [47]. 29
- 3.4 Block diagram of the BMBPU. Image source: Watt&Well [48]. 31
- 3.5 BMBPU internals overview. 31
- 3.6 High-level regulation and measurements diagram of the BMBPU-R2. Image source: Watt&Well [48]. 32
- 3.7 Diagram of the Internet Protocol-based networking setup used when carrying out experiments with the Watt&Well EVSE. Devices within the grey area are part of the EVSE itself. 34
- 3.8 Diagram of the final measurement setup used when carrying out experiments. The system is configured for CCS charging in this view (zoom in for details). 35
- 3.9 Rear, internal view of the Watt&Well EVSE showing various measurement points and probes. 36
- 3.10 Oscilloscope screenshot showing an example of an activation time measurement. The yellow trace is the sync signal and the green trace is a DC current measurement. 37
- 3.11 Keysight Charging Discovery System installation at ElaadNL. 40
- 3.12 Screenshot from the Keysight Charging Communication Interface Tester "Verisco box" software, while performing an ISO 15118-20 BPT session and discharging at -22 kW sourced from the grid via the DC emulator shown in figure 3.11b. 41

3.13	Screenshot of the EVI GUI showing the EVSE control view with different sections annotated. Image source: Watt&Well [66]	42
3.14	Simplified control architecture for CCS charging with the Watt&Well EVSE.	45
3.15	Screenshot of the EVI GUI highlighting the allocation, limitation, and SECC control sections.	48
3.16	Test patterns used for the "Parker test". Image source: [1].	50
3.17	Test patterns used when performing experiments.	51
4.1	Picture of the infotainment system in the tested Volkswagen ID.4 showing bidirectional charging information.	54
4.2	Screenshot of the Keysight CCIT "Verisco box" interface while performing Reverse Power Transfer of 17 kW using SL1800A DC emulators and the Watt&Well EVSE.	54
4.3	Example of the data output from an efficiency test using test pattern a (figure 3.17a), showing both AC and DC side power measurements as well as the auxiliary power. Emulated voltage at 400V and a single BMPU. Referring to figure 3.8, AC main power is measured by the PEL104, and AC auxiliary Power is measured by PEL106. Note the different units and scales for main and auxiliary AC power.	58
4.4	AC/DC conversion efficiency of two BMPU in series configuration performing CCS2 BPT. EV and battery are emulated at three different voltage levels 600, 700, and 800V using Keysight CDS.	59
4.5	AC/DC conversion efficiency a single BMPU performing CHAdeMO BPT. The vehicle was the Nissan LEAF listed in table 4.1.	59
4.6	Efficiency heatmaps, comparison between measured values (a) and BMPU datasheet (b). Color scales are matched as closely as possible.	60
4.7	Heatmap of single BMPU conversion efficiency, measured using Keysight CDS and battery emulation. No interpolation.	60
4.8	Plot of active and reactive power as well as power factor over time, while performing tests with the real vehicle capable of ISO15118-20 BPT. The middle section shows a test pattern (figure 3.17a), while the start and end are various switches from charging to discharging and not part of a test. Referring to figure 3.8, quantities are measured by the PEL104.	61
4.9	Current ripple heatmaps, comparison between measured values (a) and BMPU datasheet (b).	64
4.10	Heatmap of peak-to-peak DC side ripple current, with no interpolation and full-color scale.	64
4.11	Oscilloscope screenshot showing a DC side current waveform with a peak-to-peak (pk-pk) ripple value of 12.2 A and a ripple frequency measured at 705 Hz (Freq). The DC operating point is 8A and 475 V.	65
A.1	Table with BMPU-R2 electrical characteristics. Source: Watt&Well [48].	83
A.2	Peak-to-peak current ripple at the battery side filtered at 5kHz given for grid conditions three-phase with neutral 400V/50Hz and SW version 2.5.4r (build 19020). Source: Watt&Well [48].	83
A.3	Typical BMPU-R2 efficiency in three-phase mode without neutral under grid conditions 400V/50Hz at 25°C. Source: Watt&Well [48].	84
A.4	Battery Side Safe Operating Area under grid conditions 400V/50Hz at 25°C. Source: Watt&Well [48].	84
A.5	BMPU Charging and discharging current limitations block diagram. Source: Watt&Well [48].	85

A.6	BMPU Charging and discharging AC side current limitations block diagram. Source: Watt&Well [48].	85
A.7	Schematic diagram of the contactor configuration in the EVIX. Image source: Watt&Well [52]	86
A.8	Block diagram of a typical AC forward and reverse power transfer system. Source: ISO Central Secretary [10].	87
A.9	Block diagram of a typical DC forward and reverse power transfer system. Source: ISO Central Secretary [10].	87
A.10	Diagram illustrating the message sequence for an ISO 15118-2 DC charge. Image source: [31]. Note that an AC version of this diagram is available as a vector image in appendix A.11.	88
A.11	Diagram illustrating the message sequence for an ISO 15118-2 AC charge. Image source: [27].	89
A.12	Diagram illustrating the message sequence for an ISO 15118-20 DC charge. Image source: [31].	90
A.13	CHAdeMO V2G charger efficiency map for charging/discharging DC set- points from -10 kW to +10 kW with steps of 400W. Image source: [1]. . . .	102

List of Tables

2.1	Energy Transfer Modes and Offered Charging Services in ISO 15118-2. Adapted from table 63 [25].	15
2.2	ISO 15118-20 table 5: TLS versions and their supported communication protocols. Source: [16].	17
2.3	ISO 15118-20 Power transfer Service IDs and their corresponding service names and descriptions, adapted from ISO 15118-20 table 204	19
2.4	ISO 15118-20 Configuration parameters for DC BPT service. Adapted from [16].	19
3.1	Predefined contactor configurations settable via the EVI GUI and EVIX-IO board. These are provided by Watt&Well as JSON files.	30
3.2	Table of all measurement equipment in use, the selected measurement and range and the applicable uncertainty for that range.	38
3.3	Overview of EV and EVSE emulation and High Level Communication sniffing products. In this table, <i>All</i> in the protocols column refers to support for DIN SPEC 70121, ISO 15118-2, and ISO 15118-20. An extended version of this table is found in appendix A.2.	40
4.1	Table showing all vehicles tested with brand, model, trim and year information, and the software version reported in the infotainment system. Also included are EV emulators. The column Priority/SupportedAppProtocols indicates which schemas the EV supports and their priority, as sent by the EVCC in the SupportedAppProtocols message. For emulators, only the schema capable of BPT is listed. If BPT was tested working with an EV/emulator, this is also included. Some details have been left out, as the EV OEM did not wish to have these disclosed.	55
4.2	Activation and ramp time test. Confidential real vehicle with CCS2/BPT support, 575V battery voltage, 2 BMPU in series, power limited at ± 10 kW.	61
4.3	Activation and ramp time test. Emulated vehicle with CCS2/BPT support, 575V fixed voltage, 2 BMPU in series, power limited at ± 10 kW.	62
4.4	Activation and ramp time test. Emulated vehicle with CCS2/BPT support, 575V fixed voltage, 2 BMPU in series, power limited by BMPU constraints.	62
4.5	Activation and ramp time test. Emulated vehicle with CCS2/BPT support, 400V fixed voltage, 1 BMPU, power limited by BMPU constraints.	62
4.6	Activation and ramp time test. Emulated vehicle with CCS2/BPT support, 400V fixed voltage, 2 BMPU in parallel operation, power limited by BMPU constraints.	63
4.7	Activation and ramp time test. Emulated vehicle with CCS2/BPT support, 800V fixed voltage, 2 BMPU in series operation, power limited by BMPU constraints.	63
4.8	Activation and ramp time test. Real vehicle with CHAdeMO/BPT support, 385V battery voltage, 1 BMPU, and power limited by BMPU constraints.	63
4.9	Table of OCPP 1.6J messages tested, and whether the implementation was working and compliant with the OCPP 1.6 specification.	66
A.1	ISO 15118-20 configuration parameters for AC BPT service. Adapted from [16].	91

A.2 Extended overview of EV and EVSE emulation and High Level Communication sniffing products. In this table, *All* in the protocols column refers to support for DIN SPEC 70121, ISO 15118-2 and ISO 15118-20. *TLS decrypt* refers to whether the system in question claims to be able to decrypt TLS-encrypted communication. 92

1 Introduction

With the electrification of transport, an ever-increasing amount of the global vehicle fleet will contain batteries. The basic need of Electric Vehicles (EV) is to charge their DC-based batteries with energy from the AC-based electric grid. To facilitate the charging, Electric Vehicle Supply Equipment (EVSE) is used, with the actual conversion from AC to DC either happening within the EVSE (off-board charging) or in the EV itself (on-board charging). However, interest is growing in also being able to discharge EV batteries, with the combined charging and discharging operation known as Bidirectional Power Transfer (BPT). If the discharged energy is fed back to the grid, the technology is referred to as vehicle-to-grid (V2G), which leverages the flexibility and large energy storage capacity of EVs to provide critical grid services such as frequency regulation and demand response. The simplest part of BPT is to convert DC to AC, which can either happen on-board the vehicle or off-board in the EVSE, using the well-known technology of grid-tied inverters.

The much more complicated part of vehicle-to-grid technology is the communication between EV and EVSE, as well as the wider grid. BPT and V2G have already been demonstrated many times using the legacy CHAdeMO connector and CAN bus-based communication interface, including numerous studies and trials conducted at DTU [1, 2, 3]. Since the publication of these studies, the CHAdeMO connector has been superseded by the Combined Charging System (CCS) connector in Europe, which is now mandated on all DC charging infrastructure [4]. This means almost all new vehicles made for the European market are delivered with a CCS connector. Compared to CHAdeMO, CCS uses a completely different communication interface based on the HomePlug Green PHY physical layer. In addition to the physical layer, the ISO 15118 family of standards describes the communication interface used for, among other things, bidirectional power transfer.

This thesis will seek to test the ability to perform BPT using the state-of-the-art ISO 15118-20 standard, which promises interoperability between EV and EVSE on the market today equipped with the CCS connector. The application will be centered around the Watt&Well V2X EVSE, a *vehicle-to-everything* experimental EVSE platform developed by French power electronics company Watt&Well. This thesis will also propose a control and measurement system to characterize the performance of the Watt&Well EVSE, to enable comparison with other EV-EVSE combinations, as well as an assessment of the possibility of participating in various grid services.

1.1 Background

Currently, the transportation sector is a major contributor to green house gas emissions, accounting for approximately one-quarter of global emissions from fossil fuel combustion [5]. Electrification of transport thus plays an important role in the the green transition and global effort to reduce green house gas emmissions. According to the International Energy Agency (IEA), the number of electric vehicles on the road is expected to reach as high as 245 million by 2030 [6], up from 40 million in 2023 [7]. This surge in EV adoption is part of broader efforts to transition towards greener, more sustainable energy systems.

This green energy transition also involves increasing the share of renewable energy sources like wind and solar in the energy mix. These sources are essential for reducing dependence on fossil fuels and lowering greenhouse gas emissions. However, they also introduce challenges to the grid, such as intermittent production and low inertia. Wind and solar power generation depend on weather conditions and time of day, leading to variability

and unpredictability in electricity supply. Additionally, these renewable sources contribute less to grid inertia, making it harder to maintain grid stability during disturbances.

Batteries can help solve these challenges by providing energy storage solutions that mitigate the intermittency of renewable energy. They can store excess energy generated during peak production periods and release it when production is low or demand is high, thereby balancing supply and demand. Moreover, batteries can enhance grid stability by providing ancillary services such as frequency regulation and voltage support [2].

A significant portion of new battery production is going into EVs. By 2030, the battery demand for EVs alone could reach up to 4,300 GWh annually [8]. To put this into perspective, S&P Global projects that the global battery manufacturing capacity could reach approximately 6,500 GWh per year by 2030 [9]. This means that the global battery demand for EVs would account for 66% of the total battery production capacity. Such a substantial share highlights the dominant role of EVs in the battery market and underscores the importance of optimizing the use of these batteries beyond their primary function of powering vehicles.

Using Bidirectional Power Transfer, it is possible to harness the energy stored in EV batteries when the vehicles are not in use for driving. When aggregated, the energy stored in parked EV batteries represents a significant resource that can be harnessed to support the grid, thereby enabling the green transition.

1.2 Overview of Bidirectional Power Transfer Technologies

Bidirectional Power Transfer (BPT) is often referred to as vehicle-to-grid, abbreviated V2G, with the intent to refer to power transfer from the vehicle to an existing grid. However, many different bidirectional power transfer technologies exist, which are not all grid-connected. Regardless, the ISO 15118 family of standards is named *Road vehicles — Vehicle to grid communication interface*, which has led to the V2G abbreviation being used extensively in these standards. For example, the standard ISO 15118-1 *Road vehicles - Vehicle to grid communication interface - Part 1: General information and use-case definition*[10] defines V2G in definition 3.1.74 as:

plug-in electric vehicle (311.30) interaction with the electric grid, including charging as well as discharging and bi-directional communication interface.

From this, it is clear that V2G not only covers power transfer but also communication between the EV and the grid. The words *charge* and *charging* also carry different meanings within the standards in the field. From the same ISO 15118-1 standard, definition 3.1.12 refers to *charge* as:

store electrical energy in the vehicle battery

Note 1 to entry: In the first edition of this document, the words "charge" or "charging" were used intensively as a generic term. In this edition, in order to be more precise and to cover with one word forward (3.4.1) and Reverse Power Transfer (3.4.2) the terms "charge" and its declinations have been replaced by "energy transfer" when appropriate. When energy transfer is used in a sentence, this means that both directions of power flow are possible.

Note 2 to entry: The term "charge" (and the associated verb) has in this text a precise definition in relation to the amount of energy stored in the EV battery which can be different than the total energy transferred to the E V.

Note 3 to entry: In some sentences, the word "charging" is still used. For example, the words "charging site" are still used.

The referenced definitions 3.4.1 and 3.4.2 for Forward Power Transfer (FPT) and Reverse Power Transfer (RPT) state *power transfer from the external power supply to the vehicle battery via the EVSE* and *power transfer from the vehicle battery to home, loads or grid via the EVSE*, respectively. Based on these definitions for FPT and RPT, definition 3.1.10 then states that Bidirectional Power Transfer (BPT) is a *combination of forward or reverse power transfer sequences* [10].

Due to the intense coverage of the ISO 15118 family of standards, this thesis will take special care to not use the abbreviations and terms *V2G* and *BPT* interchangeably. However, for the benefit of the reader, the terms *charging* and *discharging* will be used to cover forward and reverse power transfer, as these terms have less potential to be misinterpreted.

To make matters more complicated, the term *V2X* is sometimes used as an umbrella term for various BPT technologies, with the meaning *vehicle-to-everything*. A self-evident example is the equipment this thesis is based around, the Watt&Well *V2X* EVSE. The problem is that the *V2X* term is also used beyond power transfer technologies to cover various communication types in the automotive space. These include vehicle-to-vehicle (*V2V*) and vehicle-to-infrastructure (*V2I*), covering the (wireless) exchange of information between vehicles and infrastructure along the roads for purposes such as road safety [11]. Since some of the technologies often lumped under the *V2X* term are automotive, but not power transfer related, the thesis will abstain from the *V2X* term and instead exclusively use BPT to cover the collection of various power transfer technologies.

1.3 Research Questions

The main objective of the thesis is to test and characterize the bidirectional power transfer capabilities of EV - EVSE combinations, with the goal of injecting power from the vehicle battery into an existing AC grid. The primary focus will be on vehicles equipped with the Combined Charging System (CCS) connector paired with a Watt&Well *V2X* EVSE.

Based on the background for the thesis, the thesis will seek to answer the following research questions:

- Why are vehicle-to-grid charging technologies relevant, and which use cases are envisioned for them?
- How can bidirectional power transfer be achieved with CCS technology?
- What technical characteristics are important for the vehicle-to-grid (*V2G*) charging technology under investigation?

2 State of the Art

Reverse power transfer and grid-following implementations are not new concepts and were first proposed in a paper by Willett Kempton and Steven E. Letendre in 1997 [12]. In the 2010s, Nissan led reverse power transfer efforts with their LEAF vehicle models, based on the CHAdeMO standard, and DTU has carried out much research with CHAdeMO-based technology. Particularly noteworthy is the Parker project demonstration with Frederiksberg Forsyning in Denmark, which has been contributing to the FCR-N market since 2016 and continues to do so [13].

The previous research done by DTU also covers the important topic of battery degradation in publications such as Thingvad et al.: *“Empirical Capacity Measurements of Electric Vehicles Subject to Battery Degradation from V2G Service”*[3] and Thingvad and Marinelli: *“Influence of V2G Frequency Services and Driving on Electric Vehicles Battery Degradation in the Nordic Countries”*[14]. Both of these publications find only small reductions in capacity observed after long-term participation in grid services. As long as the service energy requirements are relatively low, short-term power flows have a limited effect on the battery degradation [14]. Even after long provision periods, it is observed that the degradation is not much higher than from normal driving usage [14].

Bidirectional power transfer capabilities bring many use cases, as well as possible savings both in terms of cost and greenhouse gas emissions. These can range from providing backup power to homes, buildings, and industry in the event of power outages, to balancing local production from intermittent, renewable resources such as solar. Being able to buy electricity when the spot price is low, and use it while tariff and spot prices are higher, is also seen as a benefit by many consumers. Finally, grid-connected batteries like BPT-capable EVs are also seen as an important enabler of the modern power system with 100% renewable generation, as they can participate in for example demand response schemes as well as faster markets for frequency services. This is particularly important for the intermittent production, low inertia power system of the future. In DTU publications such as Thingvad, Ziras, and Marinelli: *“Economic value of electric vehicle reserve provision in the Nordic countries under driving requirements and charger losses”*[15], the monetary value of the services possible with bidirectional charging technology is investigated.

In figure 2.1, a catalog sourced from the aforementioned Parker project is included, showing the different services possible with bidirectional charging. The figure includes brief technical requirements, including whether a specific service necessitates two-quadrant control of active power or four-quadrant control of both active and reactive power.

Parker “service catalog” 2.0

Domain	Categories	Service examples	Short description	EV and EVSE	Technical requirements	USER	Incentives
Region (Transmission)	Power balancing	Synthetic inertia	Mimic inertia of rotating machines.		-Fast activation -Controllable ramping rate -Bidirectional (V2G)		Availability payment
		Frequency containment	Keep the frequency within a required interval.				
Neighborhood (Distribution)	Energy balancing	Wholesale energy	Responsiveness to varying energy prices.		(no special performance requirements)		Savings on energy costs / Renewable-based charging
		Regulation	Balancing energy schedules/portfolios.				
		Marginal emission	Defer charging based on CO2 cost of marginal consumption.				
Neighborhood (Distribution)	Grid contingencies	Loading issues	Mitigate overloading of transformers and cables in LV network. May also include phase load balancing.		- 4Q / Reactive power capabilities		Savings on connection costs /compensation from utility
		Voltage issues	Mitigate overvoltage and voltage drops in distribution systems.				
Building (behind the meter)	Energy autonomy	Bilateral trading	Local peer-to-peer trading of energy.		- Bidirectional (V2B)		Savings/independence/ renewable support
		Self consumption maximization	Ensure the highest possible utility of locally produced energy.				
	Building (behind the meter)	Islanded operation	Back-up power	Sustain a small power system temporarily disconnected from the grid.		- Bidirectional (V2B) -Islanding capability	
Fully off-grid			Sustain a small power system permanently disconnected from the grid.				
Building (behind the meter)	Mobile load serving	Vehicle-to-tool	Provide a mobile power-source for equipment during in-field use.		- Bidirectional (V2L)		Access to mobile power source
		Vehicle-to-Vehicle	Provide energy directly from one vehicle to another.				

Figure 2.1: Service catalog from the Parker Project providing an overview of possible use cases for bidirectional power transfer capabilities. Image source: Parker Project[2].

2.1 Categorization of BPT technologies

Below the V2X umbrella, many terms with the V2 structure besides V2G (vehicle-to-grid) are found. Some examples are V2L, V2H, V2B, G2V and V1G. The definitions of these terms are however not standardized in the same way as FPT, RPT, and BPT are in the ISO 15118 family of standards. It is however possible to look towards the ISO 15118 family for definitions that can be used to classify these technologies. ISO15118-20 covers three different BPT service types; AC_BPT, DC_BPT and DC_ACDP_BPT. The first two cover an AC and DC connection between the EV and EVSE, respectively. The latter also covers a DC connection, but via an *Automated Connection Device Pantograph*[16]. Thus one distinguishing factor for different BPT technologies can be whether the connection between the EV and EVSE is AC or DC-based, also known as AC or DC-linked. This is most often given by the location of the DC/AC bidirectional power converter and the difference in location is illustrated in ISO 15118-1 with appendix A.8 showing a bidirectional converter placed within the EV (on-board) and appendix A.9 showing an off-board bidirectional converter placed within the EVSE.

In addition to AC or DC, BPT technologies, and especially AC-based technologies, are also classified in the ISO 15118 standards by their *generator mode*. In ISO 15118-20, the `GeneratorMode` parameter indicates if the system consisting of EV and EVSE operates as a grid-following generator (only injecting active and reactive power into an existing grid) or as a grid-forming generator. The type `GridForming` is defined as a system that can control the voltage and frequency of the network and power wires that would not be powered otherwise. The `GridForming` generator mode should be selected, for example, if the system consisting of EV and EVSE is powering up a remote load or the microgrid of a house [16]. The other mode `GridFollowing` should be used in situations when the system is connected to the upstream distribution network, and would not act as one of the main grid-forming generators of the network [16].

With these two means to classify the technologies in hand, the aforementioned V2X technologies can be characterized as such:

- **V2G - vehicle-to-grid** The main technology of concern for this thesis. Can either be AC or DC-linked, but always grid-following.
- **V2L - vehicle-to-load** This technology is more or less universally accepted to be powering a single load [17] and is only RPT capable, using an AC-linked, grid-forming topology.
- **V2H - vehicle-to-home** This technology is loosely defined but found to most often cover AC-linked, grid-forming topologies with multiple loads, such as found in a home and optionally using a transfer switch to isolate the home from the wider grid. With such a system, the EV can provide backup power in the event of a grid outage. The technology could also be grid-following or even DC-linked where the energy is then supplied to a battery energy storage system.
- **V2B - vehicle-to-building** Same considerations and utilizations as V2H, but tied into a larger (commercial) building.
- **V2V - vehicle-to-vehicle** Charging one vehicle with energy from the battery of another vehicle, such that one vehicle is doing FPT and one RPT. Can be either AC or DC-linked, primarily grid-forming. In some cases, the formed grid might be DC instead of AC. As an added curiosity, this thesis demonstrates DC-linked, AC grid coupled V2V, see section 4.4.1.
- **G2V - grid-to-vehicle** Most often refers to FPT, charging the vehicle from the grid.
- **V1G** Most often refers to technology only capable of unidirectional charging, FPT from grid to vehicle.

One of the most common technologies and thereby terms is vehicle-to-load (V2L). This technology is commercially available in some of the most sold electric vehicles on the Danish market [18]. While being commercially available, it is exclusively a grid-forming technology, restricted to a single appliance, and does not offer the possibility of switching the direction of power flow. That means it is not capable of many of the applications envisioned for true bidirectional technologies, both grid-forming and grid-following. For this reason, it will be largely disregarded in this thesis.

2.2 Overview

The worldwide for market electric mobility market is growing at an incredible pace, and there are numerous competing standards and protocols on the market aiming to ensure interoperability. This thesis focuses primarily on the European and North American markets, the interoperability mechanisms used within them, as well as how they can be used to support BPT. Figure 2.2 provides an overview of standards and protocols touched upon within this thesis. The figure shows the different actors in the ecosystem as green circles, along with the interoperability mechanisms employed for communication between them. In the following sections, these standards are described in detail, with a special emphasis on how they may enable bidirectional charging. Worthy of note is the fact that the term *Secondary Actor* comes from the ISO 15118 family of standards, where it is used to cover both the CSMS and other parties. In figure 2.2 and this thesis, the CSMS and other actors will be separated, and an architecture where the secondary actors are mainly electricity grid actors such as utilities is assumed. In some cases, the protocols and standards placed between CSMS and these grid actors might be used to communicate directly to the EVSE instead. Such use cases are not covered by this thesis.

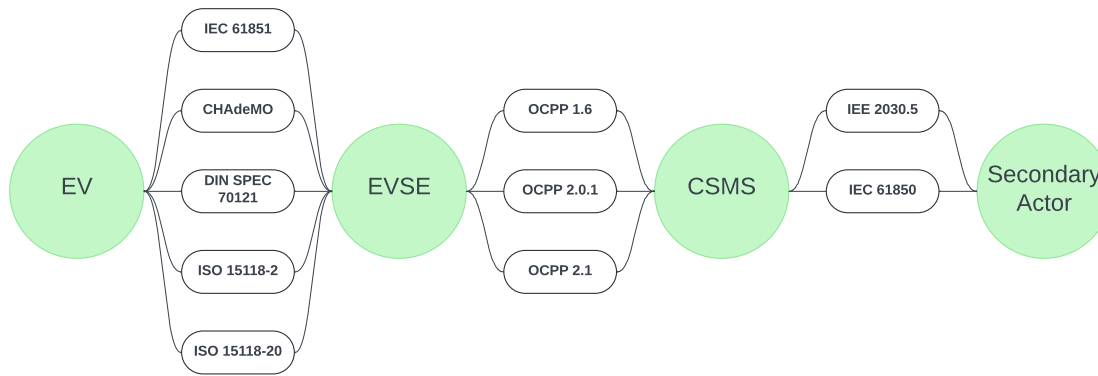


Figure 2.2: Overview of the interoperability mechanisms in the electric mobility ecosystem covered by this thesis. Secondary Actor refers to grid actors beyond the CSMS.

2.3 EV-EVSE communication

Interoperability between the EV and EVSE can be regarded as the first and most important step in enabling BPT. It is between the EV and EVSE that the actual power transfer happens, and as such the interoperability means used here not only concern themselves with communication but also user and equipment safety. Most of the connectors and communication protocols are built on top of the standard IEC 61851-1 *Electric vehicle conductive charging system – Part 1: General requirements*, which as the title suggests, outlines the general requirements. The different physical connectors used are detailed in the IEC 62196 family of standards, namely IEC 62196-3 *Plugs, socket-outlets, vehicle connectors, and vehicle inlets - Conductive charging of electric vehicles - Part 3: Dimensional compatibility requirements for DC and AC/DC pin and contact-tube vehicle couplers*.

2.3.1 CHAdeMO

The CHAdeMO standard differs a bit from the rest covered in this section. It was introduced in 2009 by the Tokyo Electric Power Company (TEPCO) and several automotive OEMs as both a connector and communication protocol. CHAdeMO is also the name of the CHAdeMO association that develops the standard. It is included in IEC 62196-3 as configuration AA [19]. CHAdeMO uses analog signaling through multiple control and proximity pilot pins and high-level digital communication with a physical and data link layer based on CAN bus. In figure 2.3, the CHAdeMO connector is shown with two large DC+ and DC- pins, as well as multiple smaller communication pins. The CAN bus interface uses the C-L CAN-low and C-H CAN-high pins shown on the lower half. In contrast to CCS, which uses single-ended signaling and HPGP for HLC, CHAdeMO and CAN bus use differential signaling on these two pins. The differential signaling makes the CAN bus a lot more resilient to interference than the HPGP interface used in CCS, and CHAdeMO does not use SLAC (Signal Level Attenuation Characterisation) or similar methods to avoid crosstalk.

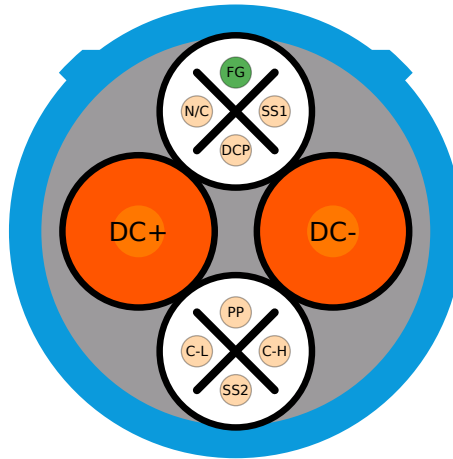


Figure 2.3: CHAdeMO connector. Image source: Wikimedia Commons [20].

CHAdeMO natively has bidirectional capabilities, and projects using the grid-following, DC-coupled RPT capacities of the CHAdeMO protocol have been going on around the world since 2012. As of today, CHAdeMO is the only charging protocol in the world with bidirectional charging functionality enabled, with mass-market production, and the certification system in place to ensure interoperability across EVs and EVSE. To date, there are more than 20 bi-directional charger models available, and over 10,000 such units are installed in Japan and the world [21]. As a hindrance to the adoption of BPT technology, the CHAdeMO connector and protocol were falling out of favor in the European and North American markets by the end of the 2010s, being replaced by the CCS plugs. This was partly driven by legislation from the European Union mandating CCS plugs be included in public charging infrastructure [4]. Because of this change, this thesis will not cover the CHAdeMO communication for bidirectional charging in detail, since the future of interoperable bidirectional charging in Europe and North America seems to be based on the ISO 15118-20 standard described in section 2.3.2.4.

2.3.2 Combined Charging System

Of most importance to this thesis is the Combined Charging System CCS2 connector, since this is one of the connectors that the Watt&Well EVSE used throughout the project is equipped with. It is also the by far most popular connector in use in Europe in 2024. On the Monta electric mobility service provider (eMSP) platform, 78% of the DC fast charging outlets are CCS, while only 22 % are CHAdeMO ¹. The Monta Platform covers many European countries with more than 100,000 fast-charging outlets.

In IEC 62196-3, the CCS2 connector is referred to as configuration FF, and it is shown in figure 2.4. The upper part of the connector is identical to the Type 2 connector used for AC charging, covered by IEC 62196-2. The Type 2 connector uses IEC 61851-1 Annex A *Control pilot function through a control pilot circuit using a PWM signal and a control pilot wire* and Annex B *Proximity detection and cable current coding circuits for the basic interface*[22] for signaling. These annexes only cover AC charging, so when the Type 2 connector was extended with the DC+ and DC- pins seen in figure 2.4 to form a combined AC and DC charging system (CCS), an additional signaling standard was needed. This standard was supposed to be ISO 15118, but as an interim solution, DIN SPEC 70121 was created, to get the market up and running until ISO 15118 was released [23]. When information about which protocols/standards the EV supports is exchanged at

¹Internal data provided by Monta

the beginning of a CCS charging session, the different protocols/standards are referred to as *schemas*. The following sections will cover the three different schemas most commonly encountered: DIN SPEC 70121, ISO 15118-2 and ISO 15118-20.

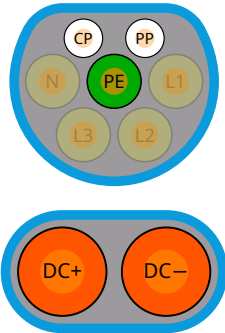


Figure 2.4: CCS2 connector, also known as configuration FF. Image source: Wikimedia Commons [24]

2.3.2.1 DIN SPEC 70121

The DIN SPEC 70121 is a specification published by the German Institute for Standardisation². It was first published in 2012 and is based on an early, unpublished version of the ISO 15118 standard [23]. It appears that even today, 10 years after the publication of ISO 15118-2:2014, DIN SPEC 70121 is still the go-to means of interoperability for DC charging. However, no concrete evidence of this fact has been found by this project, except the schema prioritization presented in section 4.1.

Since ISO 15118-2 and DIN SPEC 70121 are very similar, this thesis will not cover DIN SPEC 70121 in detail. They use the same initial handshake and very similar XML schemas, but are not identical and not cross-compatible. An EV that only supports DIN SPEC 70121 can therefore not start a charging session with an EVSE that only supports ISO 15118-2 or 15118-20 [23]. The main differences between ISO 15118-2 and DIN SPEC 70121 are highlighted in figure 2.5. DIN SPEC 70121 only supports EIM (External Identification Means), whereas ISO 15118-2 adds support for PnC (Plug and Charge). DIN SPEC 70121 also does not support Load Management, meaning it is not possible to renegotiate and schedule charging for smart charging purposes. Not included in the figure is support for AC charging mode, which exists within ISO 15118-2 [25], but not in DIN SPEC 70121 [23]. Moreover, both ISO 15118-2 and DIN SPEC 70121 lack support for BPT, so neither can be used to enable interoperable, bidirectional charging.

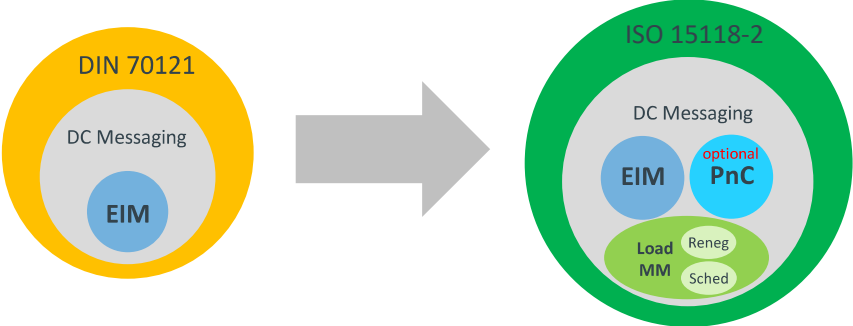


Figure 2.5: Difference between DIN SPEC 70121 and ISO 15118-2. Image adapted from CharIN [26].

²German: Deutsche Institut für Normung

2.3.2.2 ISO 15118 - overview

The ISO 15118 family of standards defines a *vehicle to grid communication interface*, as the name of the standards suggests. The scope of the standard is to enable communication between an EVCC (Electric Vehicle Communication Controller) and a SECC (Supply Equipment Communication Controller). This is illustrated as connection 1 in figure 2.6. In addition, the standards message definitions also consider use cases for communication between the SECC and a Secondary Actor [16], illustrated as connection 2.

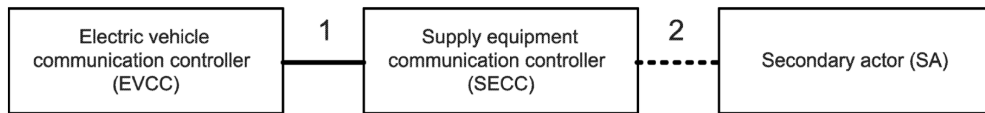


Figure 2.6: Scope of the ISO 15118 standards. Image source: [16].

Figure 2.7 illustrates the relationship between all parts of ISO 15118 and how they map to the seven communication layers as defined by the Open Systems Interconnection (OSI) model. This reference model defines how applications communicate across a network [27].

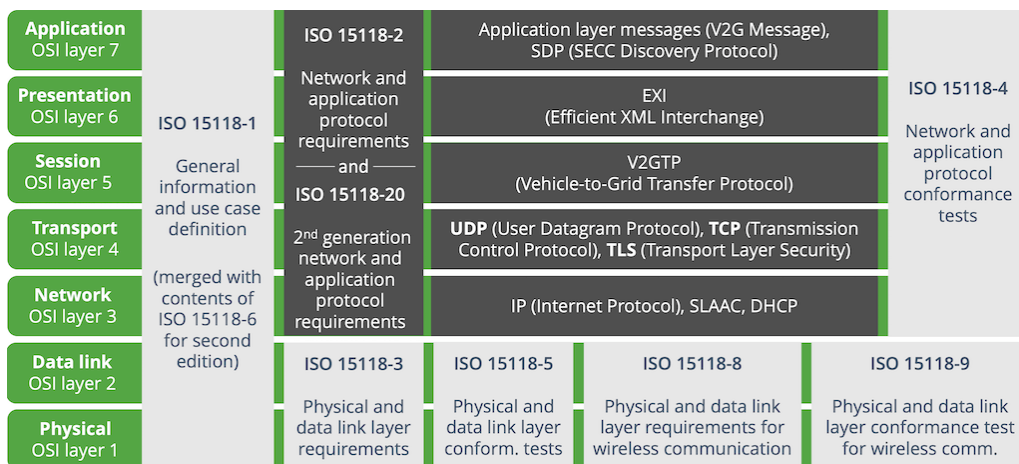


Figure 2.7: Diagram of the ISO 15118 standards and how they fit in the OSI model. Image source: *What is ISO 15118?*

Part 1 of ISO 15118 is called "General information and use-case definition". It outlines the intention of the specification and explains the overall goals of the standard by defining terms and use cases [27]. This part thus covers all seven layers of the model.

ISO 15118-2, titled "Network and application protocol requirements" serves as the central component of the international standard. It specifies the technical details for application layer messages and their parameters exchanged between electric vehicles (EVs) and EVSEs. It covers layers 3 through 7 of the OSI model, including all of the technologies in the dark grey area of figure 2.7. By following ISO 15118-2, many of the use cases outlined in ISO 15118-1 can be effectively implemented to establish successful communication and charging sessions [27]. Crucially, this standard does not cover BPT, even though it is part of 15118-1 [10].

ISO 15118-3 focuses on the "Physical and data link layer requirements" for wired charging. It defines communication at the lowest levels of the OSI model — the data link layer and

the physical layer. Specifically, it leverages PowerLine Communication (PLC), based on the HomePlug Green PHY specification, to encode digital signals onto the Control Pilot (CP) pin within the connector. These layers serve as the foundation for the higher-level communication outlined in ISO 15118-2 and ISO 15118-20. Additionally, ISO 15118-3 addresses the interaction with the IEC 61851-1 standard, as briefly touched upon in the DIN SPEC 70121 section. By enhancing the IEC 61851-1 described charging process with digital High Level Communication (HLC), ISO 15118 builds upon the safety-related IEC standard.

ISO 15118-4 and ISO 15118-5 address conformance tests for the requirements outlined in ISO 15118-2 and ISO 15118-3, respectively. These tests ensure compliance with the specified standards, and will not be covered in this thesis. Similarly, parts 6, 7, 8, and 9 cover wireless communication, and are also not covered.

The OSI model divides communication between two network endpoints into seven functional layers. In an electric vehicle charging scenario, the EVCC and the SECC act as endpoints. The EVCC's message moves through all seven layers, from the application layer down to the physical layer, before being transmitted via a physical medium like a charging cable or Wi-Fi. The EVSE then processes the message through the layers in reverse, from the physical layer up to the application layer. On the application layer, ISO 15118 defines two types of messages: SDP (SECC Discovery Protocol) and V2G (Vehicle-to-Grid) messages. SDP messages consist of a single request and response used during communication setup to exchange IP addresses and ports between the EV and the EVSE. V2G messages handle the remaining communication tasks, including starting, maintaining, and ending a charging session [27].

The application layer sends data packets to the presentation layer, which translates the application data into a specific format that both the sending and receiving sides understand. To speed up transmission, the presentation layer compresses the data using Efficient XML Interchange (EXI) for V2G messages. EXI is a binary representation of XML data structures, and all V2G messages in ISO 15118 are defined in XML format. The EV's application layer encodes an XML message into EXI format before delivering it to the session layer. The EVSE decodes the EXI back into XML upon receipt. Notably, EXI is not used for SDP messages [27, 25].

The session layer manages communication sessions between the EV and the EVSE using the Vehicle-to-Grid Transfer Protocol (V2GTP). The V2GTP header includes crucial information about the payload type, indicating whether it is an EXI-encoded V2G message or an SDP message. This information ensures both the EV and the EVSE correctly process incoming messages [27, 25].

The transport layer establishes a TCP/IP connection for reliable data transmission between the EV and the EVSE, ensuring error recovery and retransmissions if needed. All V2G messages are transmitted using TCP (Transmission Control Protocol), and Transport Layer Security (TLS) is used for encryption when data security is required. In contrast, SDP messages are transmitted using the User Datagram Protocol (UDP). UDP prioritizes quick transmission of data packets from point A to point B, without ensuring reliability or order. The EV and EVSE exchange addresses within SDP messages, which can be sent multiple times, and the order of reception does not matter. Some messages may be lost without affecting the outcome, as long as at least one message is successfully received and processed. However, V2G messages require a reliable transmission mechanism like TCP or TLS to maintain the correct order, which is crucial for the state machines controlling the information flow during a charging session [27, 25].

On layer three, the network layer, TCP uses Internet Protocol (IP) to assign unique IP addresses to the EVCC and SECC, enabling data packet routing between them. Additional protocol mechanisms used at this layer include Stateless Address Autoconfiguration (SLAAC) and Dynamic Host Configuration Protocol (DHCP) [27, 25].

On the very lowest layers 1 and 2, the data is transmitted by electrical signals such as a changing voltage. In the case of charging via the CCS, the first part of the process and handshake is done within the IEC 61851-1 Annex A Control Pilot domain. The Control Pilot pin, designated *CP* in figure 2.4, carries a ± 12 V signal generated within the EVSE. This signal is then modulated via rectification and fixed resistances on the EV side, to generate positive half-waves of 12, 9, 6, and 3 V. These are then mapped to states within IEC 61851-1 Annex A called A, B, C, and D, which are used to signal the readiness of the EV to receive power. The EVSE can then inform the EV of the maximum current via PWM (Pulse Width Modulation) of 1 kHz with a varying duty cycle [22]. Within the IEC 61851-1 standard, the duty cycle of 5% is reserved for instructing the EV to use digital communication per table Table A.7 *PWM duty cycle provided by EV supply equipment*[22]. The ISO 15118-3 standard builds upon this signaling used in IEC 61851-1, by using the same Control Pilot pin/wire to also carry digital communication in the form of PLC (PowerLine Communication). This method takes its name from the original use of carrying digital communication over electrical powerlines and is described by the HomePlug Green PHY (HPGP) specification. HPGP is intended for single-ended signaling and uses advanced modulation in a frequency band of 1.8 to 30 MHz [29]. This has the consequence that crosstalk might be present, as is illustrated in figure 2.8. Here, EV 1 is connected to EVSE A, and EV 2 is connected to EVSE B. The two EVSEs are electrically on the same mains connection, and this might lead to a coupling between the two allowing the EVCC in EV 1 to "see" the SECC of EVSE B. To get around this crosstalk and avoid attempting to start a transaction on the wrong EVSE, Signal Level Attenuation Characterization (SLAC) is used. The SLAC mechanism then uses special *sounding* packets to measure the attenuation of the signal at the various SECC and a link is formed with the SECC having the lowest attenuation. As a small curiosity, the upcoming Megawatt Charging System (MCS) will use differential signaling over Unshielded Twisted Pair (UTP) for HPGP, similar to how the CHAdeMO standard uses CAN bus. This produces much less crosstalk and means that the SLAC mechanism can be eliminated on MCS, which should reduce complexity and accelerate startup/handshake times [30]. MCS will also be based on ISO 15118 and CharIN recommends that MCS should only support ISO 15118-20 [30].

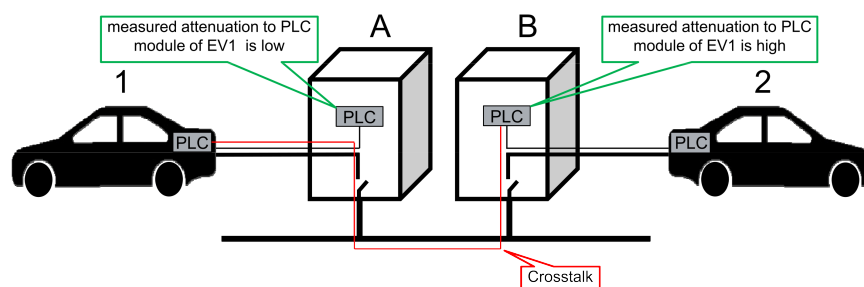


Figure 2.8: Diagram illustrating how SLAC crosstalk. Image source: [29].

To establish an ISO 15118-2 or 15118-20 session with a wired (CCS) connection, the following general steps are taken:

1. **CCS** connector is plugged in.

2. **EVCC** detects the Proximity Pilot resistance and changes the Control Pilot state to B1.
3. **SECC** detects the change from state A to state B1 and enables PWM with a duty cycle of 5%, thus switching state to B2.
4. **SECC** starts listening for SLAC sounding packets.
5. **EVCC** sends SLAC sounding packets.
6. **SECC** responds to the sounding packets with an attenuation characterization.
7. **EVCC** picks the SECC with the best connection and uses the SECC Discovery Protocol to exchange IP address and port information to form a connection.
8. **EVCC** can request TLS if needed and a TLS handshake will be performed.
9. **EVCC** sends the first V2G message, the *supportedAppProtocolRequest*.

2.3.2.3 ISO 15118-2

This section will describe some of the message sequences of a 15118-2 session, highlighting why 15118-2 lacks support for BPT. Appendix A.10 is a sequence diagram of a DC session and includes the IEC 61851-1 control pilot state changes in addition to ISO 15118 V2G messages. In appendix A.11, a similar diagram for an AC session is found, which will not be covered in detail.

The steps 1 through 9 in the previous section are covered by the first part of the diagram, where the state changes from A to B and IP-based PLC is established. After this, the *supportedAppProtocolRequest* is made, which is used by the EVCC and the SECC to agree on a protocol version. Both must support the same versions of DIN SPEC 70121, ISO 15118-2, or ISO 15118-20. The EVCC will send a prioritized list and if the SECC cannot match any of them, a charging session cannot be initiated [31, 27, 25]. This message exchange is what is used to form the table in section 4.1 on vehicle compatibility.

With the *ServiceDiscovery* messages the EV requests information from the EVSE about its available services, which may include AC single-phase or three-phase charging, various DC charging options, identification mechanisms (such as External Identification Means (EIM) or PnC), and optional value-added services like Internet access. The EV can request further details on each service using the optional *ServiceDetailRequest* message. Part of the *ServiceType* sent by the SECC is the *EnergyTransferMode* that the EVSE supports, from which the EV will pick one. In ISO15118-2, these are all *charging* services and are included in table 2.1. For a CCS charging session, the *DC_extended* mode would be offered by the SECC.

EnergyTransferMode	Offered charging service
AC_single_phase_core	AC single phase charging according to IEC 62196.
AC_three_phase_core	AC three phase charging according to IEC 62196.
DC_core	DC charging according to IEC 62196 on the core pins.
DC_extended	DC charging using the extended pins of an IEC 62196-3 Configuration EE or Configuration FF connector.
DC_combo_core	DC charging using the core pins of an IEC 62196-3 Configuration EE or Configuration FF connector.
DC_unique	DC charging using a dedicated DC coupler.

Table 2.1: Energy Transfer Modes and Offered Charging Services in ISO 15118-2. Adapted from table 63 [25].

Once the service type has been agreed upon, the session will progress towards power delivery. Using the *ChargeParameterDiscovery* messages, the EV and the EVSE exchange their technical charging limits, including maximum and minimum voltage levels and current. The EV can also communicate energy needs and the driver's desired departure time. The SECC calculates and proposes a charge schedule, detailing the maximum charging power allowed.

Next, a *CableCheck* will be initiated for safety reasons. The EV sends a *CableCheckReq* to inquire about the EVSE's cable check status, indicating if the connector is locked and if the EV is ready to charge. The SECC responds with a *CableCheckRes*, providing the cable check status and EVSE information. During the cable check, the DC EVSE will enable its power converter and apply a DC voltage to the cable higher than the maximum voltage agreed to be used during the *ChargeParameterDiscovery*. While this happens, the EV side contactors remain closed and the Insulation Monitoring Device (IMD) of the EVSE will measure if any leakage occurs. The Control Pilot state will also switch to C, indicating that dangerous voltages can now be present in the circuit. This is followed by *PreCharge*, where the EVSE output voltage is adjusted to match the EV battery voltage. Finally, the session progresses to *PowerDelivery*. At this point, the EV will close its charging contactor, allowing current flow between the EV and EVSE.

The session then progresses to the *ChargingLoop*, where in the case of DC charging, *CurrentDemand* is used by the EV and EVSE to continuously exchange the EV's requested current, target voltage, and the differences in current and voltage. The EV sends a *CurrentDemandReq* to request a specific current from the EVSE. The SECC responds with a *CurrentDemandRes*, informing the EV of the EVSE status and the current output voltage and current. This process forms a charging loop.

In addition to the lack of *EnergyTransferTypes* for BPT, the *ChargeParameterDiscovery* and *CurrentDemand* messages do not contain any elements and types useful for communicating reverse power transfer capabilities. Similarly, no framework exists to change energy transfer direction during a session, nor for the EVSE to remain in control like 15118-20 *Dynamic mode* allows.

Despite the lack of official support, some EV manufacturers like Volkswagen claim that their vehicles are capable of bidirectional charging via CCS and the ISO15118-2 standard. The following quote comes from a press release [32]:

This makes Volkswagen one of the first providers of a bidirectional charging solution based on the CCS (Combined Charging System) DC charging standard, which is widely used in Europe. Bidirectional charging is based on ISO standard 15118-2, which describes the communication between electric vehicles and wallboxes.

The solution is only compatible with the DC home power station of the S10 E COMPACT series from HagerEnergy GmbH and Volkswagen claims other home power stations are to be enabled for operation with a bidirectional charging station at a later date [32]. From this press release, it seems the claimed bidirectional capabilities are implemented using a custom subset of the ISO 15118-2 standard, as thus not interoperable between different EV and EVSE combinations.

Open source EVSE project EVerest has also demonstrated BPT using ISO 15118-2, by simply ignoring the charging-only limits of 15118-2 and switching the current flow direction. Some of the EVs tested did allow this to happen for long periods and with large energy amounts discharged, according to published logfiles [33].

2.3.2.4 ISO15118-20

The ISO 15118-20 subtitle is *2nd generation network layer and application layer requirements* and it is intended as a direct replacement for ISO 15118-2. The initial handshake process is still based on IEC 61851-1 Control Pilot signaling and the physical and data link layers are still based on ISO 15118-3 and HPGP PLC in the case of wired charging. Thus, the same sequence of 9 steps as described at the end of section 2.3.2.2 still applies. After that process, the two standards diverge.

The following things are new or improved within 15118-20:

- **Bidirectional Power Transfer (BPT) / Bidirectional Charging:** As already covered by this thesis, the ability to charge and discharge a vehicle.
- **Wireless Power Transfer (WPT) / Wireless Charging:** The definition of messages to exchange the necessary information between the vehicle and the wireless charger as a supplement to the IEC 61980 protocol.
- **Automated Connection Device (ACD):** An automatic connection and disconnection process for energy transfer by conduction. A typical example is that of the pantograph for an electric bus.
- **Dynamic Control Mode:** The EV yields full control to the EVSE, and the EVSE provides single power setpoints without negotiating charging schedules.
- **Dynamic and Scheduled Load Profiles:** Profiles can be calculated locally or provided by an external system.
- **Communication Multiplexing:** The opening of parallel communication channels; the main channel manages the charging session. These channels make it possible to renegotiate schedules, but not services, as defined in ISO 15118. They also provide the ability to send metering data without disturbing the current charging session.

- **Stronger Data Security:** TLS 1.3 is mandatory for all use cases and newer, more secure cipher suites with longer keys are added along with up-to-date cryptography algorithms. Multi-contract handling has also been improved, making it easier for the EV to identify itself to the EVSE using more than just one contract certificate for PnC.

Of these, the most relevant to the goal of achieving BPT with CCS-equipped vehicles is of course the addition of BPT support, but dynamic control mode and multiplexed communication play an important role too. On the other hand, one possible hindrance to the implementation of ISO 15118-20 is the requirement for TLS (Transport Layer Security) in all use cases. Concretely, step 8 in the initial handshake process described in section 2.3.2.2 is now a requirement, and the EVCC must request TLS before enabling 15118-20 communication. The requirements are given as such in 15118-20: [16]

[V2G20-1238] In the SDP handshake, when the SECC intends to offer ISO 15118-20 communication, it shall respond to a TLS request by the EVCC with TLS.

[V2G20-1235] V2G-CI-TLS shall always be applied for both the EVCC and SECC, if the chosen ProtocolNamespace is equal to "urn:iso:std:iso:15118:-20".

[V2G20-2646] After the message exchange of supportedAppProtocolReq/Res, usage of V2G-CI-TLS shall be confirmed.

[V2G20-1237] If the established connection between EVCC and SECC is TLS 1.2 (or lower) or TCP without TLS the EVCC shall not offer ISO 15118-20 communication in SupportedAppProtocolReq message (see Table 5).

[V2G20-2356] If the established connection between EVCC and SECC is TLS 1.2 (or lower) or TCP without TLS the SECC shall not select ISO 15118-20 communication from SupportedAppProtocolReq message (see Table 5).

The referenced table 5 is included as table 2.2. Here, the requirement for TLS version 1.3 is given. It is also stated that ISO 15118-2 with only External Identification Means (EIM) or DIN SPEC 70121 can use lower versions of TLS or no TLS at all:

TLS version	Communication protocols supported
1.3	– This document – ISO 15118-2
1.2	– ISO 15118-2
1.1 or earlier	– ISO 15118-2 EIM only
No TLS	– ISO 15118-2 EIM only – Communication specified in DIN SPEC 70121

Table 2.2: ISO 15118-20 table 5: TLS versions and their supported communication protocols. Source: [16].

In addition to the requirement for TLS 1.3 in all sessions, ISO 15118-20 also sets requirements for the cryptographic algorithms and elliptic keys used. The standard also strongly recommends the use of a Hardware Security Module (HSM) to store the private keys for the cryptographic algorithms. The HSM can either be an on-chip solutions within the

microcontrollers used or a separate hardware solution in the form of a Trusted Platform Module (TPM) of the type TPM 2.0 [16]. It seems that TPM 2.0 devices available on the market might not include support for the algorithms that 15118-20 requires [34].

Coming back to the BPT capabilities in 15118-20, the new *Dynamic* control mode is now added alongside the existing *Scheduled* mode (which uses charging schedules) in ISO 15118-2. 15118-20 differentiates between two main situations: either the EV ensures its own mobility needs (Scheduled control mode), or the responsibility for ensuring mobility needs is delegated to an off-board system, which is the EVSE (Dynamic control mode) [10].

In the Scheduled mode, the EV and the EVSE negotiate a power profile based on the information exchanged through the ChargeParameterDiscovery request and response messages also used in 15118-2. Here, the EV calculates a charging profile that meets the user's mobility needs—such as the energy required to fully charge the battery and the departure time—and the power limits of the EVSE [35]. While working with 15118-2, it is observed in this thesis that EVs do not necessarily share this information.

In the Dynamic mode, control is fully delegated to an off-board system such as the EVSE, CSMS, or other Secondary Actor and involves no negotiations. The EV sends the same charging-related parameters to the EVSE as it would in Scheduled mode. However, in Dynamic mode, the station responds with single power set points to the EV without providing pricing information or a power forecast in the form of a charging schedule. The EV must comply with these set points, and in the case of DC charging, they are directly applied in the EVSE power converter. The off-board system responsible for control ensures that the user's mobility needs are met. This mode is especially useful for scenarios requiring a fast response to provide grid services, such as frequency control [35].

The other enabling feature, communication multiplexing, uses new payload types to allow certain messages to be exchanged in parallel with the predefined message flow. These messages can include a service renegotiation, such as switching from charging to discharging energy. For instance, during a DC charging session, while exchanging the *DC_ChargeLoop* request and response messages, either the EV or the EVSE can initiate a scheduled renegotiation to change the charging profile (the amount of power used over time) without interrupting the ongoing message exchange. This renegotiation occurs in a parallel side stream with a different payload type. This is particularly beneficial for the DC charging process, where it is now possible to switch power flow direction without opening the contactors. In the ISO 15118-2 charging process, the charging session would need to be interrupted because the contactors must be opened and closed during the renegotiation of a charging schedule [35].

The message sequence to start, loop, and end a session in 15118-20 is quite similar to 15118-2. Appendix A.12 illustrates such a sequence. Of concern to bidirectional power transfer is how the service is configured. The EVCC will send a ServiceDiscoveryReq message, which will cause the SECC to send information about all services offered by the SECC. Additionally, the EVCC can restrict specific services by transmitting a list of supported service identifiers. Upon receiving the ServiceDiscoveryReq message from the EVCC, the SSECC responds with the ServiceDiscoveryRes message. This message will contain a list of ServiceIDs, and those IDs that pertain to power transfer have been included as table 2.3.

ServiceID (unsignedShort)	ServiceName	Description
1	AC	AC energy transfer, physical layer according to ISO 15118-3 and ISO 15118-8
2	DC	DC energy transfer, physical layer according to ISO 15118-3 and ISO 15118-8
3	WPT	WPT, physical layer according to ISO 15118-8
4	DC_ACDP	DC Charging with ACDP, physical layer according to ISO 15118-8
5	AC_BPT	AC Charging with BPT, physical layer according to ISO 15118-3 and ISO 15118-8
6	DC_BPT	DC Charging with BPT, physical layer according to ISO 15118-3 and ISO 15118-8
7	DC_ACDP_BPT	DC Charging with ACDP and BPT, physical layer according to ISO 15118-8

Table 2.3: ISO 15118-20 Power transfer Service IDs and their corresponding service names and descriptions, adapted from ISO 15118-20 table 204

ParameterName	ParameterType	Values	Description
Connector	intValue	1: Core 2: Extended 3: Dual2 4: Dual4	Usage of the connector.
ControlMode	intValue	1: Scheduled 2: Dynamic	Selection of which party (SECC or EVCC) is responsible to fulfill the mobility needs of this service session.
MobilityNeedsMode	intValue	1: Mobility needs provided by EVCC 2: Mobility needs provided by SECC allowed	Indicate who can provide mobility needs information. Value 2 indicates that not only EVCC but also SECC can provide mobility-needs information (however, the EVCC shall always provide an initial mobility-needs information including DepartureTime). Value 2 can be selected only if DynamicControlMode was selected.
Pricing	intValue	0: No pricing 1: Absolute Pricing 2: Price Levels	Providing information about which pricing structure will be used in the offered schedules.
BPTChannel	intValue	1: Unified 2: Separated	Type of installed power transfer channel. Unified: Single channel Separated: Dual channel
GeneratorMode	intValue	1: GridFollowing 2: GridForming	Power converter behavior. For details see the IEC/TS 62898 series.

Table 2.4: ISO 15118-20 Configuration parameters for DC BPT service. Adapted from [16].

The EVCC can also request and receive additional details about services with the ServiceDetailReq/Res message pair. For a DC BPT with ServiceID 6, these parameters are

listed in table 2.4. These include the connector type and the control mode, which can be scheduled or dynamic, as already described. The parameters also indicate the source of user mobility needs, such as departure time and required energy, as well as the pricing type. The BPTChannel parameter informs the EVCC whether a single, bidirectional meter exists, or two different meters are in use. Finally, the GeneratorMode informs the EVCC whether the power converter in the EVSE is grid forming or grid following. If these parameters are acceptable by the EVCC, it will send a ServiceSelectionReq requesting either ServiceID 5 for AC or ServiceID 6 for DC. In the case of AC BPT, a few additional parameters are included, these are found in table A.1 in the appendix. These include EVSENominalVoltage, informing the EVCC of the EVSE grid conditions, GeneratorMode letting the EVCC know if it is expected to work in grid-forming or grid-following mode, and GridCodeIslandingDetectionMethod, which relates to how the EV is expected to detect islanded grid conditions.

Once a service has been selected, the EVCC/SECC will exchange ChargeParameterDiscovery messages to negotiate the energy transfer parameters. These are the EV and EVSE minimum and maximum charging and discharging power and current, as well as EV and EVSE minimum and maximum voltages. In the case of AC BPT, these include the nominal frequency and other grid-related parameters like frequency and per-phase power. Once an agreement has been reached, the ScheduleExchange occurs. Here the EV can inform about its mobility needs, such as target SoC, departure time, and required energy to reach the target SoC. Following this, cable check and precharge sequences similar to ISO 15118-2 happen, and a final PowerDeliveryReq/Res message exchange occurs before the power transfer begins. The system now enters the charge loop, and the EV will request a certain current from the EVSE. Also, the target voltage, current, and voltage difference are transferred. In the case of dynamic mode, the EVSE will be in control and just make sure to not exceed the limits given in ChargeParameterDiscovery and ChargeLoop messages. An example of the elements sent by the EVCC to the SECC as part of the ChargeLoop for a DC BPT session in Dynamic mode is included as figure 2.9.

Once the DC session is over, similar *WeldingDetection* and *SessionStop* messages as those used in 15118-2 will be exchanged. Since each message exchanged in a session will have the potential to make it fail, it will often be displayed as part of the status in SECC and EVCC emulation software. As an example, the upper green and yellow bar in the Keysight software in figure 4.2 shows the session progress of a 15118-20 session through SLAC, SDP, SupportedApp, SessionSetup, Authorization, ServiceSetup, ChargeParameterDiscovery, ScheduleExchange, CableCheck, PreCharge and finally ChargingLopp in yellow. As the session is still active, SessionStop is grey.

2.4 EV-CSMS communication

While the physical charging hardware and EV-EVSE communication have been standardized internally by the IEC and ISO standards described in this chapter, there exists no globally agreed-upon standard for the control of EVSE. However, the Open Charge Point Protocol is the closest candidate to a standard for connected Charge Points. Furthermore, the IEC has on the 7th of June 2024 started the fast-track procedure for OCPP to become an IEC International Standard with the anticipated IEC number for OCPP being IEC 63584 [36].

The Open Charge Point Protocol is an open, standardized protocol that allows EV charging equipment to communicate with a central EVSE management system (CSMS), also known as a backend, which then allows for external control of many processes related to the charging. It was developed in 2010 by the Open Charge Alliance, a consortium of EV

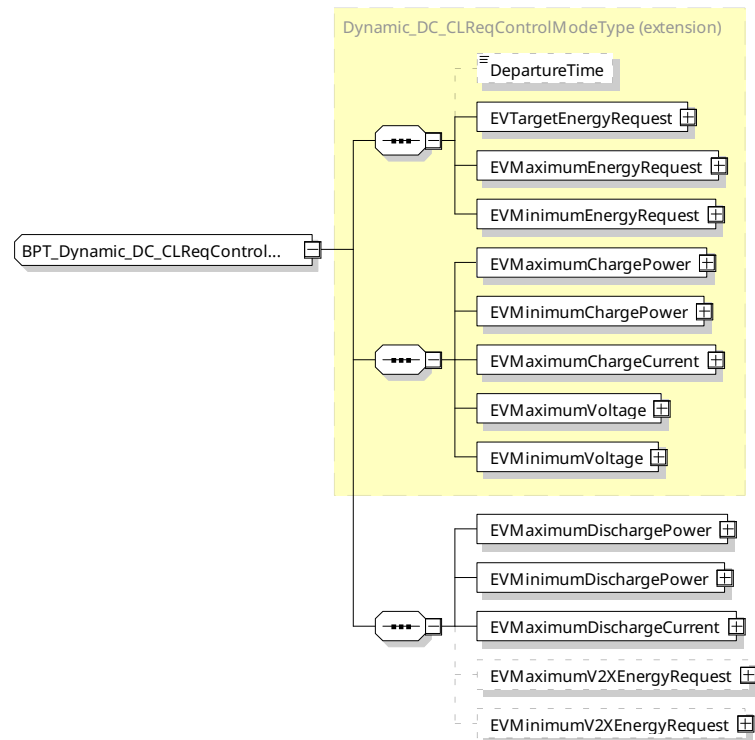


Figure 2.9: ISO 15118-20 Schema diagram 188, showing message elements for a DC BPT Dynamic ChargeLoopReq message. Image source: [16].

charging equipment manufacturers and service providers. The main purpose of OCPP is to provide a uniform way and standardized protocol for EVSE to interact with CSMS. This allows different EVSE manufacturers to interoperate with different CSMS providers. The primary usage is to manage the charging process, also known as the transaction, which entails the starting and stopping of charging sessions, monitoring the current charging status, and finally, fetching the energy amount for billing purposes [37]. In addition to managing the charging process, OCPP can be used to directly control the power or current setpoints set by the EV/EVSE combination for a session, which can be used for load balancing, smart charging, and other grid flexibility services.

OCPP versions 1.6, 2.0.1, and 2.1 all communicate between EVSE and the CSMS using WebSocket. WebSocket (ws) is a communications protocol, widely adopted from around 2010, that allows for real-time, bi-directional communication between a client and a server over a single, persistent connection. It uses a handshake process to establish a connection between the client and the server, after which both parties can send and receive data simultaneously. It is an upgrade to traditional HTTP-based communication, which requires a new connection to be established for each request and response. WebSocket is efficient and lightweight, making it useful for communication with EV charging equipment, that requires the transfer of data in near real time. It also uses TCP which has built-in failsafe checksum for messages [37]. The WebSocket protocol is illustrated in figure 2.10.

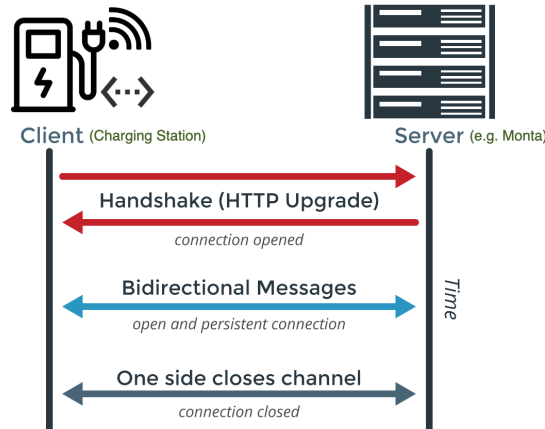


Figure 2.10: Graphic representation of the WebSocket protocol.

The following sections will provide an overview of how the different versions of OCPP can be used to enable control of BPT-capable EVSE.

2.4.1 OCPP 1.6

OCPP 1.6 comes in two variants, JSON and SOAP, and was first released in 2015. The JSON-variant, often referred to as 1.6J, is as of today the most widely adopted version of OCPP and is used throughout the world for EVSE-CSMS communication.

OCPP 1.6 does not include any native support for BPT, however, it does include the optional feature of Smart Charging. When included in OCPP 1.6 implementations, the CSMS gains the ability to influence the charging power or current of a specific EV or the total allowed energy consumption on an entire EVSE / group of EVSE, for instance, based on a grid connection, energy availability on the grid, or the wiring of a building. Influencing the charge power or current is based on energy transfer limits at specific points in time. Those limits are combined in a Charging Profile [38]. The limit in a charging profile is given with a *ChargingrateUnit*, which can be either Watts or Ampere. The limits in a profile are not directly limited to positive current or power values by the specification, but the behavior with negative values is not standardized. This means that OCPP 1.6 could be used to set negative power or current setpoint, but interoperability between different EVSE and CSMS is unknown. Another important aspect of operating both unidirectional and bidirectional EVSE is receiving measured electrical quantities at regular intervals. OCPP 1.6 supports this using the *MeterValue* message, which can contain different *measurands*. The OCPP 1.6 specification includes a list of allowable options for measurands, and the definition:

Import is energy flow from the Grid to the Charge Point, EV or other load.
 Export is energy flow from the EV to the Charge Point and/or from the Charge Point to the Grid.

The list of measurands includes *Current.Export*, *Power.Active.Export*, *Power.Reactive.Export*, *Energy.Active.Export.Register* and *Energy.Reactive.Export.Register*. The measurerand section of OCPP 1.6 is thus somewhat prepared for bidirectional technologies.

OCPP 1.6 does not support ISO 15118 messages. However, some OCPP implementers have asked the Open Charge Alliance if an intermediate solution, combining both OCPP 1.6 and the ISO 15118 Plug & Charge functionality would be possible [39]. To meet that demand, the Open Charge Alliance has released an application note detailing how some

of the 15118 messages about the handling of certificates and the PnC authentication method can be implemented in OCPP 1.6 in a standardized way [39]. The application note does not include any functionality related to BPT and in part uses the OCPP 1.6 mechanism of vendor-specific data transfer, which allows for the exchange of data or messages not standardized in OCPP. As such, it offers a framework within OCPP for experimental functionality that may find its way into future OCPP versions. Experimenting can be done without creating new (possibly incompatible) OCPP dialects. Secondly, it offers the possibility to implement additional functionality agreed upon between specific CSMS and RVSE vendors [39]. Many different custom DataTransfer mechanisms exist but in the case of BPT, OCPP 1.6 support via DataTransfer would not ensure true interoperability.

In addition to DataTransfers, some CSMS vendors and EVSE manufacturers also implement customizations around the standardized OCPP 1.6 messages. One notable example is described by Italian DC charger manufacturer Alpitronic in the document *Load management manual - Hypercharger HYC50 / HYC200 / HYC400 (50kW – 400kW) ultra-fast charging system for electric vehicles*. The manual details: [40]

Moreover, an extension to OCPP capability is provided to control reactive power, via the chargingRateUnit key: if "VAR" is specified as unit of measure, the profile will be treated as a reactive profile and it will be added to a dedicated profile database, independent of the active profile database.

The same manual claims that the power modules in the equipment can operate in the interval +14 kVAR (capacitive) to -15 kVAR (inductive) [40]. With this implementation, it would be able to set the *reactive* bidirectional power transfer setpoint to both import and export via OCPP 1.6.

2.4.2 OCPP 2.0.1

The newest released version of OCPP is 2.0.1, and this version was initially released in 2020. The third edition of version 2.0.1 was released in 2024 [41], and it is this edition that, at the time of writing, is being fast-tracked towards becoming an IEC standard. Adoption of OCPP 2.0.1 is increasing, and EVSE manufacturer EVBOXs latest models Livo and Liviqo only support 2.0.1. The CSMS platform Monta is also releasing OCPP 2.0.1 support for early adopters in June 2024.

OCPP 2.0.1 is not an incremental update and is not backward compatible with OCPP 1.6. Key changes include a revamped transaction handling system, necessary for supporting configurable start and end conditions for transactions, and the introduction of the device model, which offers enhanced configuration and monitoring capabilities. The update also adds more security features, and display customization and includes "full support" for ISO 15118-2. This covers the PnC and certificate features also added to OCPP 1.6 via an application note, as well as smart charging input from the EV, such as handling the user mobility needs and renegotiation process when a charging schedule needs to be updated [42].

Crucially, the OCPP 2.0.1 specification only covers ISO 15118-2, and the possibilities with the Metering and Smart Charging functionalities also included in OCPP 1.6 do not change significantly nor add any BPT support. To achieve BPT management via 2.0.1, it is therefore still necessary to go beyond the specification and use non-standardized messages or DataTransfer.

2.4.3 OCPP 2.1

The next version of OCPP is scheduled to be 2.1, with an unknown release date. Drafts of the protocol are currently being written, and these are available to members of the Open Charge Alliance only [43]. The draft v0.48 contains primarily additions to version 2.0.1 that cover support for ISO 15118-20 and BPT functionalities. As the content is not finalized, this section will not contain details. However, a summary of the drafted additions related to this thesis will be included.

The term V2X has been so far chosen by the draft to cover bidirectional power transfer between an EV and the grid, home, building, or load. The draft takes special care not to use the term V2G, to avoid confusion with the same term used in ISO 15118. This section will still use the term BPT.

The draft adds BPT additions to the existing Smart Charging functionality found within OCPP 2.0.1. The two control modes scheduled and dynamic in ISO 15118-20 are supported and differentiated between. The charging schedules in a charging profile have been extended with additional attributes to control discharging operations. The draft suggests that the *limit* setting in Watt or Ampere is only used for positive (charging) values, while two new fields *setpoint* and *dischargeLimit* are added. The former represents the target value for either charging or discharging depending on the sign, while the latter only deals in negative values for setting the maximum discharge limit [43].

Multiple new operating modes are also added, dictating what kind of control is to be used and the source of the setpoint and/or limits. The mode LocalLoadBalancing expands on the modes with fixed setpoint and/or limits, and instead of centralized control hands of control to the EVSE based on measurements of building consumption and local energy production from for example photovoltaic systems.

A LocalFrequency mode is also suggested, during which the EV takes part in frequency containment reserve (FCR) services or automatic Frequency Restoration Reserve (aFRR). The power setpoint for FCR support is determined from a power/frequency (Freq-Watt) curve, based on the locally measured frequency. The curve is a field in ChargingSchedule, *v2xFreqWattCurve*, which contains a list of at least two coordinates [43]. The aFRR capacity is instead activated by a signal from the TSO to the CPO³. The signal is passed on to affected EVSE via the *AFRRSignalRequest* message. The amount of upward or downward aFRR for a charging station is set in the *v2xSignalWattCurve* element in the ChargingSchedulePeriodType [43].

Another operating mode is CentralFrequency, which is similar to LocalFrequency, only in this case the setpoint for frequency support is determined by the CSMS. This is used, for instance, when calibrated frequency measurements are to be used that cannot be installed in each EVSE. This mode is intended to be used in a charging profile with ChargingProfileKind = Dynamic, such that CSMS can continually update the setpoint when the frequency changes via the *UpdateDynamicScheduleRequest* message.

On top of the BPT functionality, OCPP 2.1 drafts also include Distributed Energy Resource (DER) control, since utilities consider an EVSE (or group of EVSE) that is performing bidirectional charging/discharging as a DER. Such DER needs to adhere to the local grid codes that govern how it should react in case of grid anomalies. This is controlled by a range of settings and curves that determine how to respond to frequencies or voltages that are too high or too low. The draft specification assumes that the utility does not directly interface with EVSE or EVs for DER control, because the EVSE is only controlled

³Charge Point Operator

by the Charge Point Operator, and the EVs have no interface with the utility. Instead, the CPO acts as an aggregator who controls (groups of) EVSE. The CSO, as an aggregator, is assumed to take care of scheduling DER control messages towards EVSE when the utility sends a schedule of DER control messages [43]. The OCPP 2.1 draft assumes that the interface from CPO, via the CSMS to an EVSE, is the OCPP protocol. As such, the OCPP interface will also be used for DER control messages, and interfacing with the EV is then done via the ISO 15118-20 interface [43]. The draft points towards IEC 61850 and IEEE 2030.5 as possible protocols used for communication between the CSMS/CPO, acting as aggregator, and the utility or other secondary actor. These two protocols will be covered in more detail in the following sections.

The DER functionality is intended to provide secondary actors with standardized information about the available assets (EV/EVSE) and real-time data. It will also provide a mapping between active or reactive power setpoints or limits sent from the secondary actor, which are then forwarded to the EVSE via already supported OCPP charging profiles. Other control settings, such as a fixed power factor and frequency droop, can be transferred to the EVSE via a new *SetDERControlRequest* message. These can also include trip and ride-through curves and Volt and Watt curves [43].

2.5 CSMS-Secondary Actor communication

With the anticipated widespread adoption of BPT and especially grid-following applications, EVs will essentially become generators, and aggregated together they become virtual power plants from the grid's perspective. In that case, the combination of EV and EVSE must follow the Requirements for Generators (RfG) network code just like other DER and therefore must be able to control their electrical power output and withstand grid faults [44].

At this point in time, there are several different views on how utilities and grid operators would interact with EVs as "Generators". It could be directly with the EV, directly with the EVSE, or via secondary actors such as smart meters, Energy Management Systems (EMS), or Grid Connection Point Controllers [44]. Since the EVSE is already assumed to be connected to a CSMS for billing, management, etc. purposes, the topology might very well involve the CSMS. When a collection of distributed EVSE is aggregated by a Charge Point Operator via a CSMS, the CPO/CSMS will act as an aggregator of the DER towards the utility [44]. This topology is proposed by the Open Charge Alliance in the white paper *OCPP & IEC 61850: a winning team*, using figure 2.11 as an illustration. As ISO 15118-20 and OCPP 2.1 have already been covered in the previous section, this section will focus on the last link towards the grid (Secondary Actor), assuming that the CSMS will act as an intermediary broker.

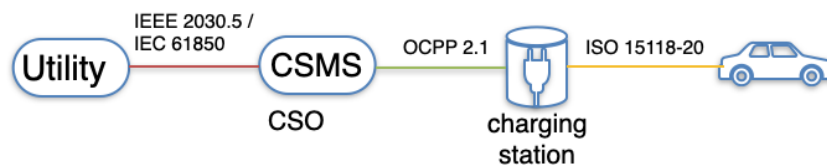


Figure 2.11: Illustration of the utility-CSMS-EVSE-EV interoperability ecosystem. Image source: [44].

2.5.1 IEC 61850

IEC 61850 is a standard for the automation of electrical substations, providing a framework for communication and interoperability among grid devices. Its application extends

to DERs, including EVs with bidirectional power transfer capabilities. Key aspects of IEC 61850 include interoperability, scalability, real-time monitoring and control, and standardized data models. IEC 61850 ensures that various grid components can communicate seamlessly, including EVs, EVSE, and utility control systems. This interoperability is vital for integrating EVs as active participants in the power grid [44].

The standard supports scalable deployment of DERs, accommodating the increasing number of EVs and other renewable energy sources. This scalability is essential for future-proofing grid infrastructure. Furthermore, IEC 61850 enables real-time monitoring and control of DERs, providing utilities with the ability to manage grid stability and respond to fluctuations in energy supply and demand effectively. The standard defines logical nodes and data models for various grid functions, ensuring consistent and accurate communication of operational parameters across the grid [44].

The Open Charge Alliance has released a whitepaper, *Ocpp & IEC 61850: a winning team*, describing how the IEC 61850 can be integrated into OCPP. It claims that the combination of ISO 15118-20 and IEC 61850 can significantly enhance the integration and management of EVs within the smart grid. The synergy between these standards offers several advantages, such as enhanced DER management, improved grid stability, optimized energy utilization, and future-proof infrastructure. By leveraging the bidirectional power transfer capabilities of ISO 15118-20 and the robust communication framework of IEC 61850, utilities can efficiently manage DERs. This includes dynamic control of charging and discharging processes to balance supply and demand in real-time [44]. The integration enables the grid to utilize EVs as mobile energy storage units, providing ancillary services such as frequency regulation and voltage control. This contributes to overall grid stability and resilience. Real-time data exchange facilitated by IEC 61850 allows for optimized energy dispatch from EVs to the grid. As the number of EVs increases, the combined use of ISO 15118-20 and IEC 61850 ensures that the grid infrastructure can adapt and scale accordingly [44]. The specific messages to be implemented, as suggested in the whitepaper, are also included in the OCPP version 2.1 draft described in section 2.4.3.

2.5.2 IEEE 2030.5

IEEE Standard for Smart Energy Profile Application Protocol, standardized as IEEE 2030.5-2018 by the Institute of Electrical and Electronics Engineers, is a communication standard designed to facilitate interaction between the smart grid and end-users [45]. The use cases include residential, commercial, and industrial consumers, and the standard leverages Internet of Things (IoT) concepts to provide a robust framework for managing energy usage, DERs, and grid stability [46]. IEEE 2030.5 is mostly used in North America, whereas IEC 61850 finds more use in Europe and Asia [43]. IEC 61850 mostly targets substation automation and large-scale grid management, while IEEE 2030.5 is more focused on enabling smart energy management and DER integration at the consumer level. However, both documents offer standardized data models and communication protocols beneficial for broader smart grid applications, and as such the OCPP 2.1 draft includes support for both [43].

3 Experimental Design

3.1 Overview of Watt&Well V2X EVSE

The Watt&Well V2X EVSE, hereafter referred to as the EVSE or the W&W EVSE, is an experimental vehicle-to-everything (V2X) Electric Vehicle Supply Equipment capable of charging and discharging electric vehicles. This EVSE formed the basis of the experimental part of this thesis. The EVSE is assembled by Watt&Well from Watt&Well manufactured main components, as well as some off-the-shelf support components. The EVSE is built in a 19-inch rack cabinet, seen from the front in figure 3.1. The main components of the EVSE are:

- 4 EVI and EVIX control boards
- 2 BMBPU R-2 bidirectional AC/DC power converters
- 2 DC side vehicle couplers - CHAdeMO and CCS2
- 9 DC side contactors
- 1 AC side Main plug, three-phase
- 1 AC side Auxillary plug, single-phase
- AC side protection and control elements for residual and overcurrent protection, interlock functionality, and power on/off switching.

3.1.0.1 AC side electrical equipment

The EVSE is connected to the mains grid via two plugs; a 63A, three-phase CEE plug for power import/export to/from the grid for the power converters, and a single-phase Schuko plug supplying auxiliary power for control, communication, and cooling systems. In addition to the mains plugs, the EVSE has various AC side protective and control devices in the form of circuit breakers, residual current devices, indicators, a contactor, a power switch, and an emergency stop. These devices are placed on the front and back sides of the EVSE. The single-phase auxiliary supply also feeds a low-voltage power supply providing 24 V DC to the control boards, DC side contactors, and the BMBPU control and cooling circuitry. In figure 3.8, a very generalized schematic of the AC and DC circuitry within the Watt&Well EVSE is found. In figure 3.1 below, the front panel is shown. In figure 3.9, some of the electrical components inside the EVSE are seen from the rear side.

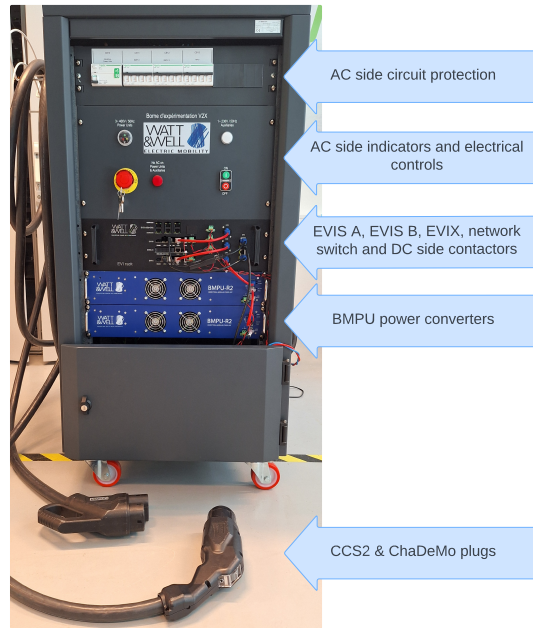


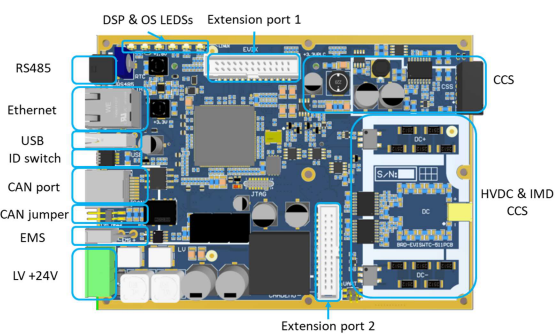
Figure 3.1: Front view of the Watt&Well V2X EVSE with components labeled.

3.1.0.2 Communication and control boards

The communication and control part of the Watt&Well EVSE is comprised of several printed circuit board assemblies (boards). The main board is the EVI (Electric Vehicle Interface), of which the SECC part is referred to in Watt&Well documentation as the EVIS. A photo of the EVI board is included in figure 3.2a. The board comes with multiple connectors and interfaces, which are labeled in figure 3.2b. In the lower right corner of the PCB sits the high voltage DC (HVDC) and insulation monitoring device (IMD) circuitry, which measures the DC side voltage and insulation resistance before and during charging. In the EVSE used for this thesis, two EVI boards are included; EVIS A and EVIS B, handling CCS and CHAdeMO charging respectively.



(a) Photo of the EVI printed circuit board assembly.



(b) EVI board rendering with connectors labeled. Image source: Watt&Well [47].

Figure 3.2: Watt&Well EVI board.

The EVI board handles multiple functionalities of the EVSE. The main processor is an ARM-based system-on-chip, running embedded Linux. On EVIS A, the Linux distro is *Debian GNU/Linux 10*, whereas the EVIS B, an older version of the board, runs *Raspbian*

GNU/Linux 10. For lower-level signaling and safety functions, an additional microcontroller-based chipset is included on the EVI board. This chipset runs its own firmware and is connected to the main processor via CANOpen. Finally, a Qualcomm QCA7000 series-based PLC module is included on the board for HPGP communication with CCS vehicles. These three devices are the main chips on the board, while the rest of the components are smaller integrated circuits and passive components.

In figure 3.3, a block diagram of the EVI is shown. The white rectangles show hardware components such as the three main chips; the embedded Linux system, chipset, and PLC module. Black arrows show hardware communication interfaces and their protocols, while grey rectangles show software-based components in the three main chips. The dashed lines in figure 3.3 illustrate the electrical isolation between the CCS and HVDC/IMD sections and the rest of the board.

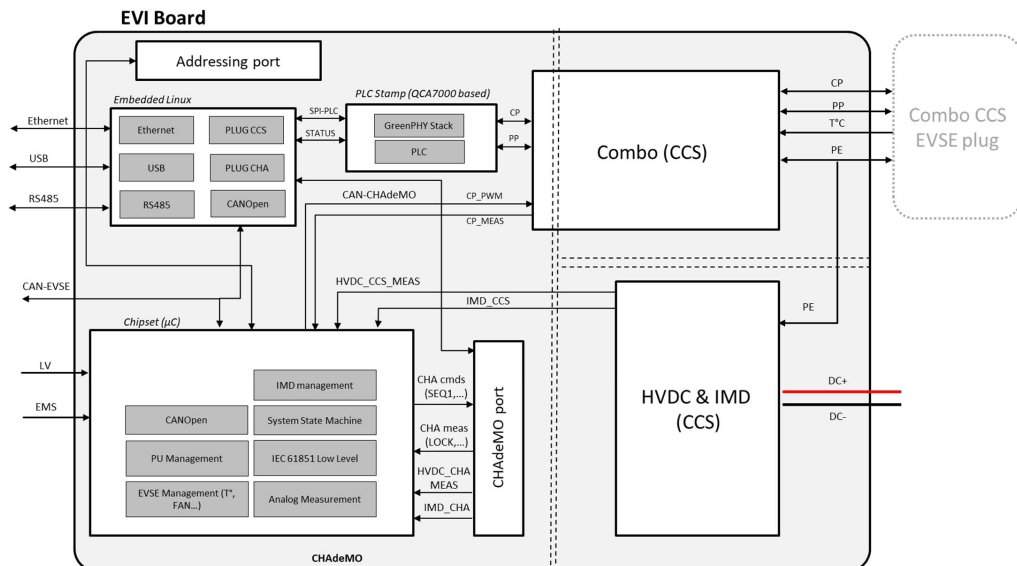


Figure 3.3: Block diagram of the EVI board. The dashed lines indicate isolation. Image source: Watt&Well [47].

The two white multi-pin board-to-board connectors marked as *Extension port 1* and *Extension port 2* on figure 3.2b are used to connect to extension boards. The configuration used for this thesis and illustrated in figure 3.1 includes two such extension boards; the *EVIX-IO* and *EVIX-AD6-CHA*. The former board adds multiple GPIO (General Purpose Input/Output), analog inputs, etc. to EVIS A, which in the Watt&Well EVSE configuration are used to control and monitor 9 DC contactors. For this exact purpose, the EVIX has 10 high current digital outputs (DSO Power), which can source up to 4 A at 24 V DC [47]. These outputs drive the coils of 9 contactors used to configure the two power modules in the EVSE electrically. In addition, the DSI inputs on the EVIX-IO are wired to the auxiliary terminals on the contactors, to monitor the correct operation of the contactors. The contactor configuration is included as appendix A.7. The manufacturer included 10 predefined contactor configurations for various charging scenarios, found in table 3.1.

Number	Configuration file name	Configuration
1	PARALLEL_CCS1	CCS2: Both BMPU in parallel
2	SERIES_CCS1	CCS2: Both BMPU in series
3	PU1_CCS1	CCS2: BMPU1 only
4	PU2_CCS1	CCS2: BMPU1 only
5	PARALLEL_CHA	CHAdEMO: Both BMPU in parallel
6	SERIES_CHA	CHAdEMO: Both BMPU in series
7	PU1_CHA	CHAdEMO: BMPU1 only
8	PU2_CHA	CHAdEMO: BMPU2 only
9	PU1_CCS1_PU2_CCS2-CHA	CCS2: BMPU2 and CHAdEMO: BMPU1
10	PU2_CCS1_PU1_CCS2-CHA	CCS2: BMPU1 and CHAdEMO: BMPU2

Table 3.1: Predefined contactor configurations settable via the EVI GUI and EVIX-IO board. These are provided by Watt&Well as JSON files.

3.1.0.3 Bidirectional Modular Power Units

The power converters employed in the EVSE are Watt&Well made BMPU-R2-500-32 units, where BMPU is short for Bidirectional Modular Power Unit. These units are 2U, 19-inch rack format power converters capable of up to 10.5 kW of charging power and -11 kW of discharging power. The converter can operate at up to 500 V DC and up to 30 A of charging current or -32 A of discharging current. All electrical characteristics of the converter can be found in the table from the datasheet [48] in appendix A.1. In the datasheet, the various limits are summarized into a Safe Operating Area figure provided in appendix A.4.

The BMPU can be operated in three different modes [48]:

1. **G2V/V2G – AC power control mode:** converter is operating as a current-controlled source where AC side active and reactive powers are controlled. DC side voltage is not controlled.
2. **G2V/V2G – DC voltage control mode:** converter is operating as a current-controlled source where DC side voltage is controlled. Active and reactive powers are not controlled.
3. **V2L mode:** converter is operating as a voltage-source inverter (VSI) where AC side voltage and frequency are controlled and set by the user.

In the first two modes, the converter operates as a grid-following/grid-tied inverter when injecting active power into the grid, which is the operating mode covered by this thesis. In the V2L mode, the converter is instead operating as a grid-forming inverter. Reading and changing the mode configuration was not possible, so the converter is assumed to have been operating in mode 2 (G2V/V2G – DC voltage control) for all experiments.

In the block diagram of the BMPU (shown in figure 3.4), there are several labeled elements, some also shown in the internal view in figure 3.5. Starting from the left side of the block diagram, there is an AC side EMI (Electromagnetic Interference) filter for Electro-Magnetic Compatibility (EMC) reasons. Next is the bidirectional Active Front End (AFE), which also acts as active Power Factor Correction (PFC). According to Watt&Well, the PFC stage uses a four-phase topology, allowing operation with both three-phase + neutral grid connection and single-phase connection [48]. Following this is a DC bus capacitance and a DC/DC converter with a transformer for full galvanic isolation between the AC and

DC sides. The DC/DC converter uses a full resonant topology with SiC (silicon carbide) active devices, according to Watt&Well [48], but more details on the exact topology are not provided. Resonant converters, such as the LLC topology¹, are common in e-mobility due to their bidirectionality and high efficiency, as covered in the author's previous work [49]. After the DC/DC stage, there is a DC side EMI filter, a DC fuse, and a fast discharge circuit that can reduce the remaining voltage on DC output capacitors to below 60 V DC within 1 second for safety reasons [48]. At the bottom of the block diagram, the control and protection section is found, along with the fan control for forced air cooling. Notably, this section has a 12/24V DC supply separated from the three-phase supply. There is also a bidirectional CAN connection. Like with the other Watt&Well components in the EVSE, the communication protocol used by the BMPU-R2 is CANopen. Within the control section, there is a state machine that controls the behavior of the BMPU-R2 based on state requests and the selected power mode. There is also a PFC control section that regulates AC side phase currents, reactive power, and DC bus voltage in G2V/V2G operating mode, as well as the AC voltage and frequency in V2L operation. Additionally, there is a DC/DC control section that regulates AC side active power, DC side current, and voltage. The controller manages AC and DC side pre-charge and operation relays and contains software protection against over/under-voltage, over/under current, over-temperature, and communication loss [48].

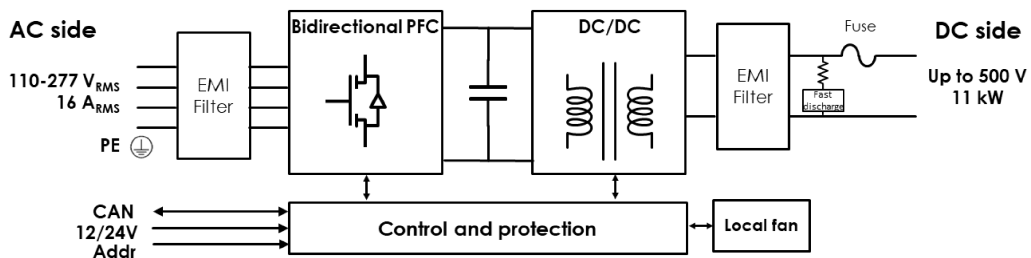


Figure 3.4: Block diagram of the BMBPU. Image source: Watt&Well [48].



Figure 3.5: BMBPU internals overview.

The regulation and measurement of the BMBPU-R2 are illustrated in figure 3.6. The left-side regulation section depicts the regulation structure with incoming CANopen mes-

¹Inductor-inductor-capacitor topology

sages. Messages shown in black are valid for all power modes, while messages shown in colors correspond to the operating mode indicated in the legend in the corner. Since the assumed operating mode for this thesis is *G2V/V2G – DC voltage control mode*, only the blue *DC voltage setpoint* is relevant. This voltage is set by CANopen messages within the control architecture shown in figure 3.14, but it was not directly configurable within the scope of this thesis. This level of control was also not particularly useful and could potentially cause battery damage if the DC voltage setpoints were incorrect. Instead, the parameter indirectly changeable by the control setup described in section 3.5 was the *Charging current limitation* and *Discharging current limitation*, shown in black on figure 3.6. In addition to the DC voltage setpoint, this current limit seems to be the main regulation parameter in the DC/DC stage of the converter. In the appendix, figure A.5 shows a block diagram illustrating how this DC side current limit is calculated internally from limitation curves, thermal derating factors, set limits, and the user input as shown in figure 3.6. This calculation also factors in AC side limits, as determined by the block diagram in appendix A.6, where the DC side voltage (battery voltage) is necessary to convert from DC power to DC current.

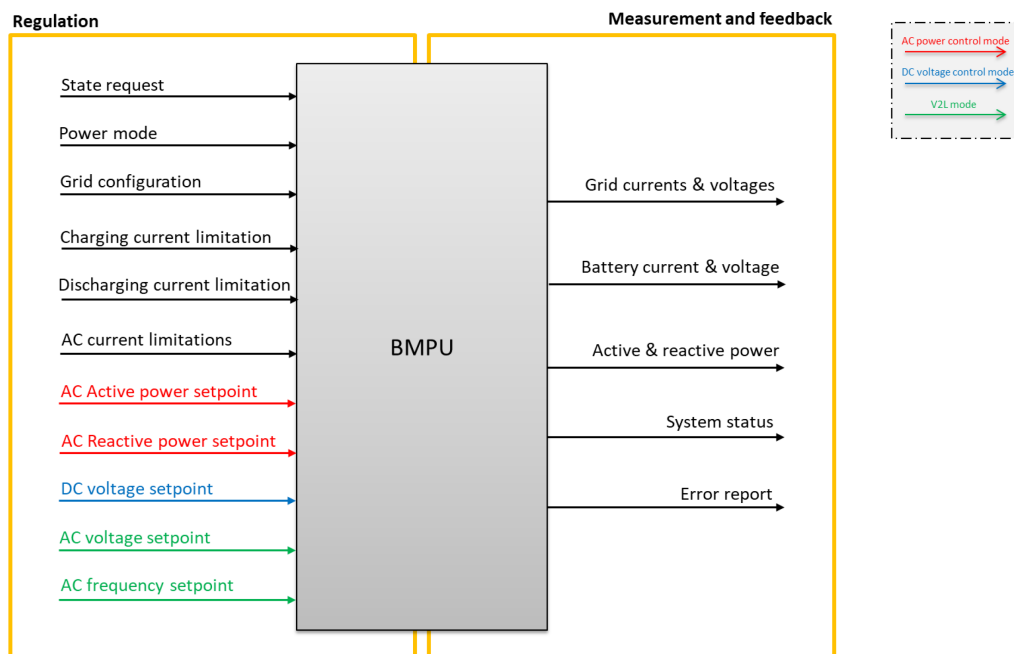


Figure 3.6: High-level regulation and measurements diagram of the BMPU-R2. Image source: Watt&Well [48].

In addition to the BMPU-R2-500-32 model, Watt&Well also offers a DC/DC version called BMPU-R2-DC. This version is intended for connecting EVSE to DC grids or energy storage systems [50]. Since this thesis primarily deals with AC-based grids, it is not particularly relevant, but an interesting offering. Watt&Well also offers the MPU range of unidirectional power converters for EVSE, which can only operate in grid-to-vehicle mode [51].

3.2 Network setup

The Watt&Well EVSE internally uses a wealth of communication protocols and physical layers, some of which are shown in figure 3.3. For external access and control, the main interface was the Ethernet-based network already set up in the EVSE from the manufac-

turer, comprised of the EVIS A board, EVIS B board and a switch mounted on the front panel shown in figure 3.1. The user manual [52] described how these two devices were set up in an IPv4 based subnet 192.168.200.XXX/24. On this network, EVIS A has a fixed address of 192.168.200.11 and EVIS B 192.168.200.12. The user manual suggested connecting to this network by setting your device NIC (Network Interface Controller) with a static address in the 192.168.200.XXX/24 subnet range, excluding 11 and 12. By configuring this and connecting the NIC ethernet port to the EVSE switch with a patch cable, it was possible to connect to the EVIS A and B at their respective addresses, as described in section 3.5.

It was quickly realized that while this simple setup worked, it had some drawbacks. Most importantly a lack of internet connectivity, which was necessary both for correct timestamps in the logs obtained from the EVI boards as well OCPP connectivity as described in section 3.5.2. First, an attempt was made to connect via the wired network in the lab using a router. While this did provide an internet connection, the high security of the network meant that at least HTTP traffic on port 80 and possibly also other traffic was blocked. To circumvent these restrictions, the group opted to use a Teltonika model RUT951 Industrial router with a built-in 4G cellular modem. The router's LAN port was configured to be part of the 192.168.200.XXX/24 subnet with a static address of 192.168.200.1 and connected to the EVSE switch. At the same time, the router was set up to allow internet connection via the 4G modem on this LAN network as well as an optional WLAN network with a DHCP server² set up for the 192.168.200.XXX/24 subnet. To maintain connectivity with EVIS A and B, their IPv4 addresses were given static leases in the DHCP server. To form an internet connection from the EVI boards, the command `sudo route add default gw 192.168.200.1 eth1` was run within the embedded Linux system command line interface. This sets the Teltonika router as the default gateway for the system.

When the measurement setup described in section 3.3 came to need a Raspberry Pi single board computer, this device was connected to the EVSE switch as well, and the device LAN interface `eth0` set up with address 192.168.200.123. This was added as another static lease within the Teltonika router. The resulting network is illustrated as a diagram in figure 3.7. In the diagram, the grey area indicates devices that are part of the Watt&Well EVSE.

²DHCP is short for Dynamic Host Configuration Protocol and is a common network management protocol used to dynamically assign devices' IP addresses. With DHCP, there is no need for manually configuring connections in the network [53].

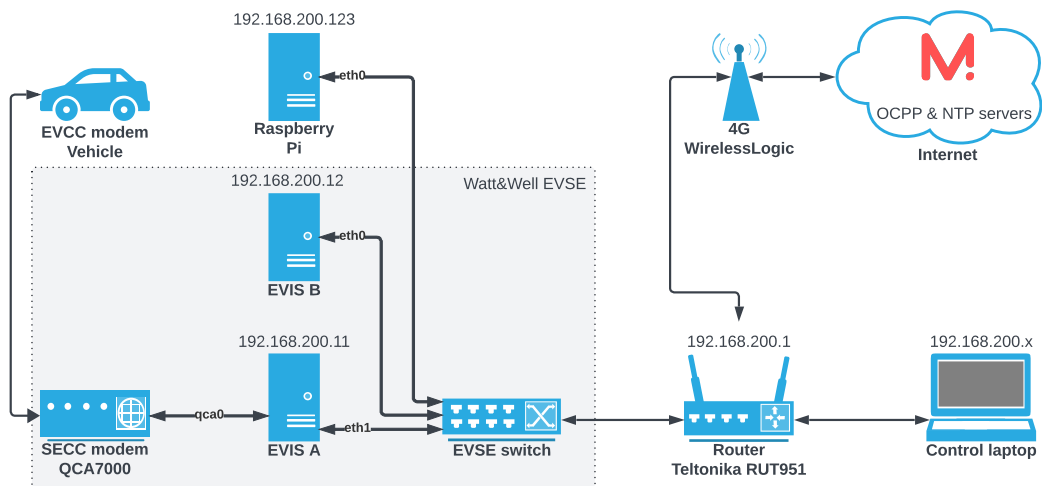


Figure 3.7: Diagram of the Internet Protocol-based networking setup used when carrying out experiments with the Watt&Well EVSE. Devices within the grey area are part of the EVSE itself.

The network setup in figure 3.7 provided all the control and access needed for the experiments carried out as part of this thesis. To carry out experiments, the user would connect their laptop to the router via either WLAN or LAN and be assigned an IPv4 address in the 192.168.200.XXX/24 subnet. The user would then be able to interact with the EVIS A and B as well as the Raspberry Pi, and these devices would be able to connect to internet-based servers using OCPP and NTP³ protocols for CSMS and timekeeping functionality respectively. For illustration purposes, the QCA7000-based HPGP modem used in the SECC part of EVSE, as well as the corresponding EVCC HPGP modem on the vehicle side is also included. While these devices were not directly interfaced with, they still communicate on Internet Protocol (IP) based networks, and the QCA7000 modem was found to be attached to the embedded Linux system of EVIS A as `qca0`.

3.3 Measurement setup

For data collection during experiments, a large part of this thesis's work was spent designing and implementing a measurement system. As described in section 3.1 and 3.5, the Watt&Well EVSE performs internal measurements and logging. However, this data was quickly found to be either inaccessible or hard to work with, so the focus early in the project shifted towards using external measurement equipment. Looking towards earlier research in the field, concurrent measurement of AC and DC side quantities were needed to obtain most metrics [1]. On the grid (AC) side, measurements should include voltages and currents for a normal 230/400 V three-phase grid, as well as derived quantities such as active and reactive power and power factor. On the vehicle (DC) side, it should be capable of measuring up to ± 65 A and 1000 V, the maximum quantities achievable with the two BMPU power converters in the EVSE. From this, DC power can easily be determined by simple multiplication. The measurements should also have a time granularity, accuracy, and precision sufficient for the test cases determined in section 3.6.

A key issue identified in previous works by the author such as "Smart from Start: Ex-

³Network Time Protocol

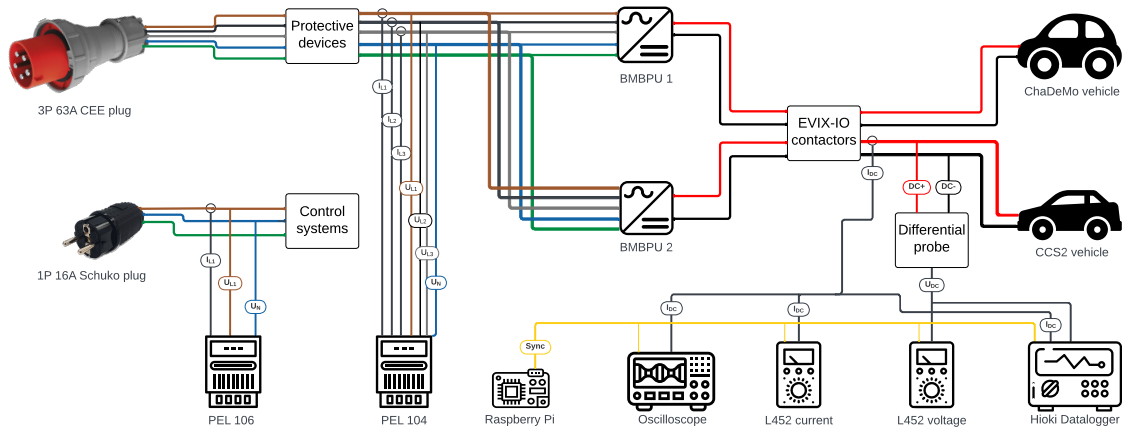


Figure 3.8: Diagram of the final measurement setup used when carrying out experiments. The system is configured for CCS charging in this view (zoom in for details).

perimental Validation of Dynamic Charging Limits via EVSE”[54] and “Development of Harmonized Electric Vehicle Smart Charging Tests”[49] was the synchronization of measurements. Since this project would involve both AC and DC side measurements, a way to synchronize these to ensure simultaneous measurement was needed. Unfortunately, no single piece of equipment with enough measurement channels and capabilities to measure both three-phase AC current and voltage as well as DC current and voltage was available. As an alternative, the Chauvin Arnoux PEL 10x series of power/energy loggers was taken into consideration, as multiple units were available. One of these devices could either perform three-phase AC measurements or DC measurements up to 1000V. However, even though the logger device itself was DC-capable, the included Chauvin Arnoux model MA193 was only capable of AC measurement. The probes used a Rogowski coil-type sensor, which only works with AC. To make matters worse, the PEL 10x series power/energy loggers used a proprietary current sensor connector, making substitution of the MA193 sensors difficult.

To stay within the Chauvin Arnoux ecosystem, an alternative DC measurement method was investigated, using Chauvin Arnoux L452 dataloggers. These devices use a simple modular connector, so they can easily be connected to the available current probes. Nevertheless, these devices had another shortfall, as the input was only rated for $\pm 10V$. A differential voltage probe was identified as a solution to get around that limit. To connect the differential probe safely, some modifications of the Watt&Well EVSE were necessary. The DC positive and negative leads going to both the CHAdeMO and CCS2 connector were split to form a Y-connection after the EVIX-IO contactor array. Appropriately sized wire attached to this point was connected to a fuse rated for the high DC voltage that can be present on these wires, and downstream from the fuse 4mm banana plugs were connected. The fuses ensure that in the event of a short circuit in the measurement system downstream from the fuses, the short circuit current will not exceed the capabilities of the small cross-section measurement wires. In figure 3.9, these added fuse holders and banana plug terminals are marked with an orange highlight (DC voltage). To perform the measurement, a differential probe Hioki model P9000-01 was connected to the banana

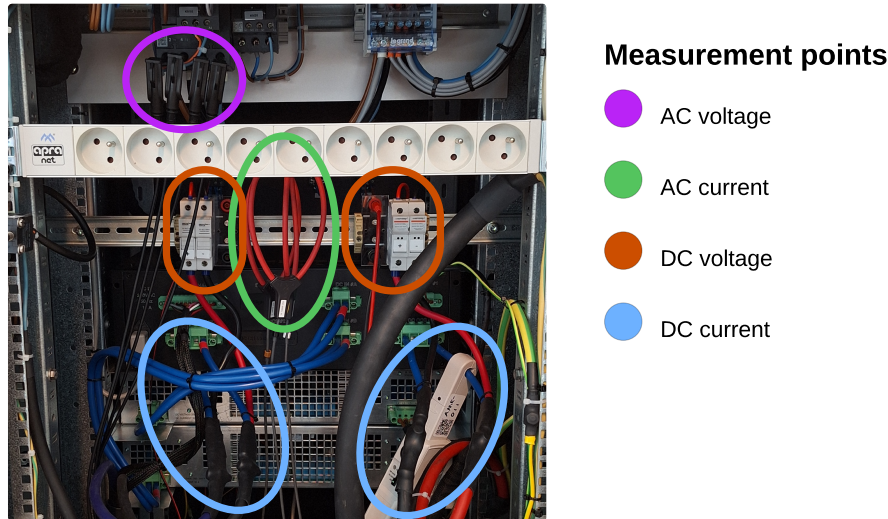


Figure 3.9: Rear, internal view of the Watt&Well EVSE showing various measurement points and probes.

In figure 3.9 the DC side current measurement point is also shown, marked with a light blue circle. Here, a current probe Keysight model 1146B is clamped around the DC positive wire going to the CCS2 or CHAdeMO connector. This probe can measure from DC up to 100 kHz AC at up to 70 A RMS using a Hall effect-based sensor [55], making it ideal for this application. Also shown in the figure is the AC voltage measurement point in purple, where magnetic probes are attached to the screw holes of the main contactor. Finally, the figure also shows the AC-current measurement point in green, where three Rogowski coils are placed around L1, L2, and L3.

With all these measurement points selected and wired in, testing of the system was started. A Chauvin Arnoux PEL104 was connected for AC side measurements and the Chauvin Arnoux L452 datalogger for DC side measurements. Multiple attempts were made to find a way to sync and start both measurements at once, but the measurement management software *PEL Transfer* and *Data Logger Transfer* did not allow this. Instead, each device had to be set into *recording mode* separately. With both AC and DC side equipment logging data, a test sequence with sudden, large changes in active power was started. The goal was to see if the AC and DC side measurements were in sync and could remain synchronized over a duration of time. It was found that the offset between AC and DC measurements was a fixed quantity of less than 1 second and remained the same throughout 45 minutes. To confirm that the delay between AC and DC measurements was not contributed by the B MPU power converter, another test was run with the PEL104 in DC mode, measuring the same DC side voltage as the L452 data logger. This again showed a consistent, less than 1-second shift between the two measurements. With this result, it was decided that the system was good enough for efficiency measurements.

As described in section 3.1, the Watt&Well EVSE has two mains connections, one three-phase connection for the B MPU power converters, and one single-phase supply for all the control systems. The control circuitry and forced air cooling within the B MPU is also supplied from the single-phase supply. That means that the efficiency heatmap for the B MPU provided in the datasheet and included in appendix as A.3 is purely characterizing the power converter, not the losses in the control system and cooling. This separation allows the characterization of both the pure power converter efficiency, but also the overall

system efficiency of the EVSE, including control, communication and cooling consumption. To capture this data, an additional Chauvin Arnoux model PEL106 power and energy logger was placed in line with the single-phase supply. In figure 3.8, both of these PEL10x devices are shown on the left side.

With the AC side measurements taken care of and initial testing showing decent performance, the focus shifted towards the DC side. When a method to set the DC side current or power setpoint via a script was finally found, as described in section 3.5, measurement of activation and ramp time was possible. Using a technique developed in the project “Smart from Start: Experimental Validation of Dynamic Charging Limits via EVSE” [54], a script controlling the charging process via API can change the state of a digital I/O pin on a development board such as an Arduino [54] or Raspberry Pi. For this project, a Raspberry Pi was chosen, since this has support for both Python and GPIO⁴ directly accessible via Python [56]. By setting one of the digital pins on the Raspberry Pi board high when an API call was made to change the current/power setpoint, this signal could be used to measure the activation time. In figure 3.10, an example of such a measurement is included. Here, the yellow trace is the sync timing signal from the Raspberry Pi and the green trace is a DC current measurement. Using the built-in cursor functionality of the oscilloscope, the time elapsed between sending the command to reduce current, and the DC current starting to change is measured as 1.2 seconds (ΔX).

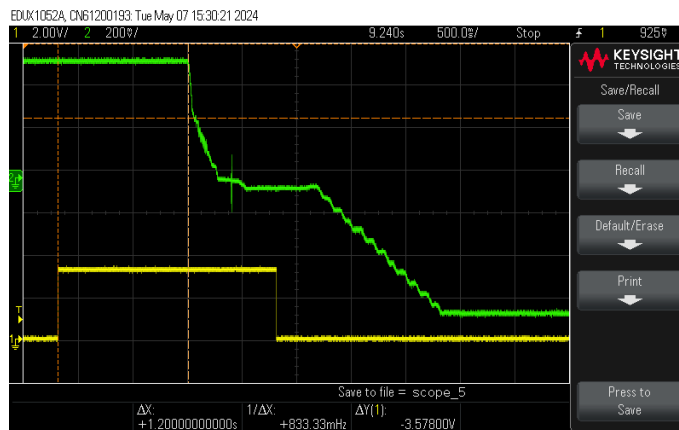


Figure 3.10: Oscilloscope screenshot showing an example of an activation time measurement. The yellow trace is the sync signal and the green trace is a DC current measurement.

Two additional issues surfaced with the L542 data loggers while working with the DC side measurement; the measurement range and dropped measurements. For the first point, the dataloggers could either be configured for a $\pm 10V$ or $\pm 1V$ input range, which applies to both inputs. This meant that it was not possible to use the full measurement range of both the current probe and differential voltage probe at the same time. To solve this issue, an additional L452 datalogger was added, with one handling current and the other handling voltage. This also freed up a channel on each logger, which was then connected to the Raspberry Pi-generated sync signal. This configuration is illustrated on the measurement setup diagram in figure 3.8. The other issue with dropped measurement was however still present. The issue materialized as the logged value for both current and voltage suddenly dropped far below the expected range. To investigate whether this was caused by the data

⁴General Purpose Input/Output

loggers, the measurement probes, or maybe noise coupled into the system, a different datalogger was placed in parallel with the two L452. This was a Hioki model LR8431-20 with 10 channels, capable of logging all channels simultaneously at 1 ms intervals. This solved the problem, indicating that the issue did indeed lie with the L452 data loggers. In addition, the Hioki output data was deemed to be and remain in sync over time with the AC side. To avoid the dropped measurements affecting future work, it was decided to keep the Hioki datalogger in the system.

The final measurement setup was thus found and is illustrated in figure 3.8. In this figure, standard European wire colors for the AC side three/single-phase supply are used, and red/black for the DC side positive and negative. Current measurement probes are shown as a circle around the wire and direct voltage measurement as a branch.

3.3.0.1 Table of measurement equipment

Brand	Model	Measurement	Applicable uncertainty
Chauvin Arnux	PEL 104/106	AC voltage	$\pm 0.2\% R \pm 0.2 V$
		AC current (MA193)	$\pm 0.2\% R \pm 0.02\% I_{nom}$
		Active power	$\pm 0.5\% R \pm 0.005\% P_{nom}$
		Reactive power	$\pm 1\% R \pm 0.01\% Q_{nom}$
		Power factor	± 0.05
Chauvin Arnux	L452	Voltage $\pm 1V$	$1 mV \pm (0.5\% + 1 cts)$
Hioki	LR8431-20	Voltage 1V	$\pm 0.1\%$
Hioki	P9000-01	Voltage 1:1000	$\pm 0.5\%$
Keysight	1146B	Current 10 mV/A	4%

Table 3.2: Table of all measurement equipment in use, the selected measurement and range and the applicable uncertainty for that range.

3.4 Vehicle emulation and sniffing

Before the Watt&Well EVSE became available, it was already clear that getting access to a vehicle with support for ISO 15118-20 and especially DC BPT would be a challenge. In anticipation of this, some market research on alternatives was done. In general, test equipment manufacturers offer four different solutions:

- **EV emulation** where the EVCC and associated systems are emulated. These can be communication-only or also include battery emulation to support charging and discharging.
- **EVSE emulation** where the SECC and associated systems are emulated. These can be communication-only or also include power converters to emulate an AC grid or DC charger.
- **Man-in-the-Middle (MitM)** testing, where the communication and power flow between EV and EVSE are intercepted and measured by placing the device in the middle.
- **Sniffing** where the communication is "sniffed" through non-invasive means.

EV emulation was deemed the most interesting option of these four, as it would likely allow this project to achieve BPT via CCS2 without a compatible vehicle. However, sniffing

equipment was also investigated as a possibly useful tool for this project. In previous projects by the author, Control Pilot-based EV-EVSE communication used for AC charging has been intercepted and decoded using an oscilloscope [54] or custom software running on a microcontroller [49]. However, such methods were no longer feasible due to the complexity of the HPGP communication and Efficient XML⁵ Interchange (EXI)-encoded messages used in the ISO 15118 domain. Instead, sniffing might be the only option to capture and decode the exchange of messages between EV and EVSE, especially in the case that the Watt&Well EVSE did not provide such communication logs. That was a very real concern, as the authors' experience with other DC charging systems was a complete lack of low-level logging of the EXI-encoded data stream sent via the HPGP interface. If this also proved the case with the Watt&Well EVSE, it would be hard to gain hands-on experience with the ISO 15118 communication standard and HPGP, as well as pinpoint exactly why an attempt at BPT might fail.

As such, both EV emulators and sniffing tools were researched, and the findings were compiled into table 3.3. In the appendix A.2, an extended version of this table can also be found. In the table, the brand and model names of the different offerings on the market are indicated. In the protocols column, *All* represents support for DIN SPEC 70121, ISO 15118-2, and ISO 15118-20. Some systems, such as numbers 5 and 7, also support additional protocols and connector types such as GB/T and CHAdeMO [57, 58], which are not listed. The features column highlights the specific capabilities of a system, characterized as above. The extended table A.2 also lists model numbers of both hardware and software products, if the equipment supports powered testing, and whether it claims to decrypt TLS.

Fortunately, the project did not end up in need of a sniffer tool, as the Watt&Well EVSE provided logs of all EV-EVSE communication. There were however still, as anticipated, major difficulties with finding a suitable vehicle with CCS2, ISO15118-20, and BPT support, which is outlined by the vehicle compatibility results in section 4.1. To attempt to perform an ISO 15118-20 BPT session, a visit to the ElaadNL Testlab in Arnhem, Netherlands was arranged. In this lab, no less than system numbers 1, 3, and 5 from the table 3.3 was available for testing, and results from this are included in section 4.1.

The main system at ElaadNL Testlab is the number 5, Keysight Charging Discovery System (CDS). In figure 3.11a, the rack depicted is the CDS high-power version configured for MitM testing. On the top left a CCS2 inlet is found, used for EV emulation and MitM testing. On the right of this, a DC outlet is found, used for EVSE emulation and connecting to the EV in case of MitM testing. The middle section is an AC inlet and outlet, used for AC EV and EVSE emulation as well as MitM testing. Finally, the lower part shows the DC positive and negative connections for DC emulator hookup for both EV and EVSE emulation, here connected for EV emulation. On the very top of the CDS rack depicted in figure 3.11a sits a small black box. This is the number 2 Keysight Charging Communication Interface Tester, also colloquially called the "Verisco box" after the manufacturer Verisco, who is now acquired by Keysight. The Verisco box is fully integrated with the Keysight CDS and can act as EVCC or SECC, controlling the charging process via the CDS. For the tests performed with the Verisco box, the physical CCS2 plug of the Watt&Well EVSE was therefore plugged into the CDS.

⁵Extensible Markup Language

No.	Brand	Name	Protocols	Features
1	Trialog	ComboCS4M [59]	All	EV emulation
2	Trialog	Sniffer [59]	All	Sniffing
3	Keysight	Charging Communication Interface Tester [60]	All	EV emulation EVSE emulation
4	Keysight	CCS Charging Protocol Tracer [61]	All	Sniffing
5	Keysight	Charging Discovery System [57]	All	EV emulation EVSE emulation MitM
6	Comemso	EVCA Flex [58]	All	EV emulation EVSE emulation MitM
7	Comemso	EVCA Multi Mobile [58]	All	EV emulation EVSE emulation MitM
8	Comemso	EVCA ComOnly [62]	All	EV emulation EVSE emulation Sniffing
9	IoTecha	PilotShark [63]	All	Sniffing
10	VertexCom	GreenPHY Sniffer [64]	No ISO-20	Sniffing
11	Applus	CCS V2G Decoder [65]	No ISO-20	Sniffing

Table 3.3: Overview of EV and EVSE emulation and High Level Communication sniffing products. In this table, *All* in the protocols column refers to support for DIN SPEC 70121, ISO 15118-2, and ISO 15118-20. An extended version of this table is found in appendix A.2.



(a) Keysight "Verisco box" (top) and Charging Discovery System.



(b) Keysight SL1830A regenerative DC emulator.

Figure 3.11: Keysight Charging Discovery System installation at ElaadNL.

In figure 3.11b, the regenerative DC emulator for the ELaadNL system is depicted. This grid-connected, bidirectional DC power supply consisting of two Keysight model SL1830A can sink and source up to 360 kW to/from the AC grid to emulate battery charging and discharging at high power. In figure 3.12 and figure 4.2, screenshots of the software used for the Verisco box are included. For the depicted test in this screenshot, the Watt&Well EVSE was connected to the CDS rack via CCS2. The Verisco box was acting as the EVCC, controlled via the shown software, and the DC emulator was sourcing 22 kW from the grid, emulating a battery being discharged.

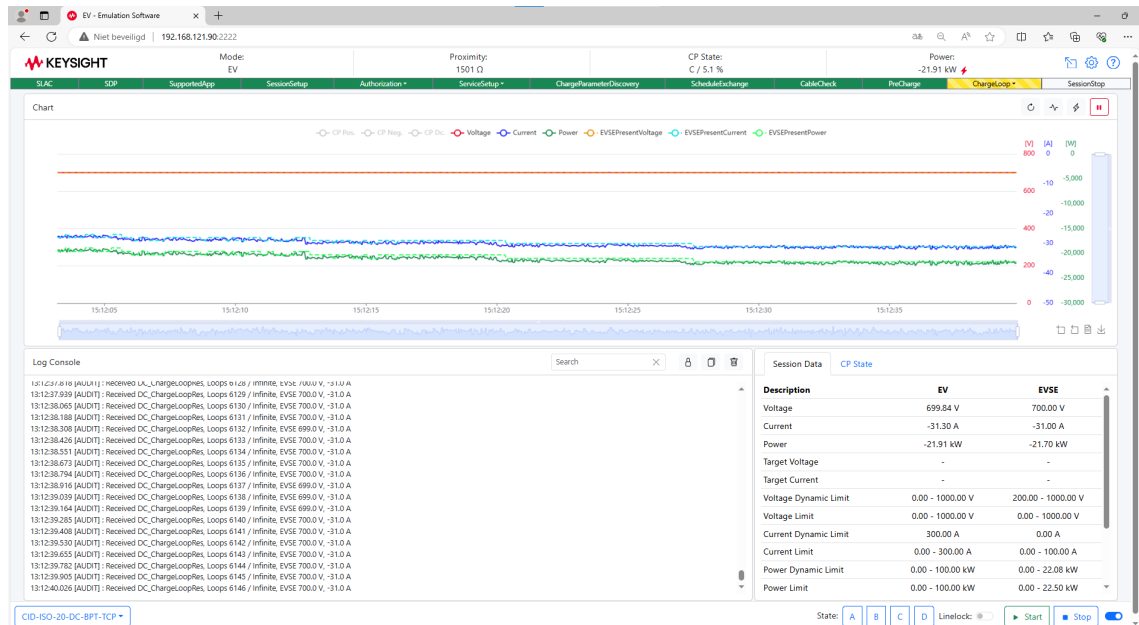


Figure 3.12: Screenshot from the Keysight Charging Communication Interface Tester "Verisco box" software, while performing an ISO 15118-20 BPT session and discharging at -22 kW sourced from the grid via the DC emulator shown in figure 3.11b.

3.5 Control setup

The Watt&Well EVSE offers multiple control and configuration methods. This section covers those applied for this project, with a special emphasis on achieving four goals:

1. The ability to start and stop power transfer sessions.
2. The ability to change configurations of the EVSE.
3. The ability to obtain logs and/or live data showing messages exchanged via High Level Communication with CCS2 vehicles.
4. The ability to dynamically update electrical setpoints, to run various semi-automated and timing-critical experiments.

Watt&Well provided various documentation for interfacing with the EVSE. The most user-friendly interface is the EVI GUI⁶, which runs on a web server within the EVI board [66]. Both EVIS A and EVIS B offer this GUI and are served on port 8333 via HTTP and Web-Socket protocols. To connect to the GUI, a browser (client) located within the subnet as described in section 3.2 was simply pointed to <http://192.168.200.xx:8333>, where xx is either 11 for EVIS A or 12 for EVIS B. This would serve the user with a login page where

⁶Graphical User Interface

Watt&Well-provided credentials must be entered. Watt&Well provided two sets of credentials, basic and expert. The expert credentials will unlock extra functionality that could be dangerous if used incorrectly. In figure 3.13, a screenshot of the GUI in expert mode is included.

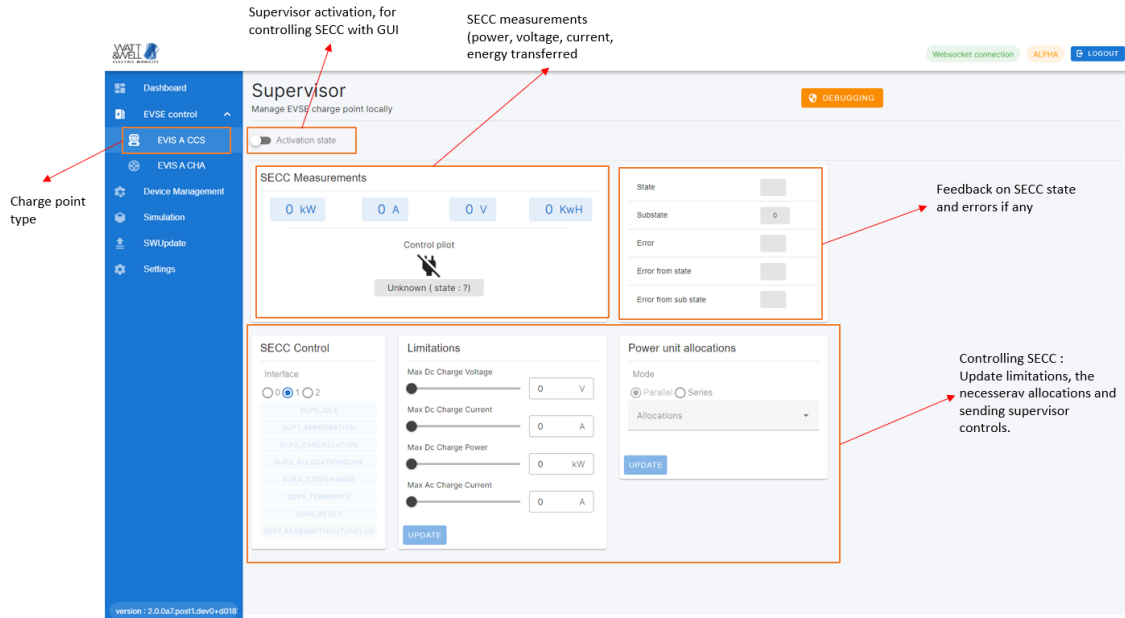


Figure 3.13: Screenshot of the EVI GUI showing the EVSE control view with different sections annotated. Image source: Watt&Well [66]

On the left side in figure 3.13 is the blue-colored menu to switch between different views. These are:

- **Dashboard** showing an overview of charging sessions.
- **EVSE control** where it is possible to allocate power modules, set limitations and control the SECC to start and stop the charging process.
- **EVIX IO** (not shown) where it is possible to control and monitor the EVIX input/outputs described in section 3.1. This was used to apply the contactor configurations described in table 3.1.
- **Device management** where it is possible to see and configure the different devices on the CANopen bus within the EVSE.
- **Simulation** which was unfinished and not used for this project.
- **SWUpdate** where software updates for the EVI board could be carried out.
- **Settings** which was unfinished and not used for this project.

In order to start a charging EVSE session via the GUI, the following steps were taken:

1. **Contactor configuration** was set within the EVIX IO view on EVIS A.
2. **EVIS** was selected, EVIS A for CCS2 or EVIS B for CHAdeMO.

3. **EVSE control** view was selected, either EVIS A or B and the *Supervisor* set active.
4. **BMPUs allocated** in the *Power unit allocations* section according to the contactor configuration set in step 1.
5. **Interface option** in section *SECC Control* was set; 1 for Forward Power Transfer and 2 for Bidirectional Power Transfer.
6. In the case of BPT, the mode selection was set to *Discharge compatible, Dynamic*, and either *Charge* or *Discharge*.
7. **Limitations section** was filled in with the maximum values intended during the session.
8. **SUP buttons** in the *SECC Control* section were operated to control the state machine and start the session as described in the EVSE manual [52] and technical reference manual [67].
9. **Update limitations** During the session, the limitations/setpoints could be manually changed in section *Limitations* and reapplied by setting state SUP3_ALLOCATIONDONE. The same method could also be used to switch between charging and discharging modes.
10. **Stop** To stop a session, the state machine was again operated according to the documentation.

In addition to the GUI, the EVIS A and B also include a CLI⁷, as described in the EVI getting started manual [68]. This interface is accessed via SSH⁸ on port 22. The interface has several utilities (commands) used for this project:

- **WDM** Watt Device Manager which is used to interact with devices on the CANopen bus. A scan of the bus is initiated by the command `wdm scan`.
- **PM logs** to show logs of the ongoing charging process via the Linux tool `journalctl`. Typically initiated by command `sudo journalctl -u evis-ccs-pm -f` for the CCS plug module, with some additional, optional arguments possible.
- **Nano** a text editor used to edit text files directly in the CLI. Typically initiated by command `sudo nano <filename>`.
- **Systemctl** used to start, stop, or restart specific services or the whole embedded system. Typically used to restart services after changes were made via the command `systemctl restart <service name>`.
- **Supcli** used to interact with *supervisors* and start a new supervisor with specific configurations via command `supcli ./path/to/config.ini`.
- **Route** used to change network configurations, as described in section 3.2 on networking.
- **Python** for executing scripts written in Python within the embedded Linux environment, the command `python3 <filename>` was used.

One of the main uses of the CLI command `nano` was to change settings in the file `evis-ccs-pm.ini`, which is the initialization file used by the CCS plug module. This file contained settings that were not exposed elsewhere and became quite important to the project, as described

⁷Command Line Interface

⁸Secure Shell

in section 4.1. The CLI also featured SFTP⁹ for transfer of files in and out of the embedded Linux environments file system.

With a combination of the EVI GUI, PM logs, and some settings like this only available via the CLI, the first three goals outlined at the beginning of this section were achieved; starting and stopping sessions, changing configurations, and obtaining logs. However, the final goal of dynamically updating electrical setpoints was not achieved. To achieve that, the way the Watt&Well EVSE handles charging sessions needs to be understood.

3.5.0.1 Control architecture

The control architecture of the EVI board is derived from the block diagram in figure 3.3. Within the CLI, the command `wdm scan` can be used to show all nodes on the CANopen network. The output for the Watt&Well EVSE is the following table:

```
Detected a total of 9 valid node(s)
```

Node ID	Device name	Hardware revision	Serial number	Software version
0x10(16)	Watt & Well EVIS ChipSet	EVIS_5X1	401449	5.1.3r
0x11(17)	PM CCS EVIS A	-	0	--version error
0x20(32)	Watt & Well EVIS ChipSet	EVIS_401	1018	5.1.3r
0x21(33)	PM CCS EVIS B	-	0	unavailable
0x23(35)	PM CHA EVIS B	-	0	unavailable
0x3e(62)	BMPU DC/DC	AA	4294967295	2.5.9r
0x3f(63)	BMPU DC/DC	AA	4294967295	2.5.9r
0x5e(94)	BMPU	AA	325	2.5.9r
0x5f(95)	BMPU	AA	234	2.5.9r

Listed in this table are the DC/DC section of the two BMPUs (ID 62 and 63) and their Active Front End/Power Factor Correction stages (ID 94 and 95). Also listed are the two chipsets on EVIS A (ID 16) and EVIS B (ID 32), these are the EVI microcontrollers responsible for power unit management and IO interactions with the vehicle. Their internal state machine is representative of the charging process state [68]. In addition, three other nodes are found on the bus; PM CCS EVIS A, PM CCS EVIS B, and PM CHA EVIS B. They are the *plug modules* of EVIS, a piece of software running within the embedded Linux environment responsible for communication with the EV and the CAN communication with the Chipset. They exist in either CHAdeMO (CHA) or CCS variants [68]. When the CLI command `sudo journalctl -u evis-ccs-pm -f` is used to obtain logs from a CCS session, the log output is thus coming from the plug module.

The plug module is not directly controlled by user input, instead another piece of software running within the embedded Linux environment called the *supervisor* is used. This software handles user input and interacts with the plug module via the CANopen bus. This control architecture is simplified in figure 3.14:

⁹SSH File Transfer Protocol

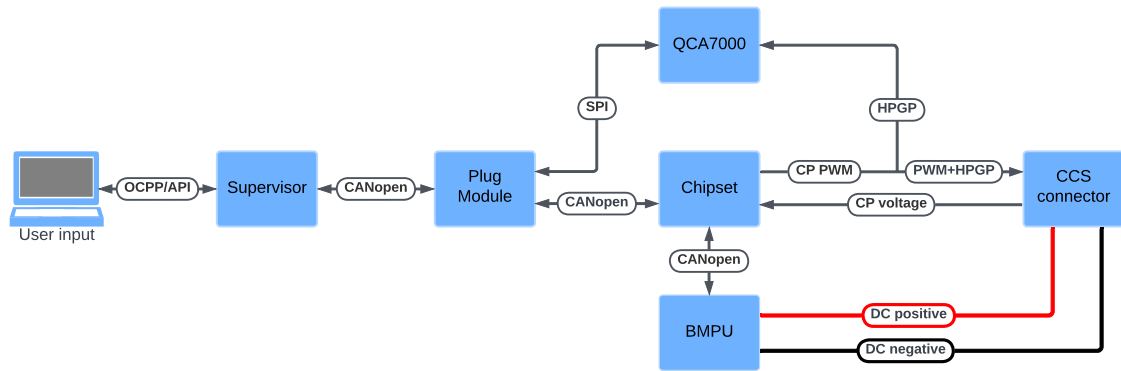


Figure 3.14: Simplified control architecture for CCS charging with the Watt&Well EVSE.

Breaking down the control architecture in figure 3.14, user input would be delivered to the supervisor via different protocols such as OCPP or HTTP, depending on which supervisor was in use. These inputs would then be translated into CAN messages and sent to the plug module via CANopen. The plug module interacts with the vehicle via two communication channels - High Level Communication is done via the QCA7000 HPGP modem, which itself is connected to the EVI board with SPI¹⁰. In the QCA7000, HPGP applied to the control pilot wire is modulated and demodulated into "normal" IP packets. The control pilot communication itself is handled by the chipset, which generates the ± 12 V square wave with 5% duty cycle. At the same time, the chipset measures the control pilot voltage with reference to earth, to determine the state of the EV. This information is available to the plug module on the CANopen bus. In addition to low-level communication with the EV, the chipset also handles control of the BMPUs via CANopen and runs the state machine responsible for the safety of the charging process. The control architecture is presumably constructed this way to avoid a crash of the embedded Linux system affecting the safety of the charging process. As an additional note, somewhere within this architecture, presumably as part of the plug module, sits the CCS stack. Watt&Well did not build the software to perform CCS charging themselves, instead using the YaCCS stack from Trialog. The YaCCS stack provides a robust and reliable communication stack to perform ISO 15118 or DIN 70121 charges with a compatible vehicle over PLC [69].

Due to the complexity of the CANopen signaling used between the plug module, chipset, and BMPUs, as well as the safety implications of bypassing these systems, it was chosen to only interact with them through a supervisor. The following sections will go through the three different supervisors available, with a special emphasis on how they might be used to apply power setpoints in an automated way.

3.5.1 Python supervisor

Well into the project period, Watt&Well provided an example of a Python script that, when run within the embedded Linux system of the EVI, should work as a basic supervisor. The original code provided is included as appendix A.4.1.1. When this script was run, it did not work. Through multiple days of debugging, it was found that there were some issues with the libraries imported from `watt_node_v2.node.supervisor` on lines 3-9. When this was corrected, the script would instead fail to connect to the CAN interface `kvaser` selected on line 21. This prompted more debugging with no results. With the help of Watt&Well, it was determined that `kvaser` was the wrong interface, and it should be `socketcan` instead.

¹⁰Serial Peripheral Interface

With this change, the script worked and a charge with predefined limits and direction could be launched.

CHAdeMO was selected as the standard for initial development, as no BPT-capable CCS2 vehicles were available. Through a lot of trial and error and reverse engineering of the `watt_node_v2.node.supervisor` libraries, a script was developed that could start a CHAdeMO session in either charging or discharging mode, with predefined limits. However, the hope was to achieve goal number 4, dynamically setting electrical setpoints via a script such as the Python supervisor. Development of a supervisor script to do this was started, and this work is included in appendix A.4.1.2. The overall goal of this script was to demonstrate the ability to:

1. Set the limitations as 5000 W charging power and 7000 W discharging power.
2. Enable the V2G interface and set the SECC as discharge compatible in dynamic and charging modes.
3. Allocate both BMPUs to the session.
4. Start the charge.
5. Update the limitations to charging power 2000 W.
6. Update the settings to discharging mode
7. Call the request code SUP3 to apply the changes to the session.

While the script A.4.1.2 was able to select the CHAdeMO interface, set the limits, BMPU allocations and start a charge, neither updating the charging power nor switching to discharge mode worked. Ultimately, the development of the Python supervisor was stopped in favor of the method described in section 3.5.3. A working supervisor for CCS was also never achieved.

3.5.2 OCPP supervisor

The EVI board from Watt&Well supports OCPP, and since OCPP was established as the main protocol used to interact with EVSE in section 2.4, this OCPP functionality was investigated. The OCPP implementation is described in the document *EVIS - OCPP documentation*[70] and uses two mandatory services and some optional. The two mandatory services are the *QOCPP* controller, which forms the WebSocket connection to the CSMS, and the OCPP supervisor, which handles authorization EV, allocates power units, and updates power limitations [70]. The two services are connected via ZeroMQ, a universal messaging library.

The OCPP functionality of the EVI was tested against Monta OCPP Toolkit, a free-to-use sandboxed OCPP 1.6J implementation available on <https://ocpp-toolkit.monta.app/>. In the QOCPP configuration file `ocpp-controller.json`, the WebSocket URL and OCPP version were set as follows:

```
"ocpp": {
  "csId": "DTU-WW-V2G-01",
  "evseId": "1",
  "url": "ws://ocpp-toolkit-api.monta.app/",
  "version": "1.6"
}
```

With configured and the OCPP controller service restarted, a WebSocket connection to the Monta OCPP Toolkit was observed. Next, a `.ini` initialization file for the supervisor was

prepared according to the documentation [70] to achieve full functionality. An example of CCS charging with two BMPUs at 22 kW is in appendix A.4.2.1. To start the supervisor, the CLI command `supcli ./path/to/config.ini` was used. Following this operation, the Watt&Well EVSE would start behaving as a "normal" EVSE connected via OCPP, requiring authorization before charging sessions could start, etc.

Following the execution of `supcli`, the CLI can be used to control and monitor the OCPP-connected session. The following commands in format `evseId,command,data` can be issued within the CLI:

- **reset** This will reset any error on the specified charge point and must be frequently used to clear all the errors.
- **authorize,tag** This will authorize a charge with the supplied tag using `Authorize.req`. This is used to emulate scanning an RFID since the Watt&Well EVSE has no RFID reader.
- **stop** This will stop an ongoing charge and send a `StopTransaction.req`.

While the above method was found to work with CCS, a working OCPP supervisor for CHAdeMO was not achieved. Additionally, it was quickly realized that the configuration key `SupportedFeatureProfiles` only listed `Core,LocalAuthListManagement,RemoteTrigger`, not `SmartCharging`, which identifies support for OCPP 1.6J Smart Charging functionality. The EVSE would also ignore any `SetChargingProfile.req` messages.

Further results from OCPP compatibility testing are provided in section 4.4.2. However, the main takeaway for this section was that the OCPP supervisor did not provide support for dynamically setting electrical setpoints, and could thus not be used for goal 4, as listed in the beginning of this section. Because of this, OCPP supervisor work was halted in favor of the method described in section 3.5.3.

3.5.3 EVI GUI supervisor

The EVI GUI previously described acts as a supervisor as well. When the activation state slider, shown in figure 3.13, was enabled client-side, a supervisor would start on the server side, inside the EVI embedded Linux environment. The controls shown in figure 3.15 would then be used to configure this supervisor with BMPU allocations (right side), electrical limitations (middle), and finally SECC commands (left). The allocation and limit settings would be sent from the client to the server when the `UPDATE` button is pressed. In the case of SECC control, the request and associated settings above will be sent once one of the `SUP` request buttons is pressed. In the view shown in figure 3.15, both BMPUs are allocated for parallel operation and the electrical limitations are set to allow maximum charging and discharging power limited only by `ChargeParameterDiscovery` and `ChargeLoop` constraints and BMPU physical limits. Additionally, the SECC control view is configured for BPT and the session will start in discharge mode.

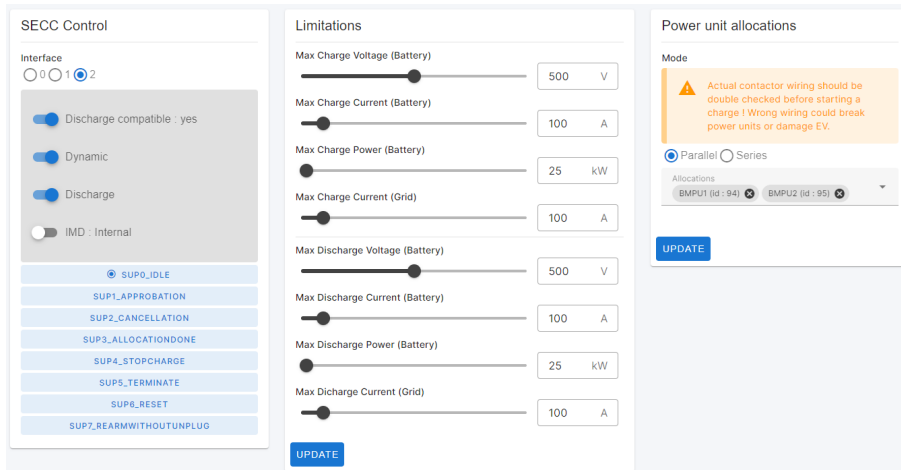


Figure 3.15: Screenshot of the EVI GUI highlighting the allocation, limitation, and SECC control sections.

The two sections SECC Measurements and SECC State shown in figure 3.13 would live update during a charging session, showing electrical power, current, voltage, and energy as well the control pilot state and SECC state and error codes. To complement this, the `evis-ccs-pm` plug module logs available via the CLI interface showed additional details.

During a charge, it is also possible to change the electrical limitations and even power transfer direction by changing the settings in the Limitations view and pressing the *UPDATE* button or toggling the slider for Charge/Discharge mode. The changes would only be applied when the `SUP3_ALLOCATIONDONE` request was sent. While this did somewhat fulfill goal number 4 of being able to dynamically change the electrical setpoint, it did not offer any documented way to automate test sequences. Because of the many issues with the two other supervisors described above, an attempt was made to reverse-engineer the GUI supervisor for the sake of automating it. Using the DevTools build into the web browser Google Chrome, using the Network panel to record a network activity log. With this method, it was possible to log the API calls being made from the GUI frontend to the backend and supervisor. It was quickly discovered that the Limitations *UPDATE* button would send a PUT request with a JSON¹¹ payload to the URL `http://192.168.200.11:8333/supervisor/secc/EVIS_A_CCs/update/limitations` for EVIS A, and a similarly structured URL for EVIS B. The JSON payload would contain the limitations set on the frontend formatted as such:

```
{
  "max_dc_discharge_voltage": 400,
  "max_dc_charge_current": 50,
  "max_ac_charge_current": 100,
  "max_dc_discharge_power": 0,
  "max_dc_charge_power": 0,
  "max_dc_discharge_current": 0,
  "max_dc_charge_voltage": 0,
  "max_ac_discharge_current": 0
}
```

Similarly, pressing the `SUP3_ALLOCATIONDONE` button would also send a PUT request,

¹¹JavaScript Object Notation

this time to http://192.168.200.11:8333/supervisor/secc/EVIS_A_CCS/update/command with JSON payload:

```
{
  "interface": 1,
  "request_code": 3,
  "discharge_compatible": false,
  "discharge_mode": false,
  "dynamic_mode": false,
  "imd_external": false,
  "imd_state": 0
}
```

Configuring the two requests in the API platform Postman was the next step. It was determined that the API required *Basic Auth* and used the same credentials as the GUI login. After experimenting with the API in Postman, it was clear that these two API calls could replace manually updating settings in the GUI. Using the Python library *requests*, two scripts were written to send API calls in an automated way.

The first script, intended to be run on a Raspberry Pi, is included as appendix A.4.3.1 and toggles between charging and discharging for a CHAdeMO session, while also pulling GPIO pin 7 high exactly when the command is sent to switch power transfer direction. This script was intended for activation and ramp time measurements, as described in section 3.3. The second script is included as appendix A.4.3.2 and uses while loops to ramp the DC power setpoint up and down in fixed power steps, with fixed step intervals. The two scripts worked exactly as intended, and thus the fourth goal outlined at the beginning of this section was achieved - it was now possible to dynamically update electrical setpoints. Based on these initial scripts, test scripts to carry out the test cases selected in the following section were written.

3.6 Selection of test cases

When the project started, the capabilities of the Watt%Well EVSE were largely unknown. Several important metrics were identified in the project plan, based on existing publications in the field and previous experience by the author. One such publication, Zecchino et al.: “Test and Modelling of Commercial V2G CHAdeMO Chargers to Assess the Suitability for Grid Services” lists seven metrics:

- (i) *Direction*: The information if an EV can provide only uni-directional or bi-directional (V2G) power flow.
- (ii) *Set-point linearity*: The discreteness of the charging/discharging power set-point.
- (iii) *Starting time and maximum activation time*: The period between receiving the set-point and activating the flexibility.
- (iv-v) *Ramp-up/ramp-down time*: The up/downwards time between activation time and full-service provision, and vice versa.
- (vi) *Accuracy*: The difference between the required and the delivered response, e.g., the acceptable response band.
- (vii) *Precision*: The variation of the delivered response for a given set-point.

The first metric was deemed the most important, and this project largely focused on determining whether it was possible to achieve bidirectional power transfer using the CCS2

connector. With access to the logs of EV-EVSE communication described in section 3.5, it was possible to determine why an attempt at BPT may or may not fail and report on the results. A range of different EVs and EV emulation systems were tested against the Watt&Well EVSE, and results based on the dissection of `evis-ccs-pm` (plug module) are included in section 4.1.

Except for this first metric on BPT capabilities, the ability to modulate the Watt&Well EVSE active power setpoint during a session was required to determine the metrics i-vii. As described in the section 3.5, this was achieved using the EVI GUI supervisor using the reverse-engineered API. In the same paper that proposed the seven metrics, a test pattern designed to allow estimation of the metrics is also proposed, included as figure 3.16. This test pattern gave inspiration for the test patterns used in this thesis. By extending the scripts developed for controlling the Watt%Well EVSE, included as appendix A.4.3.1 and A.4.3.2, it was possible to apply such test patterns to an ongoing session.

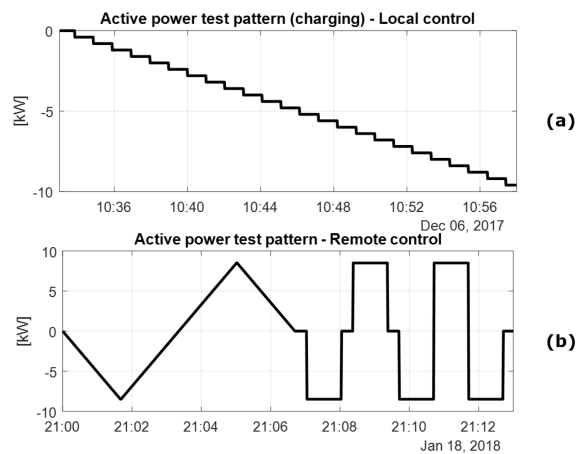


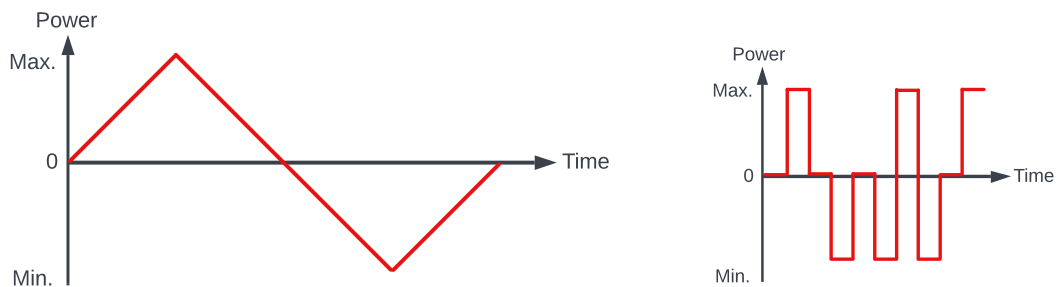
Figure 3.16: Test patterns used for the "Parker test". Image source: [1].

In addition to the seven metrics, the project plan also covered efficiency testing as a possible option. With the possibility to dynamically set the current/power setpoint gained via the EVI GUI API, it was possible to not only measure efficiency at a single operating point but sweep across the operating range. With a real EV connected, this operating range was restricted by the battery voltage, which is State of Charge (SoC) dependent. Thus, it was decided to run efficiency tests at a range of SoC values, to capture any voltage dependency. To further capture any voltage dependency and attempt to replicate the efficiency heatmap included in figure 4.6b, the battery emulator available at ElaadNL Testlab was used. This setup is described in section 3.4 and allows setting a fixed battery voltage, and thereby it was possible to test across the whole Safe Operating Area (appendix A.4) of the BMPU power converter. Because of the separated power converter mains supply and single phase auxiliary supply, it was also decided to include measurements of the auxiliary consumption in all efficiency measurements, to capture the full system efficiency. It was however decided to not include any vehicle side losses for battery conditioning and auxiliary loads.

In the early days of the project work, the reactive power capabilities of the BMPU, as described in the datasheet, were taken into consideration. As described in the section 3.1 on the Watt&Well EVSE components, the BMPU includes active power factor correction. It is also possible to set the power factor in the range of -0.4 to +0.4, with a typical value of 0.99, as seen in appendix A.1. Unfortunately, the power factor setpoint was not accessible

with the control methods described in section 3.5, so it was not possible to modulate it, nor check that it remained at the default value of 0.99. From experience in previous projects [49] and results in other works [71], it was still decided to measure and log reactive power and power factor with the PEL104 Power Energy Logger shown in figure 3.8 during sweeps of the operating range. This would allow later characterization of the performance of the active power factor correction, as well as comparison to other power converters for e-mobility. Since other papers have suggested investigating grid quality metrics such as individual current and voltage harmonics contribution [71] and Total Harmonic Distortion (THD), the PEL104 device was also configured to save this information.

After trial and error experimentation with a CHAdeMO vehicle capable of BPT, it was decided to split the test pattern into two tests. The first pattern, shown in figure 3.17a was intended to sweep the operating range of a given configuration of vehicle and BMPU power converters. Such a pattern would provide data for the determination of (ii) set point linearity, (vi) accuracy, and (vii) precision as well as the additional metrics efficiency, reactive power and/or power factor, individual harmonics, and THD. The other pattern shown in figure 3.17b was instead designed to provide data for more time-sensitive analysis of (iii) activation time and (iv-v) ramp times.



(a) Test pattern type a used for efficiency, set point linearity, accuracy, precision, current ripple, reactive power, THD, and harmonics measurements.

(b) Test pattern type b used for activation and ramp time measurements.

Figure 3.17: Test patterns used when performing experiments.

While sweeping the operating area of the BMPU, it was also discovered that the DC side current ripple was quite significant at specific points, enough to make the DC side current measurements unreliable. Since the ripple was significantly higher than the figures given in the datasheet, it was decided to take advantage of the capabilities of the EV emulation equipment at ElaadNL Testlab and also characterize the current ripple across the charging part of the Safe Operating Area (appendix A.4).

4 Results

4.1 Vehicle compatibility

This section covers the results from testing different EV and EV emulators against the Watt&Well EVSE. The table 4.1 lists all vehicles and emulators tested with the brand, model, and for the vehicles additional information trim/configuration, the model year, and software version shown in the on-board infotainment system. Also listed are the schemas sent via the SupportedAppProtocolsReq message and their priority. This data was obtained by dissection of the Plug Module logs, coming from the `evis-ccs-pm` service. Finally, the rightmost column indicates whether it was possible to achieve Bidirectional Power Transfer with the specific EV or not. For one of the vehicles, marked as brand/-model [Confidential], the OEM asked the project group not to disclose specific information. This vehicle was a real, road-legal, and registered EV with prototype software. To highlight the difference between the prototype vehicle's software/hardware and a production version, a similar brand and model was tested. To avoid disclosing the brand/model of the prototype, this production vehicle has been marked as [Same as above], and the specific software version has not been disclosed.

In all three EV emulators tested against the Watt&Well EVSE, it was possible to pick the schemas, and in the case of the Trialog ComboCS4M even pick multiple schemas and set their priority. To not list all the possible schemas, only the ISO 15118-20 based schema expected to be able to support BPT has been listed. For the Keysight Charging Discovery System (CDS), number 5 in the table 3.3, a handshake with ISO 15118-20 picked as the schema was not achieved. With the number 3 in table 3.3, the Keysight Charging Communication Interface Tester (CCIT/"Verisco box"), BPT was achieved with the Keysight CDS and SL18000A series DC emulator handling the physical power transfer. Finally for the number 1 in table 3.3, the Trialog ComboCS4M, no power converters were connected. As a result, it was possible to configure a DC BPT session and enable discharge mode, but no power was flowing.

in the Volkswagen ID.4 tested with details as per table 4.1, a mention of bidirectional charging was found within the infotainment system. A picture of this information has been included as figure 4.1.

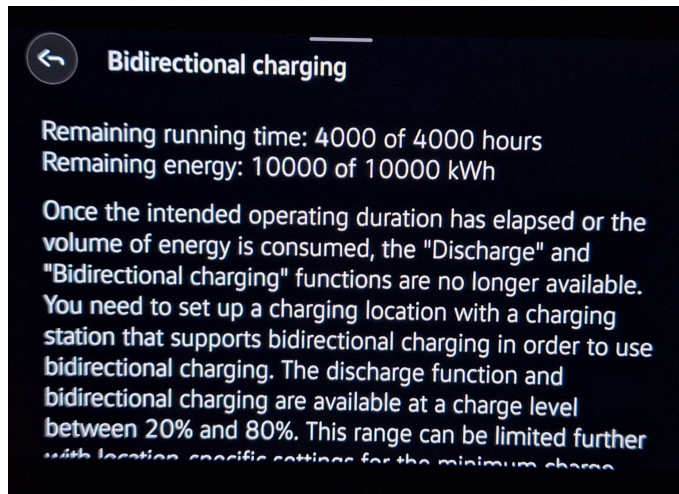


Figure 4.1: Picture of the infotainment system in the tested Volkswagen ID.4 showing bidirectional charging information.

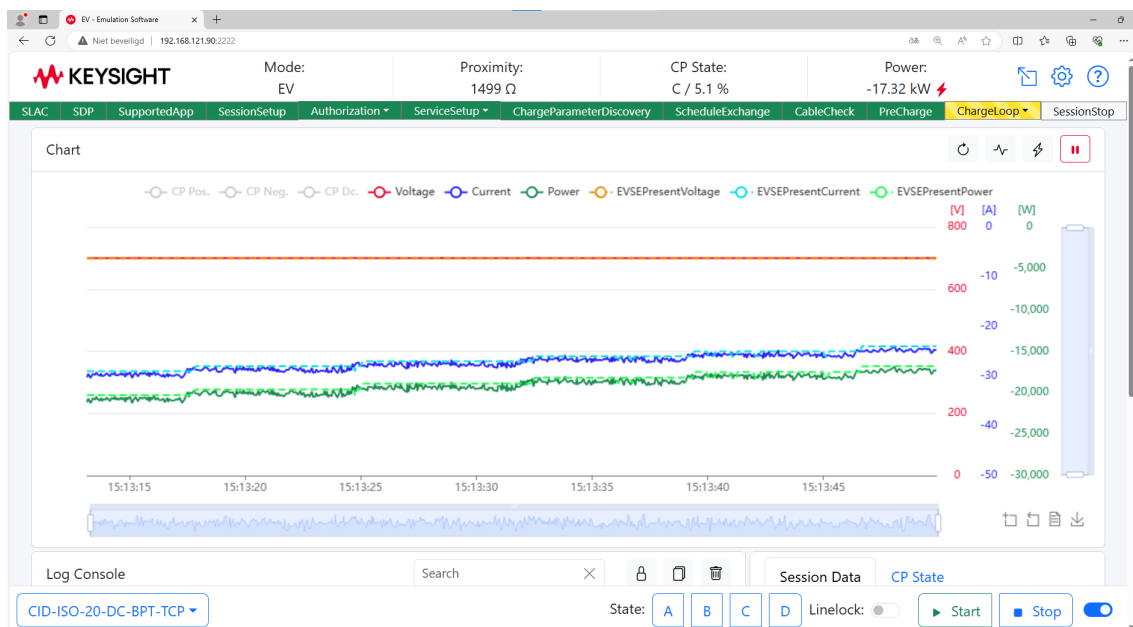


Figure 4.2: Screenshot of the Keysight CCIT "Verisco box" interface while performing Reverse Power Transfer of 17 kW using SL1800A DC emulators and the Watt&Well EVSE.

Brand	Model	Trim/year	Software version	Priority / SupportedAppProtocols	BPT working
Nissan	LEAF	2017	Unknown	CHAdEMO	Yes
Opel	Corsa-e	Elegance 2021	psag3_ar_19.1	1 urn:din:70121:2012:MsgDef DIN 2 urn:iso:15118:2:2013:MsgDef ISO2	No
Polestar	2	LRSM 2WD 2023	P2.14.3	1 urn:din:70121:2012:MsgDef DIN 2 urn:iso:15118:2:2013:MsgDef ISO2	No
Volkswagen	ID.4	Pro 77 kWh 2023	3.5.0	1 urn:din:70121:2012:MsgDef DIN 2 urn:iso:15118:2:2013:MsgDef ISO2	No
Kia	EV9	GT line 2024	MV1.EUR.116	1 urn:din:70121:2012:MsgDef DIN 2 urn:iso:15118:2:2013:MsgDef ISO2	No
Tesla	Model Y	RWD 2023	v12 (2024.20.1)	1 urn:tesla:din:2018:MsgDef 2 urn:din:70121:2012:MsgDef DIN	No
[Confidential]	[Confidential]	Unknown	Prototype	1 urn:din:70121:2012:MsgDef DIN 2 urn:iso:15118:2:2013:MsgDef ISO2 3 urn:iso:std:iso:15118:-20:DC ISO20_DC 4 urn:iso:std:iso:15118:-20:AC_[redacted]	Yes
[Same as above]	[Same as above]		Production	1 urn:din:70121:2012:MsgDef DIN 2 urn:iso:15118:2:2013:MsgDef ISO2	No
Keysight	CDS	N/A	N/A	urn:iso:std:iso:15118:-20:DC ISO20_DC	No - no handshake
Keysight	CCIT (Verisco)	N/A	N/A	urn:iso:std:iso:15118:-20:DC ISO20_DC	Yes - via CDS
Trialog	ComboCS4M	N/A	N/A	urn:iso:std:iso:15118:-20:DC ISO20_DC	Yes - unpowered

Table 4.1: Table showing all vehicles tested with brand, model, trim and year information, and the software version reported in the infotainment system. Also included are EV emulators. The column Priority/SupportedAppProtocols indicates which schemas the EV supports and their priority, as sent by the EVCC in the SupportedAppProtocols message. For emulators, only the schema capable of BPT is listed. If BPT was tested working with an EV/emulator, this is also included. Some details have been left out, as the EV OEM did not wish to have these disclosed.

4.1.1 TLS investigation

As detailed in section 2.3.2.2, ISO 15118-20 mandates TLS encryption for all use cases. This section will detail how the logs from the CCS plug module `evis-ccs-pm`, as well as some additional logging and configuration options in the EV emulators tested, were used to investigate TLS support of the Watt&Well EVSE and the ISO 15118-20 capable EV and EV emulators tested. When the Watt&Well EVSE was first testing against the Keysight CCIT "Verisco box" at ElaadNL, TLS was disabled on the EVCC (emulator) side. This was done to hopefully get a 15118-20 DC BPT session up and running without dealing with certificates and Public Key Infrastructure (PKI). Once the test plan was completed, an attempt was made to enable TLS on the EVCC side. In the Watt&Well EVSE, the PKI is directly accessible via the CLI and SFTP and configured via the `evis-ccs-pm.ini` file. By inspecting the certificates of the SECC PKI, it was found that all certificates, including the root certificate, were signed by Trialog - the provider of the YaCCS stack used by Watt&Well.

The Keysight/Verisco system offered a few different preconfigured PKIs, but not any provided by Trialog. The different preconfigured PKIs were tested against the Watt&Well EVSE and failed to establish a TLS connection. To get around this, a new PKI entry DTU `test2` was configured in the Keysight system using the PKI from Watt&Well/Trialog found inside the EVI file system. This EVCC side PKI configuration also failed against the Watt&Well SECC. From the Keysight/Verisco system, the following log was obtained:

```
1 [AUDIT] de.verisco.emu.api SmartChargingSetup SLAC matching process successful
2 [AUDIT] de.verisco.emu.api SmartChargingSetup Sending router solicitation...
3 [INFO] de.verisco.emu.evcc EvccStateContext Updating apphand service supported
  protocol list...
4 [INFO] de.verisco.emu.apphand ApphandServiceImpl Add supported protocol
  namespace urn:iso:std:iso:15118:-20:DC
5 [AUDIT] de.verisco.emu.sdp EvccSDPClient Send SDPReq (TLS), retry: 0
6 [AUDIT] de.verisco.emu.sdp EvccSDPClient Received SDPRes from /fe80:0:0:0:c0d:
  c6ff:fe48:3fe9%3:15118
7 [AUDIT] de.verisco.emu.sdp EvccSDPServiceImpl SDP successful
8 [AUDIT] de.verisco.emu.api SmartChargingSetup SECC supports TLS connection
9 [AUDIT] de.verisco.emu.api SmartChargingSetup Starting TLS connection to IPv6:
  fe80:0:0:0:c0d:c6ff:fe48:3fe9%enp2s0 & port: 59806
10 [AUDIT] de.verisco.emu.security TlsContextServiceImpl V2G TLS context of DTU
  test2 initialized
11 [INFO] de.verisco.emu.webserver WebSocket onConnect: New client connected from
  /127.0.0.1:59540. Client size: 2
12 [ERROR] de.verisco.emu.api SmartChargingSetup TLS connection to IPv6: fe80
  :0:0:0:c0d:c6ff:fe48:3fe9%enp2s0 & port: 59806 failed! javax.net.ssl.
  SSLHandshakeException: PKIX path validation failed: java.security.cert.
  CertPathValidatorException: Path does not chain with any of the trust
  anchors
```

In the above log, it is observed that the SECC supports TLS and that the EVCC attempts TLS using the DTU `test2` PKI. This attempt then failed. The corresponding log from the SECC side shows that the SECC was listening on the same port 59806, but did not recognize the certificate, producing a similar error state:

```
1 TcpHandler:122:3042894880          TcpHandler: start: TCP listening on
  :::59806
2 SdpHandler:110:3042894880          SdpHandler: startListening: UDP
  listening for EV SDP request on :::15118 (using TCP port 59806)
3 SdpHandler:260:3042894880          > Tx SDP response
```

```

4 TcpHandler:227:3042894880]                TcpHandler: handleAcceptConnection:
      new client connected
5 TcpHandler:230:3042894880]                TcpHandler: begin connection on port
      : 59806
6 TcpHandler:239:3042894880]                TcpHandler: close existing TCP
      server
7 TlsHandlerConnection:154:3042894880]      TLS handshake connection error:
      sslv3 alert certificate unknown, socket is open: true
8 IIEc61851Controller:186:3053161664]      CP: "A"

```

Comparing the SECC side logs from this test with the logs of testing against a real vehicle with ISO 15118-20 DC BPT support, it is clear that the real vehicle did not request TLS. Instead, the SupportedAppProtocolsReq message is sent unencrypted right after the TCP connection is established, this time on port 52116:

```

1 SdpHandler:260:3042866208]                > Tx SDP response
2 TcpHandler:227:3042866208]                TcpHandler: handleAcceptConnection:
      new client connected
3 TcpHandlerConnection:51:3042866208]      TcpHandlerConnection: start
4 TcpHandler:230:3042866208]                TcpHandler: begin connection on port
      : 52116
5 TcpHandler:239:3042866208]                TcpHandler: close existing TCP
      server
6 Handshake:38:3042866208]                 #10 urn:din:70121:2012:MsgDef DIN (
      priority 1)
7 Handshake:38:3042866208]                 #20 urn:iso:15118:2:2013:MsgDef ISO2
      (priority 2)
8 Handshake:38:3042866208]                 #1 urn:iso:std:iso:15118:-20:AC_[
      redacted] Not_Selected (priority 4)
9 Handshake:38:3042866208]                 #2 urn:iso:std:iso:15118:-20:DC
      ISO20_DC (priority 3)
10 SdpHandler:82:3042866208]                SdpHandler: Closing SDP socket...
11 MessageStateMachineManager:140:3042866208]MsgStM::
      ProcessSupportedAppProtocolReq
12 EvisIso15118Adapter:549:3053132992]      > Tx PM charge settings [
      DischargeCompatibility:1,DynamicMode:1,DischargeMode:0,InterfaceType:2]
13 Handshake:68:3042866208]                 Selected SchemaId #2 ISO20_DC
14 MessageStateMachineManager:140:3042866208]MsgStM::WaitForSessionSetupReq
15 TcpHandlerExtended:66:3042866208]        < Rx 4 SessionSetupReq
16 EvisIso15118Adapter:190:3042866208]      Configured DC BPT Charge Service
17 EvisIso15118Adapter:221:3042866208]      DC BPT service offered to EVCC

```

The same behavior as seen in these logs with no TLS was also observed on both the Keysight/Verisco system (table 3.3 number 3) and the Trialog ComboCS4M system (table 3.3 number 1). Since the PKI in the Watt&Well SECC was provided by Trialog, a TLS attempt was also made with the Trialog emulator system. Three attempts were made:

- Trialog EVCC default PKI against the Watt&Well default PKI.
- Trialog EVCC with the Watt&Well SECC PKI installed against the Watt&Well default PKI.
- Trialog EVCC default PKI against the same PKI installed in the Watt&Well SECC.

Despite both PKIs in all three combinations being provided by the same company (Trialog), all three attempts failed.

4.2 Efficiency

This section contains highlighted efficiency results from testing the Watt&Well EVSE against both real vehicles and an emulator. Referring to the measurement setup illustrated in 3.8, the AC active and reactive power to/from the BMPU(s) was measured and logged using the PEL 104. The AC auxiliary power from the single-phase supply was measured and logged using the PEL 106. Finally, the DC side current and voltage were measured by the respective probes and then logged using the Hioki datalogger. The DC side power was then found as the product of the current and voltage data logged by the Hioki. In figure 4.3, an example of the raw output from a test using the test pattern found in figure 3.17a is included. This data has been synchronized time-wise and shows the AC side power going to/from a single BMPU, as well as the DC side power and AC auxiliary power supplying the rest of Watt&Well EVSE.

From the many datasets like the one illustrated in figure 4.3, the efficiency of the BMPU was calculated as $\eta_{BMPU} = \frac{\text{DC side power}}{\text{AC side power}}$. Before this could be done, a significant cleanup of the data was needed. This work was primarily carried out by another project student, Gabriel Fabbri. A few examples of the result have been included: Figure 4.4 shows the efficiency of two BMPUs in series configuration tested against the Keysight CDS with a fixed battery voltage at 600, 700, and 800V. Figure 4.5 shows the efficiency of a single tested against a real CHAdeMO vehicle.

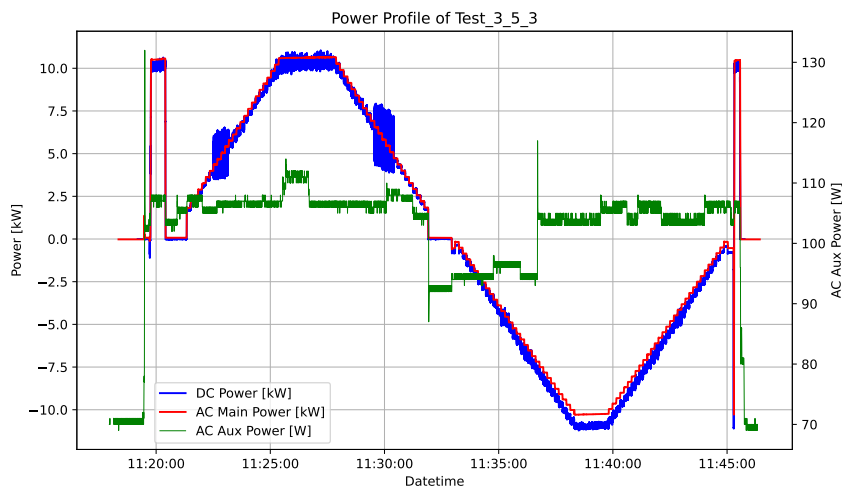


Figure 4.3: Example of the data output from an efficiency test using test pattern a (figure 3.17a), showing both AC and DC side power measurements as well as the auxiliary power. Emulated voltage at 400V and a single BMPU. Referring to figure 3.8, AC main power is measured by the PEL104, and AC auxiliary Power is measured by PEL106. Note the different units and scales for main and auxiliary AC power.

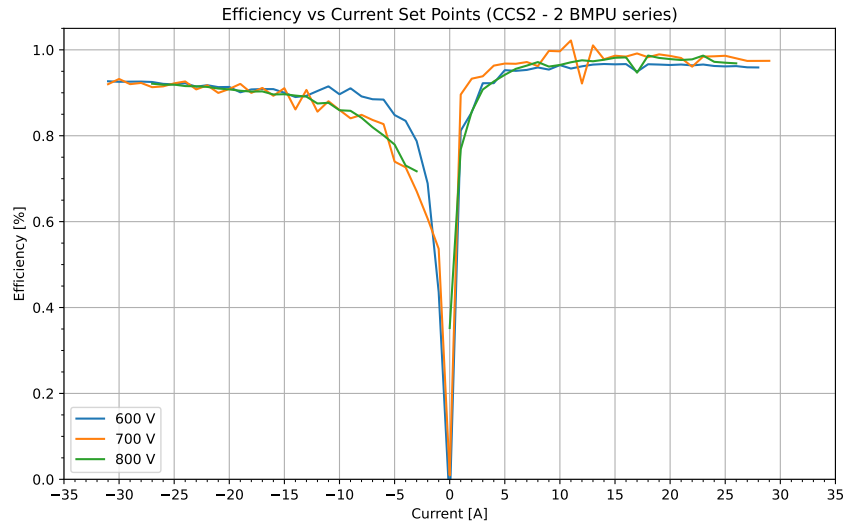


Figure 4.4: AC/DC conversion efficiency of two BMPU in series configuration performing CCS2 BPT. EV and battery are emulated at three different voltage levels 600, 700, and 800V using Keysight CDS.

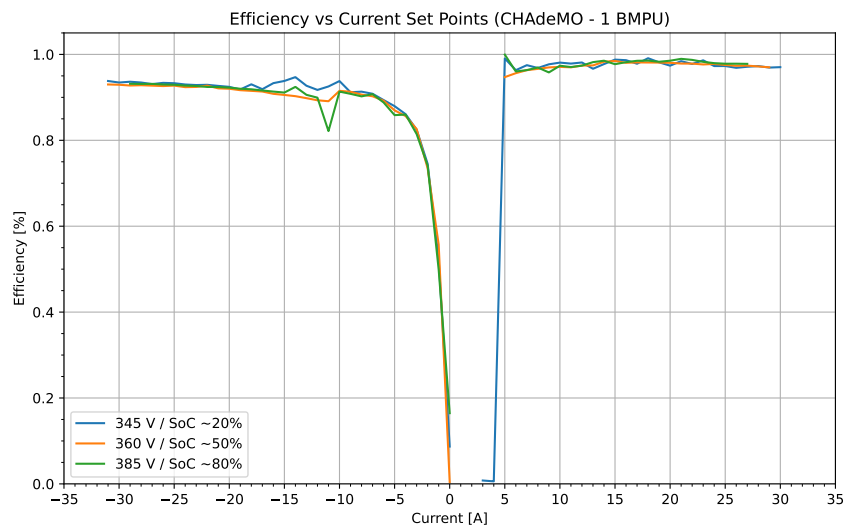
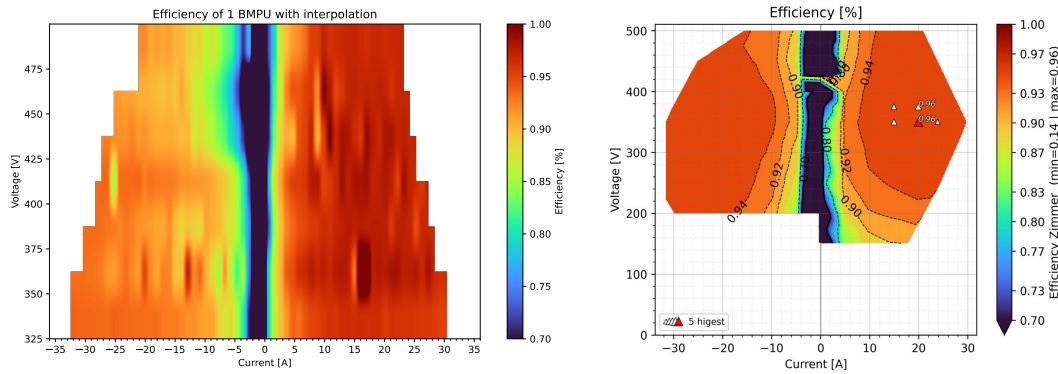


Figure 4.5: AC/DC conversion efficiency a single BMPU performing CHAdeMO BPT. The vehicle was the Nissan LEAF listed in table 4.1.

By aggregating efficiency measurements of a single BMP, using multiple sweeps of the operating area at different voltage levels set on the Keysight CDS DC emulator, it was possible to create a heatmap of the efficiency across the Safe Operating Area of the BMPU, included as appendix A.4. In figure 4.6, the result of this test campaign (figure 4.6a) is placed next to the corresponding figure from the datasheet (figure 4.6b). The color scale has been matched as close as possible, to enable direct comparison. A larger version of the same heatmap without interpolation is included as figure 4.7.



(a) Heatmap of single BMPU conversion efficiency, measured using Keysight CDS and battery emulation. (b) Typical BMPU-R2 efficiency heatmap from the datasheet. Source: Watt&Well [48].

Figure 4.6: Efficiency heatmaps, comparison between measured values (a) and BMPU datasheet (b). Color scales are matched as closely as possible.

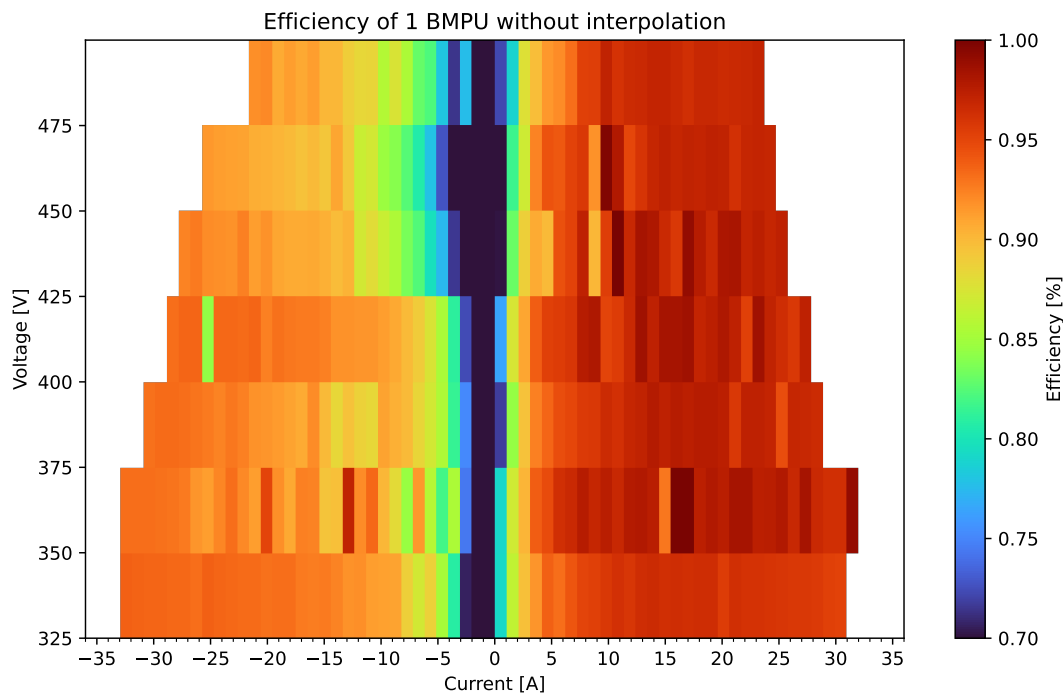


Figure 4.7: Heatmap of single BMPU conversion efficiency, measured using Keysight CDS and battery emulation. No interpolation.

4.3 System characteristics

Not all the metrics identified in section 3.6 will be reported on. As an example of active, reactive, and power factor contribution, figure 4.8 shows active and reactive power measurements as well as logged power factor over time. These measurements were logged while performing a test with the real vehicle capable of ISO15118-20 BPT described in section 4.1. The middle section shows a test pattern (figure 3.17a), while the start and end are various switches from charging to discharging and not part of a test.

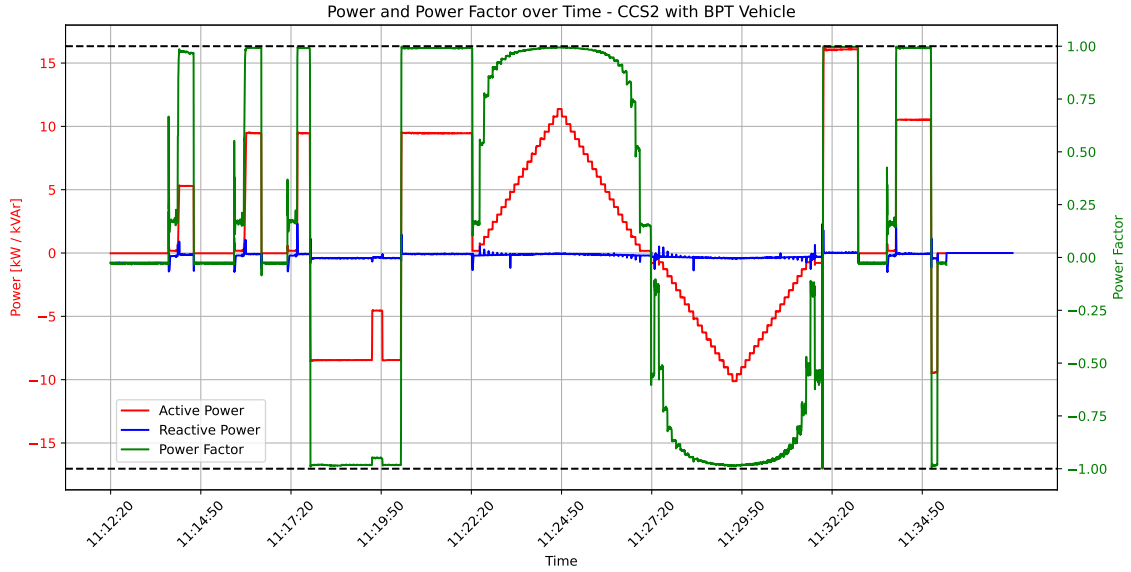


Figure 4.8: Plot of active and reactive power as well as power factor over time, while performing tests with the real vehicle capable of ISO15118-20 BPT. The middle section shows a test pattern (figure 3.17a), while the start and end are various switches from charging to discharging and not part of a test. Referring to figure 3.8, quantities are measured by the PEL104.

4.3.1 Activation and ramp times

Using the test pattern b, shown in figure 3.17b, the following data was captured for steps between the minimum and maximum power available in a given configuration. The exact BMPU and vehicle configuration are given in each table caption. The From and To columns indicate which power setpoint was stepped from and to, respectively. The Activation and Ramp columns give time measurements for the specific ramp in milliseconds, while the Total is the sum of the two. The Ramp rate column is reported in kW/s and is calculated as the difference between power before and after the step, divided by the ramp time.

From [kW]	To [kW]	Activation [ms]	Ramp [ms]	Total [ms]	Ramp rate [kW/s]
0	10	78	473	551	21.1
10	0	91	402	493	24.9
0	-10	992	724	1716	13.8
-10	0	189	309	498	32.4
0	-10	242	271	513	36.9
-10	10	1085	1048	2133	19.1
10	-10	97	1744	1841	11.5
-10	0	160	360	520	27.8

Table 4.2: Activation and ramp time test. Confidential real vehicle with CCS2/BPT support, 575V battery voltage, 2 BMPU in series, power limited at ± 10 kW.

From [kW]	To [kW]	Activation [ms]	Ramp [ms]	Total [ms]	Ramp rate [kW/s]
0	10	11	556	567	18.0
10	0	9	409	418	24.4
0	-10	940	760	1700	13.2
-10	0	59	419	478	23.9
0	-10	239	302	541	33.1
-10	10	1069	994	2063	20.1
10	-10	22	1723	1745	11.6
-10	0	58	411	469	24.3

Table 4.3: Activation and ramp time test. Emulated vehicle with CCS2/BPT support, 575V fixed voltage, 2 B MPU in series, power limited at ± 10 kW.

From [kW]	To [kW]	Activation [ms]	Ramp [ms]	Total [ms]	Ramp rate [kW/s]
0	15.6	138	800	938	19.5
15.6	0	92	536	628	29.1
0	-18.3	1200	1024	2224	17.9
-18.3	0	128	727	855	25.2
0	-18.3	292	504	796	36.3
-18.3	15.6	1104	1798	2902	18.9
15.6	-18.3	68	2406	2474	14.1
-18.3	0	89	724	813	25.3

Table 4.4: Activation and ramp time test. Emulated vehicle with CCS2/BPT support, 575V fixed voltage, 2 B MPU in series, power limited by B MPU constraints.

From [kW]	To [kW]	Activation [ms]	Ramp [ms]	Total [ms]	Ramp rate [kW/s]
0	10.5	346	334	680	31.4
10.5	0	156	540	696	19.4
0	-11	1240	436	1676	25.2
-11	0	128	518	646	21.2
0	-11	204	460	664	23.9
-11	10.5	1156	1129	2285	19.0
10.5	-11	108	1739	1847	12.4
-11	0	106	567	673	19.4

Table 4.5: Activation and ramp time test. Emulated vehicle with CCS2/BPT support, 400V fixed voltage, 1 B MPU, power limited by B MPU constraints.

From [kW]	To [kW]	Activation [ms]	Ramp [ms]	Total [ms]	Ramp rate [kW/s]
0	21	380	767	1147	27.4
21	0	77	1052	1129	20.0
0	-22	1247	1050	2297	21.0
21	0	52	1172	1224	17.9
0	-22	174	1038	1212	21.2
-22	21	1131	2262	3393	19.0
21	-22	5	2285	2290	18.8
-22	0	133	1150	1283	19.1

Table 4.6: Activation and ramp time test. Emulated vehicle with CCS2/BPT support, 400V fixed voltage, 2 BMPU in parallel operation, power limited by BMPU constraints.

From [kW]	To [kW]	Activation [ms]	Ramp [ms]	Total [ms]	Ramp rate [kW/s]
0	21	308	364	672	57.7
21	0	134	548	682	38.3
0	-22	1327	902	2229	24.4
21	0	152	530	682	39.6
0	-22	184	648	832	34.0
-22	21	1116	1728	2844	24.9
21	-22	108	2470	2578	17.4
-22	0	120	553	673	39.8

Table 4.7: Activation and ramp time test. Emulated vehicle with CCS2/BPT support, 800V fixed voltage, 2 BMPU in series operation, power limited by BMPU constraints.

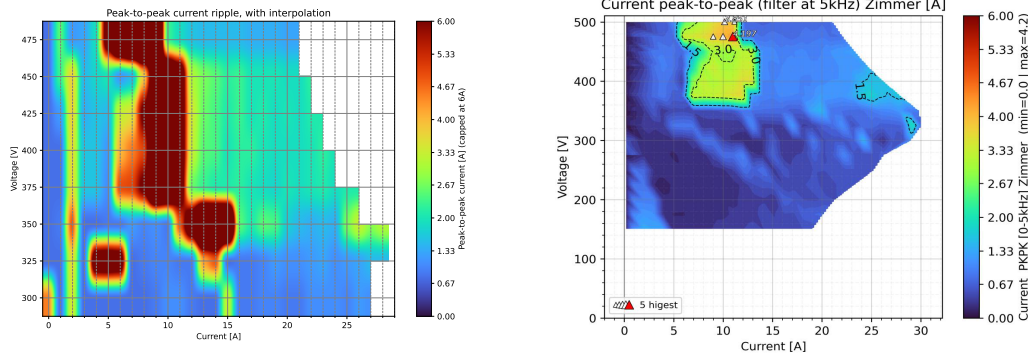
From [kW]	To [kW]	Activation [ms]	Ramp [ms]	Total [ms]	Ramp rate [kW/s]
0	10.5	977	880	1857	11.9
10.5	0	111	500	611	21.0
0	-11	1324	413	1737	26.6
-11	0	96	537	633	20.5
0	-11	215	508	723	21.7
-11	10.5	1182	1137	2319	18.9
10.5	-11	106	1624	1730	13.2
-11	0	167	543	710	20.3

Table 4.8: Activation and ramp time test. Real vehicle with CHAdeMO/BPT support, 385V battery voltage, 1 BMPU, and power limited by BMPU constraints.

4.3.2 DC current ripple

As described in section 3.6, a significant DC side current ripple was observed during initial testing. An example of the ripple influencing the measurements is seen clearly in figure 4.3 as a sudden large variation in the DC side power around the 5 A mark. In figure 4.11, an oscilloscope screenshot showing the ripple waveform at 8 A and 475 V operating point is included, showing a peak-to-peak ripple current of 12.2 A at a ripple frequency of 705 Hz. To further investigate the ripple effect, a test series sweeping across the positive/charging part of the Safe Operating Area of the BMPU (appendix A.4) was carried out.

In figure 4.9, a heatmap of the recorded values is shown as figure 4.9a next to the heatmap provided in the datasheet for the B MPU figure 4.9b. Note that the color scale has been matched as close as possible, leading to many of the measured values being out of range. In figure 4.10, a similar heatmap for the measured values are shown, with no interpolation and full-color scale.



(a) Heatmap of peak-to-peak DC side ripple current, with interpolation and scale similar to the datasheet.

(b) Heatmap of peak-to-peak DC side ripple current filtered at 5kHz. Source: Watt&Well [48].

Figure 4.9: Current ripple heatmaps, comparison between measured values (a) and B MPU datasheet (b).

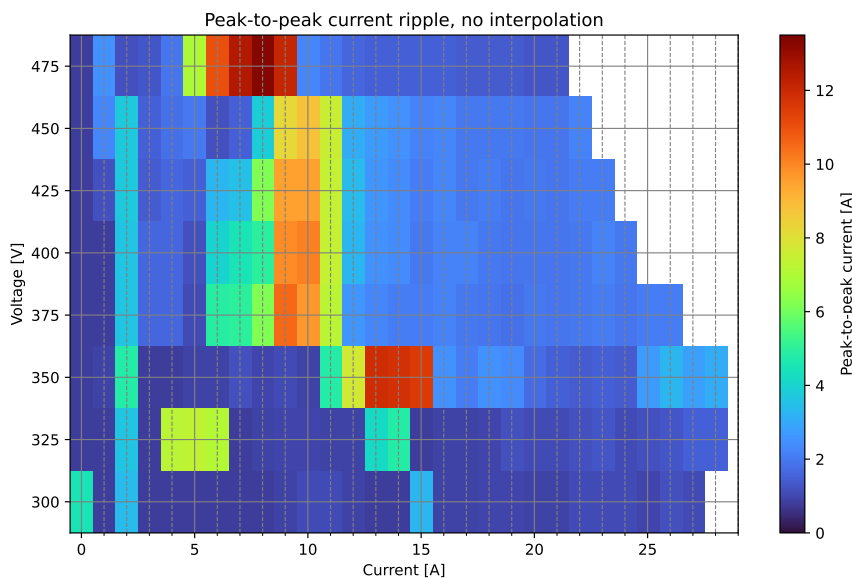


Figure 4.10: Heatmap of peak-to-peak DC side ripple current, with no interpolation and full-color scale.

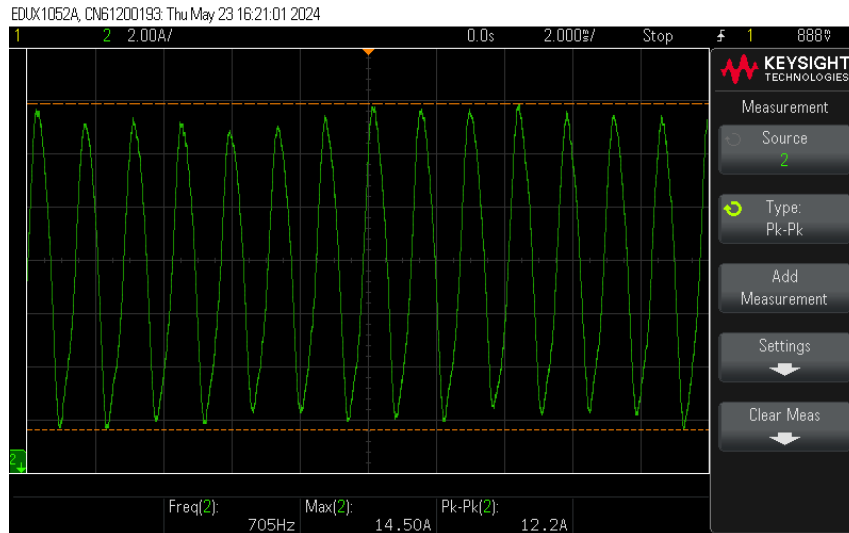


Figure 4.11: Oscilloscope screenshot showing a DC side current waveform with a peak-to-peak (pk-pk) ripple value of 12.2 A and a ripple frequency measured at 705 Hz (Freq). The DC operating point is 8A and 475 V.

4.4 Additional findings

4.4.1 Vehicle-to-vehicle power transfer

Mostly as a curiosity, a demonstration of vehicle-to-vehicle power transfer was also done as part of the project work. Since the Watt&Well EVSE has both CHAdeMO and CCS2 connectors, two separate power converters, and two SECC in the form of EVIS A and EVIS B, it should be technically possible. To test if it worked as intended, the contractor configuration file 9 from table 3.1 called `PU1_CCS1_PU2_CCS2-CHA` was loaded into the EVIX-IO section of the EVI GUI. This set the DC side contactor configuration such that BMPU 1 was connected to the CCS2 interface and BMPU 2 was connected to the CHAdeMO interface. Both BMPU remained in their fixed configuration of *G2V/V2G – DC voltage control mode*, that is grid-following, and was connected on the AC side as shown in figure 3.8.

With this setup, it was possible to start a session on the CCS2 and the CHAdeMO interface at the same time. By switching the CHAdeMO interface to discharging mode, energy was flowing from the battery of the CHAdeMO vehicle, via the two AC/grid side coupled BMPU, to the CCS2 vehicle battery. Because both BMPUs remained in the grid-following mode, the AC grid connection acted essentially as a buffer for any mismatch between the active power export from one BMPU and the active power import of the other. This configuration could be called DC-linked AC grid-following vehicle-to-vehicle power transfer or perhaps DC-linked, AC grid-coupled vehicle-to-vehicle power transfer. It was not attempted to operate the system without a grid connection, as this would require switching one of the BMPUs into the grid-forming *V2L mode*, which was not available.

4.4.2 OCPP capabilities

With the OCPP 1.6J service and supervisor configured for CCS charging as described in section 3.5, some testing of the OCPP capabilities was carried out. The testing more or less followed the test protocol described in earlier work by the author [37]. It was found that the OCPP supervisor, when connected to the Monta OCPP Toolkit, could start and stop charging sessions via the `RemoteStartStartTransaction.req` and `RemoteStopTransaction.req` messages in an OCPP 1.6J-compliant manner. This included correct Start-

Transaction.req and StopTransaction.req messages, as well as correct statuses reported via StatusNotification.req messages. When the CCS2 plug was inserted into a vehicle, the EVSE would report Preparing, when the transaction was authorized and power started flowing status was Charging and once the transaction was ended, but the plug remained inserted, the status was Finishing. It was also possible to start transactions locally by emulating RFID cars via CLI commands.

The testing also showed that the OCPP supervisor was somewhat unstable, and would often go to a faulted state and require reset commands sent via the CLI to resume. Sending Reset.req messages from the CSMS did now work. It was also attempted to switch to OCPP 2.0.1 by changing the `ocpp-controller.json` file version parameter. This did not work and resulted in the following error message printed in the OCPP controller log:

```
[OcppManager:36:ocpp] OCPP 2.0.1 not available on this build
configuration, use OCPP 1.6
```

All the OCPP 1.6J messages tested and the results of whether the message worked as defined in the OCPP 1.6 specification have been included in table 4.9:

OCPP 1.6J message	Result
BootNotification	Working, but does not contain any chargePointVendor or chargePointModel information
RemoteStartTransaction	Working, both before and after plug-in.
StartTransaction	Working.
RemoteStopTransaction	Working.
StopTransaction	Working.
MeterValues	Working, but measurands do not follow OCPP 1.6J specification.
StatusNotification	Working, reports status Preparing, Charging, Finishing, Faulted correctly.
GetConfiguration	Working, can retrieve list of all configuration keys.
SetConfiguration	Working, changes take effect.
StatusNotification	Working, reports for connector 0 and connector 1.
Authorize	Working, with emulated RFID reader.
SupportedFeatureProfiles	The configuration reported the following: Core, Firmware-Management, LocalAuthListManagement, RemoteTrigger.
SetChargingProfile	Not working, no response when a TxProfile was sent.
TriggerMessage	Not working, none or incorrect responses send.
Reset	Not working, does not have any effect.

Table 4.9: Table of OCPP 1.6J messages tested, and whether the implementation was working and compliant with the OCPP 1.6 specification.

5 Discussion

The by far most important result of this thesis is the small **Yes** in the BPT working column of table 4.1 next to the confidential, real vehicle communicating via ISO 15118-20. Since Type 2 and CCS2 are the market-dominant connectors in Europe, almost all EVs, AC, and DC charging infrastructure use them and the underlying communication protocols. Thus, the path toward enabling widespread bidirectional power transfer in Europe must include these connectors and their communication protocols. As covered in the section on DIN SPEC 70121 and the ISO 15118 family, only the latest second-generation ISO 15118-20 standard has built-in support for bidirectional power transfer. Looking at the table 4.1, a range of vehicles were tested, and only the prototype vehicle supported ISO 15118-20. This is also the only real, CCS-equipped vehicle tested that was capable of BPT. The rest of the tested vehicles only support DIN SPEC 70121 and ISO 15118-2. In the case of the Tesla Model Y, not even ISO 15118-2 is supported. Instead, it supports *Tesla DIN 2018*, likely a proprietary protocol. The results of this thesis show that with support for ISO 15118-20 on both the EVCC and SECC, true interoperability and standardized BPT implementations are possible. The result with the confidential vehicle covered by this thesis is likely one of the first times ever that independent researchers have achieved BPT using the standard ISO 15118-20 schema. Previous results have typically been done in secret, often with heavy involvement from automotive OEMs, and might not use the standardized BPT protocol in ISO 15118-20.

As a testament to the proprietary nature of other BPT implementations, Volkswagen claims bidirectional charging is possible in all new models with the 77 kWh battery and from ID. Software 3.5 or higher [32]. When a vehicle matching these exact specifications was tested, it only reported support for DIN SPEC 70121 and ISO 15118-2, as shown in table 4.1. Since Volkswagen does say the technology is based on ISO 15118-2, not 15118-20, and it is only compatible with specific charging hardware [32], it can be assumed that a proprietary subset of 15118-2 is in use. In the infotainment system of the car, information on bidirectional charging is available, as shown in figure 4.1. Interestingly, this screen contains a running count of how many hours and energy in the form of kWh have been used for bidirectional charging. The same limits are also found in the press release by Volkswagen: [32]

The discharging and bidirectional charging functions are no longer available once the intended operating time or energy quantity has been reached: Max energy quantities: Up to 10,000 kWh Discharging; Max operating hours: Up to 4,000 hours Discharging.

Such limits may hint towards a big blocker for BPT adoption among the automotive OEMs being anticipated battery degradation. On EVs, warranties for the high voltage battery are 8 years or 160,000 km on average, whatever comes first [72]. However, these warranty terms likely assume that the battery will only be used for driving. If the battery is engaged in BPT while not driving, it is possible to complete a lot of discharge cycles in 8 years. It is of course also possible to drive and fast charge a lot at high power levels in 8 years, but the 160,000 km average limit somewhat restricts such use and the resulting degradation of the battery. However, when the battery is cycled by BPT instead of driving, the odometer is not ticking towards the 160,000 km limit. Thus, there is the potential for the vehicle owner to degrade the battery without exceeding the warranty limits, and then have the battery replaced under warranty at a significant cost to the manufacturer. However, with

previous research showing that degradation from V2G can be very small [3], it might not need to be a concern for automotive manufacturers. In addition to battery degradation, the BPT use case might also stress other drivetrain components like contactors, battery conditioning, and battery management systems. In the case of AC-linked BPT, there will also be additional use of the bidirectional on-board charger. If these systems and components are not designed and tested for BPT applications, the manufacturer might risk replacing faulty units under warranty.

It seems that Volkswagen, with the limits shown in figure 4.1, tries to tackle this problem. The time and energy restriction as well as 20-80% SoC operating window restrictions is very likely intended to protect the battery from intensive BPT use and thereby degradation, saving Volkswagen from replacing batteries under their warranty. Another financially related reason that EV OEMs are slow at adopting ISO 15118-20 and BPT support might be that they are looking to monetize it. When end users buy a vehicle, they are first and foremost buying a means of transportation, but via (aggregated) BPT support they can also participate in electricity and ancillary service markets. These new use cases could potentially lead to significant earnings for the end user and/or aggregator. One example is the Monta PowerBank program, which allows end users to participate in FCR-D markets using their private, unidirectional AC EVSE. Here, end-users can earn up to 50 DKK worth of Monta Wallet credit every month [73], as part of an undisclosed revenue-sharing model. With the adoption of BPT, such earnings could increase, as the bi-directionality could allow larger contributions as well as new services and markets. It is thereby reasonable to assume that the automotive OEMs are looking for ways to monetize these capabilities themselves, to at least get a share of the earnings made with their product, before making the technology available to the mass market.

On the more technical side, the TLS requirement in 15118-20 might also pose a hindrance to the adoption of the standard. As shown in section 4.1.1, it was proven that the real vehicle with ISO 15118-20 support did not request TLS. This is not compliant with ISO 15118-20, where TLS is always mandatory. The attempts at establishing a TLS encrypted session with the different emulators also failed. Although this might very well be due to user error and lack of knowledge in the field of cryptography, it still goes to show that TLS is difficult. As covered in section 2.3.2.2, both ISO 15118-2 and 15118-20 recommend using a Hardware Security Module (HSM) to store and process the private keys for the cryptographic algorithms. Since the algorithm requirements have changed from 15118-2 to 15118-20, the EVCC hardware OEMs use might not work with the newer algorithms. This can make adding secure ISO 15118-20 support to existing EVCC hardware impossible, thereby making software upgrades of existing vehicles or EVCC designs to add BPT support not an option. Instead, the vehicle manufacturer might need to redesign their EVCC hardware with new microcontrollers or add separate cryptographic processing in the form of a Trusted Platform Module (TPM). These TPMs then pose new challenges, as the algorithms required by ISO 15118-20 do not seem to be available in current TPM 2.0 market offerings [34].

A final challenge for BPT adoption at the hardware level might be grid code compliance. For any grid-following BPT application, be it AC or DC-linked, the grid-connected power electronics must comply with specific requirements. These vary by location, which is especially a problem for AC-linked applications. For DC-linked applications, this is pretty easy to overcome, as the power electronics are located in the stationary EVSE and likely installed at a fixed location. For AC-linked applications, the power electronics are located in the vehicle, which can easily move between different grid code areas. In this case, it remains unsolved whether the EV or EVSE should ensure grid code compliance [44]. If the

EVSE is to ensure compliance, it could either directly control the EV-side power electronics via 15118-20 ChargeLoop, or communicate the location-specific parameters as part of the session setup stage. Both options might not be possible with the current edition of ISO 15118-20, as the ChargeLoop might be too slow at 250 ms, and the standardized messages in the session setup stage do not contain grid code information [44].

5.1 Electrical performance

The metrics to be investigated reported in section 3.6 were identified during the project based on previous literature in the field and the capabilities of the Watt&Well EVSE, especially paired with an EV emulation setup. These are largely based on a wish to determine the systems grid compliance and suitability to contribute to especially more demanding ancillary services like Frequency Containment Reserve (FCR) or Fast Frequency Reserve. However, the specific requirements of these services were not investigated, and the results will not be compared to such requirements. Instead, they will be compared against the figures provided in the datasheet of the BMPU power converters and other publications, namely Zecchino et al.: “Test and Modelling of Commercial V2G CHAdeMO Chargers to Assess the Suitability for Grid Services”.

Efficiency

The example power profile included in figure 4.3 shows the raw data for an efficiency measurement, with the test pattern a from 3.17a in use. The green auxiliary power curve shows the consumption of all EVSE systems except for the actual power converters. It seems to be around 70 W at standby before the session starts and once started at the 11:20:00 mark, it quickly jumps to approximately 110 W. This is very likely due to the forced air cooling fans starting up. The fan speed and thereby power draw are temperature dependent [48], and higher loading with resulting higher losses will thus increase internal temperatures and thereby fan speed. Centered around 11:35:00, the converter power is lower and the fan speed likely dropped because of the lower heat output, resulting in auxiliary power consumption dropping to 95 W. Once the power increases again, now exporting to the grid, the fan speed and power draw increases. The red curve representing AC side active power to/from the BMPU shows very little variation and follows the “staircase” test pattern. On the other hand, the blue curve representing DC side power varies a lot, and especially around the 5 kW power level, the DC current ripple is contributing to a lot of noise.

From datasets like the one in figure 4.3, efficiency curves like the ones shown in figure 4.4 and 4.5 were created. These, show first and foremost, a lot of variation in the measurements, especially the former where efficiency for 700 V jumps above 100% in two points. Some of this variation is likely caused by clashes between the significant DC side current ripple in certain operating areas clashing with the sampling rate of the data logging equipment. If the sample is taken during a minimum of the ripple waveform, such as the one shown in figure 4.11, it will show a lot lower value than a similar measurement taken in a maximum. The plot of the CHAdeMO vehicle efficiency shown in figure 4.5 operating with a single BMPU is directly comparable to a similar figure in the paper by Zecchino et al., included as appendix A.13. Here, a similar Nissan LEAF (possibly the exact same) vehicle was tested against a ± 10 kW capable bidirectional charging system and a similar efficiency figure for different SoC is included. From such a comparison, it seems the BMPU is more efficient at the maximum operating point than the Zecchino et al. system, with the BMPU achieving $\geq 96\%$ efficiency in charging mode. In discharging mode, the efficiency is more comparable to the old system at $<94\%$. Both the old system and BMPU also show a general tendency for the efficiency to be quite poor around the 0 power mark,

making low power operation not very desirable from an efficiency standpoint.

The tendency for discharge mode is also reflected in the series operating configuration in figure 4.4. With the data available, it is not possible to determine if the efficiency is genuinely lower in discharging mode, or if there is a problem with the measurements. In all efficiency measurements, there is a tradeoff between step size in the ramp, measurement time at each step, and the overall length of a test. Had more time been allowed to let the system stabilize at a given setpoint, the recorded efficiency might have been higher as the DC link voltage in the BMPU would have more time to stabilize.

To get a more comprehensive image of the efficiency and enable direct comparison with the BMPU datasheet, the battery emulation capabilities of the Keysight CDS were utilized to sweep across most of the operating area of the BMPU both in terms of voltage and current. Comparing the resulting heatmaps in figure 4.6a and 4.7 to the heatmap provided in the datasheet, figure 4.6b, they are quite similar with a distinct low-efficiency band in the middle and the highest efficiency observed in the highest power operation possible. This hints at some constant losses of the converter not dependent on loading, which has a higher impact the lower the overall power is. Some segments in the experimental data show efficiency higher than the maximum 96 % claimed by Watt&Well. This might be due to some accuracy issues with the measurement setup, or the impact of the significant ripple observed and previously described. Similar to the efficiency curves, the heatmap shows a generally lower efficiency in discharge mode, which is not seen in the datasheet figure. As described earlier in this section, the exact cause of this could not be determined.

Reactive power

In figure 4.8 a plot of active and reactive power as well as power factor over time is included, with data recorded while testing BPT with the real, ISO 15118-20 capable vehicle. As described earlier, the BMPU can operate at a power factor setpoint of -0.4 to +0.4, and it is assumed to be sat at 0.99. From the plot, it seems that the BMPU active power factor correction has no issues maintaining a power factor close to unity at higher power, but when the power is reduced below around ± 5 kW, the power factor drops significantly below the assumed set point of 0.99. The reactive power capabilities of the Watt&Well EVSE were not further investigated in this thesis, because of the lack of controllability. Such considerations are instead left for further research, where controllability can hopefully be achieved in a more user-friendly manner than injecting messages on the CANopen network.

Activation and ramp time

The BMPU datasheet shown in appendix A.1 details that the *maximum power variation* is 30 kW/s. In the datasheet, it is also stated that the BMPU can change between both operating modes and go to full power in either direction in less than 750 ms [48]. Comparing these figures to the results of testing a single BMPU in tables 4.5 and 4.8, the maximum ramp rate achieved with CCS was 31.4 kW/s and for CHAdeMO 26.6 kW/s. These were obtained either ramping from 0 to maximum charging power or from 0 to maximum discharging power, showing significant variability between the averages of all ramp rates for both CCS and CHAdeMO. The average ramp rate for CCS with a single BMPU was 21.5 kW/s and CHAdeMO 19.3 kW/s. Comparing these to the results of Zecchino et al., this paper demonstrates an average ramp up rate of 3.35 kW/s with a maximum of 8.84 kW/s and an average ramp down rate of 9.17 kW/s. Based on this, it is safe to say that the BMPU is a lot faster and it is possible to achieve the maximum rate given in the datasheet under some circumstances.

For the activation time, the control method has to be taken into account. The paper by

Zecchino et al. distinguishes between *local* and *remote* control. In the setup used in this project, the control method is very local; the commands sent via the EVI GUI API are coming from a Python script running on the Raspberry Pi located in the same Local Area Network as the EVIS device as shown in the figure 3.7. This means the network-imposed latency should be negligible, and certainly a lot lower than other projects by the author, where network round trip times in the hundreds of milliseconds were common [54]. In the same tables for single BMPU operation referenced above, activation times below 100 ms were measured for some steps, whereas the steps where the power flow direction is changed from 0 or charging to discharging mode is consistently above 1000 ms. This indicates that the system takes extra time to switch modes. Additionally, none of the tests were able to achieve the 750 ms figure from the datasheet, instead taking around 2000 ms to transition from either full discharging power to full charging power or vice versa. This is likely because the 750 ms figure is given for direct control via the CANOpen interface of the BMPU, whereas the values measured in this project have to traverse the whole control stack illustrated in figure 3.14.

Comparing the activation times achieved to the paper by Zecchino et al., the average local control activation time was 4 seconds, and the remote control was 7 seconds. This is a lot slower than the control method and BMPU combination of this project, which produced an average delay of 431 ms for the single BMPU CCS test and 522 ms for the single BMPU CHAdEMO test. Although not directly comparable, as the 575 V battery required the operation of two BMPUs in series, the test with the real BPT capable CCS vehicle in table 4.2 produced achieved an average ramp rate of 23.4 kW/s and an average activation time of 367 ms.

Current ripple

A measurement of the DC side current ripple was done, as the ripple observed in measurements such as the one included in figure 4.3 did not match the maximum ripple values given in the BMPU datasheet. The datasheet provided a heatmap of peak-to-peak ripple current across the charging mode operating range only, included as figure 4.9b. Comparing this to the heatmap for the measured values in figure 4.9, which uses the same colors and scaling, it is clear that the measured ripple is substantially greater. Peak-to-peak ripple values of up to 13 A were recorded as seen in figure 4.10, and many of the recorded values across the operating range were higher than the supposed 4.2 A maximum given in the datasheet. The IEC 61851-23 standard gives figures for maximum current ripple, either observed at rated power and maximum rated current, or in the worst case. These are 1.5 A peak-to-peak below 10 Hz, 6 A below 5000 Hz, and 9 A below 150 kHz [74]. That means the ripple shown in 4.11 of 12.2 A peak-to-peak at a frequency of 705 Hz is well above the limits in the standard, making the BMPU likely not IEC 61851-23 compliant. This is quite interesting, as the datasheet claims that the BMPU is designed to be compatible with exactly IEC 61851-23 [48].

5.2 Experimental setup

A significant amount of the work within this project was centered around understanding, configuring, and controlling the Watt&Well EVSE. The project was centered around this specific EVSE because of the inclusion of a CCS2 connector and ISO 15118-20 capable SECC. This work in the end resulted in the successful demonstration of bidirectional power transfer with 15118-20 based communication with both a real EV and EV emulators. In addition, the work on building a control and measurement system around the EVSE also allowed the collection of large amounts of data to characterize the system.

To get to this point, a comprehensive study of the relevant interoperability mechanisms

ranging from IEC 61851 to ISO 15118 was carried out. These are all required to perform a BPT session with CCS. The research presented in 2.3.2.2 provided an understanding necessary to successfully work with the Watt&Well EVSE and CCS charging. To understand the workings of the Watt&Well EVSE, all the documentation provided by Watt&Well was studied in detail. Especially the EVI board acting as the SECC and the B MPU power converters were studied closely, to understand their capabilities and shortcomings. In general, the Watt&Well EVSE is a good test platform for BPT-related studies, with many configuration options. The documentation and ease of use are however somewhat lacking, and it is clear that the system is a prototype. As an example, when using the EVI GUI, there is no *start charge* button or similar. Instead, one must engage directly with the state machine and the likelihood of error is high, which results in failed sessions. Such a start charge functionality could likely be added quite easily by Watt&Well since the other Python and OCPP supervisors investigated did include such functionality. Another issue encountered was the lack of a well-documented API, SDK¹ or similar interface to start and monitor sessions as well as change electrical setpoints during a session. Achieving this level of control was a big goal for the project, as this would allow the execution of standardized, automated test sequences similar to those used in the existing literature.

While a custom supervisor script built in Python seemed like the ideal solution to achieve this goal, the lack of documentation led to the abandonment of the development. Instead, the solution ended up being a reverse-engineering of the API used for the EVI GUI supervisor. This gave sufficient control to set power or current setpoints as well as switch the mode between charging and discharging, allowing the execution of automated test sequences. This novel control method, paired with SSH access to the EVI CLI, provided a very powerful configuration and control architecture. One important missing option was the ability to directly interact with the CANopen bus, especially the B MPU power converters. These are very well documented and provided some additional features that would have been interesting to investigate, if a way to set the related parameters had been identified. Functionality included switching from grid-following to grid-forming mode, configurable power factor setpoints to control reactive power import/export, and setting power ramp rates. The CANopen interface also provides a lot of measurement data, which if accessible, could have eliminated the need for external measurement.

On the topic of measurements, the lack of accessible, internal measurement data meant an external measurement system was constructed. The system was built within an iterative process, adding more and more measurement points and systems, without removing others. In the end, the system did provide data to assess all the identified metrics, but not without shortcomings. Despite being identified as a possible source of issues before the design of the system even started, synchronization issues persisted. On top of this, the DC side data was also affected by ripple and lost data points in the data logging equipment. Some degree of user error also snuck in, with a mismatch between data logger and voltage probe range settings meaning a loss of accuracy and significant digits. All in all, these shortcomings meant that data processing proved a challenge, and for this reason, nowhere near all of the collected data has been included in this thesis. Despite the room for improvement, the system did work to a degree acceptable enough to produce some results comparable to the B MPU datasheet and existing literature, as discussed in the previous section. Especially the test results obtained using EV emulation equipment proved useful, as the DC voltage probe issue was solved by using a fixed voltage, as set in the battery emulator.

¹Software Development Kit

In general, the use of EV emulation equipment, enabled by a visit to the ElaadNL Testlab in the Netherlands, provided a lot of additional possibilities. Testing against a fully configurable EVCC and emulated battery allowed testing ISO 15118-20 DC BPT without a real EV. The addition of battery emulation with fully configurable DC voltage gave even further options and does not come with the issues of SoC-dependent voltage that affect real batteries when used in testing. This makes it much easier to create consistent, reproducible results. At the ElaadNL Testlab, the Watt&Well EVSE was tested against not only one but three different systems from three different companies (counting Keysight and Verisco as separate companies), with results included in table 4.1. Both the ISO 15118-20 stacks of the Keysight/Verisco CCIT and Trialog ComboCS4M supported ISO 15118-20 and DC BPT, while the Keysight CDS did not. According to ElaadNL, this was a known problem that Keysight was working to solve.

6 Conclusion

This thesis has explored the implementation and feasibility of Bidirectional Power Transfer (BPT) using the ISO 15118-20 standard within the Watt&Well V2X Electric Vehicle Supply Equipment (EVSE) platform. This EVSE is capable of DC-linked, grid-following BPT. The research was driven by the increasing global electrification of the vehicle fleet and the need for efficient and flexible energy management solutions, such as Vehicle-to-Grid (V2G) technologies.

The experimental design involved setting up a comprehensive test environment to evaluate the BPT capabilities of the Watt&Well V2X EVSE. A thorough understanding of the EVSE's components and interoperability mechanisms enabled effective control and performance assessment, aided by vehicle emulation systems.

The experimental results were highly promising. Vehicle compatibility tests showed that the Watt&Well V2X EVSE could effectively communicate and perform BPT with a prototype vehicle using the ISO 15118-20 standard, as well as two separate vehicle emulation systems. These results validate the technical viability of the ISO 15118-20 standard for enabling BPT on modern vehicles with potential for widespread adoption. However, results from testing production vehicles indicated that adoption is still lacking. The result from testing the same brand and model as the prototype vehicle with normal production software showing no ISO 15118-20 support also goes to show that the protocol is still in its early days. Even when OEMs have a seemingly working software stack in their EVCC implementation, it is not made available on vehicles with production software. Several reasons for slow adoption were discussed, including battery degradation, warranty issues, and cybersecurity concerns. At the same time, the rest of the e-mobility ecosystem might not be ready either. With the architecture proposed in figure 2.11, the missing link is not the ISO 15118-20 EV-EVSE protocol, which this thesis proved is working, but instead the yet-to-be-released OCPP 2.1 specification.

This thesis also identified relevant electrical metrics for characterizing the system and assessing its suitability for grid services. Despite some measurement quality issues, the data provided useful comparisons with manufacturer documentation and previous-generation CHAdeMO-based BPT systems. Efficiency tests showed that the system could transfer power bidirectionally with up to 95% efficiency while discharging. Activation and ramp time tests demonstrated faster response times than previous-generation hardware, though not as fast as the datasheet suggests. Ripple measurements indicated that at certain operating points, the DC side ripple current exceeded IEC 61851-23 standardized limits.

The experimental validation of the Watt&Well V2X EVSE platform demonstrated its capability as a BPT test platform while also highlighting shortcomings such as lack of user-friendliness, documentation, and access to advanced features.

In conclusion, this thesis successfully demonstrated the practicality and potential of BPT using the ISO 15118-20 standard. The Watt&Well V2X EVSE platform has proven to be an effective tool for advancing V2G technologies. Future work should address remaining challenges, optimize system components, and explore large-scale implementations to fully realize the advantages of bidirectional power transfer in a sustainable and electrified future.

Bibliography

- [1] Antonio Zecchino et al. “Test and Modelling of Commercial V2G CHAdeMO Chargers to Assess the Suitability for Grid Services”. In: *World Electric Vehicle Journal* 10.2 (2019). ISSN: 2032-6653. DOI: 10.3390/wevj10020021. URL: <https://orbit.dtu.dk/en/publications/test-and-modelling-of-commercial-v2g-chademo-chargers-to-assess-t>.
- [2] Peter Bach Andersen et al. *The Parker Project: Final Report*. English. Technical University of Denmark, 2019.
- [3] Andreas Thingvad et al. “Empirical Capacity Measurements of Electric Vehicles Subject to Battery Degradation from V2G Service”. English. In: *IEEE Transactions on Vehicular Technology* 70.8 (2021), pp. 7547–7557. ISSN: 0018-9545. DOI: 10.1109/TVT.2021.3093161.
- [4] European Parliament. “DIRECTIVE 2014/94/EU OF THE EUROPEAN PARLIAMENT AND OF THE COUNCIL of 22 October 2014 on the deployment of alternative fuels infrastructure”. In: *Official Journal of the European Union* (). URL: <https://eur-lex.europa.eu/legal-content/EN/TXT/HTML/?uri=CELEX:32014L0094&from=en>.
- [5] United Nations. *Factsheet: Climate Change*. United Nations. New York, 2017. URL: https://www.un.org/sites/un2.un.org/files/media_gstc/FACT_SHEET_Climate_Change.pdf.
- [6] V. Masson-Delmotte et al. *Global EV Outlook 2020*. Analysis. International Energy Agency (IEA), 2020. URL: <https://www.iea.org/reports/global-ev-outlook-2020>.
- [7] International Energy Agency (IEA). *Trends in Electric Cars – Global EV Outlook 2024*. Analysis. IEA, 2024. URL: <https://www.iea.org/reports/global-ev-outlook-2024/trends-in-electric-cars>.
- [8] World Economic Forum (WEF). *A Vision for a Sustainable Battery Value Chain in 2030*. Report. WEF, 2019. URL: https://www3.weforum.org/docs/WEF_A_Vision_for_a_Sustainable_Battery_Value_Chain_in_2030_Report.pdf.
- [9] Aude Marjolin. *Lithium-ion Battery Capacity to Grow Steadily to 2030*. Research Report. S&P Global Market Intelligence, 2023. URL: <https://www.spglobal.com/marketintelligence/en/news-insights/research/lithium-ion-battery-capacity-to-grow-steadily-to-2030>.
- [10] ISO Central Secretary. *Road vehicles — Vehicle to grid communication interface - Part 1: General information and use-case definition*. en. Standard ISO 15118-1:2019. Geneva, CH: International Organization for Standardization, 2019. URL: <https://www.iso.org/standard/69113.html>.
- [11] Fabio Arena and Giovanni Pau. “An Overview of Vehicular Communications”. In: *Future Internet* 11.2 (2019). ISSN: 1999-5903. DOI: 10.3390/fi11020027. URL: <https://www.mdpi.com/1999-5903/11/2/27>.
- [12] Willett Kempton and Steven E. Letendre. “Electric vehicles as a new power source for electric utilities”. In: *Transportation Research Part D: Transport and Environment* 2.3 (1997), pp. 157–175. ISSN: 1361-9209. DOI: [https://doi.org/10.1016/S1361-9209\(97\)00001-1](https://doi.org/10.1016/S1361-9209(97)00001-1). URL: <https://www.sciencedirect.com/science/article/pii/S1361920997000011>.
- [13] Nuuve. *Parkeringsplads på Frederiksberg opnår international berømmelse*. 2021. URL: <https://nuuve.com/parkeringsplads-pa-frederiksberg-opnar-international-berommelse/>.

- [14] Andreas Thingvad and Mattia Marinelli. “Influence of V2G Frequency Services and Driving on Electric Vehicles Battery Degradation in the Nordic Countries”. English. In: *Proceedings of EVS 31 & EVTeC 2018*. 31st International Electric Vehicles Symposium & Exhibition & International Electric Vehicle Technology Conference 2018, EVS31 and EVTeC2018 ; Conference date: 30-09-2018 Through 03-10-2018. 2019.
- [15] Andreas Thingvad, Charalampos Ziras, and Mattia Marinelli. “Economic value of electric vehicle reserve provision in the Nordic countries under driving requirements and charger losses”. English. In: *Journal of Energy Storage* 21 (2019), pp. 826–834. ISSN: 2352-152X. DOI: 10.1016/j.est.2018.12.018.
- [16] ISO Central Secretary. *Road vehicles — Vehicle to grid communication interface - Part 20: 2nd generation network layer and application layer requirements*. en. Standard ISO 15118-20:2022. Geneva, CH: International Organization for Standardization, 2022. URL: <https://www.iso.org/standard/77845.html>.
- [17] Lisa Calearo, Marte Larsen, and Maja Sig Vestergaard. “Assessment of the regulatory framework of bidirectional EV charging in Europe”. In: (2023). URL: https://smarten.eu/wp-content/uploads/2023/12/V2X-Enables-abd-Barriers-Study_11-2023_DIGITAL.pdf.
- [18] Lisa Calearo, Marte Larsen, and Maja Sig Vestergaard. “Smartladning og V2X for virksomheder - Kortlægning af potentiale for smartladning, systemydelse og V2X for virksomheder”. In: (2024). URL: <https://www.regionh.dk/til-fagfolk/trafik/Groenne-koeretoerj/Document/Rapport%20om%20Smartladning%20og%20V2X%20for%20virksomheder.pdf>.
- [19] International Electrotechnical Commission. *Plugs, socket-outlets, vehicle connectors and vehicle inlets - Conductive charging of electric vehicles - Part 3: Dimensional compatibility requirements for DC and AC/DC pin and contact-tube vehicle couplers*. en. Standard EN/IEC 62196-3:2022. Geneva, CH: International Electrotechnical Commission, 2022. URL: <https://webstore.iec.ch/publication/59923>.
- [20] via Wikimedia Commons Mliu92 CC BY-SA 4.0 <<https://creativecommons.org/licenses/by-sa/4.0/>>. *CHAdEMO connector.svg*. 2021. URL: https://commons.wikimedia.org/wiki/File:CHAdEMO_connector.svg.
- [21] CHAdEMO Association. *V2G/VGI*. 2022. URL: <https://www.chademo.com/technology/v2g>.
- [22] International Electrotechnical Commission. *Electric vehicle conductive charging system – Part 1: General requirements*. en. Standard EN/IEC 61851-1:2019. Geneva, CH: International Electrotechnical Commission, 2019. URL: <https://webshop.ds.dk/standard/M298491/ds-en-iec-61851-1-2019>.
- [23] Marc Mültin. *The battle between ISO 15118 and DIN SPEC 70121*. 2017. URL: <https://www.switch-ev.com/blog/the-battle-between-iso-15118-and-din-spec-70121>.
- [24] via Wikimedia Commons Mliu92 CC BY-SA 4.0 <<https://creativecommons.org/licenses/by-sa/4.0/>>. *IEC 62196 Type 2 (M, DC, CCS Combo 2).svg*. 2021. URL: [https://commons.wikimedia.org/wiki/File:IEC_62196_Type_2_\(M,_DC,_CCS_Combos_2\).svg](https://commons.wikimedia.org/wiki/File:IEC_62196_Type_2_(M,_DC,_CCS_Combos_2).svg).
- [25] ISO Central Secretary. *Road vehicles — Vehicle to grid communication interface - Part 2: Network and application protocol requirements*. en. Standard ISO 15118-2:2014. Geneva, CH: International Organization for Standardization, 2014. URL: <https://www.iso.org/standard/55366.html>.
- [26] CharIN. “Recommendation of Charging Interface Initiative e.V. CharIN Guide ISO 15118 Service HPC1”. In: (). URL: <https://www.charin.global/media/pages/home/>

- technical-details-ccs-basic/9468fe8ffe-1645622498/charin-guide-iso-15118-service-hpc1-v1.2.pdf.
- [27] Marc Mültin. “ISO 15118 as the Enabler of Vehicle-to-Grid Applications”. In: *2018 International Conference of Electrical and Electronic Technologies for Automotive*. 2018, pp. 1–6. DOI: 10.23919/EETA.2018.8493213.
- [28] Marc Mültin. *What is ISO 15118?* 2021. URL: <https://www.switch-ev.com/blog/what-is-iso-15118>.
- [29] Matthias Kübel. *Design Guide for Combined Charging System*. 2015. URL: https://tesla.o.auroraobjects.eu/Design_Guide_Combined_Charging_System_V3_1_1.pdf.
- [30] CharIN. *CharIN Whitepaper Megawatt Charging System (MCS)*. 2022. URL: https://www.charin.global/media/pages/technology/knowledge-base/c708ba3361-1670238823/whitepaper_megawatt_charging_system_1.0.pdf.
- [31] Typhoon HIL. *ISO 15118-2 Protocol*. 2024. URL: https://www.typhoon-hil.com/documentation/typhoon-hil-software-manual/References/iso15118_protocol.html.
- [32] Volkswagen Newsroom. *Cleverly manage your own electricity: First ID. models support bidirectional charging*. <https://www.volkswagen-newsroom.com/en/press-releases/cleverly-manage-your-own-electricity-first-id-models-support-bidirectional-charging-17949>. Accessed on June 24, 2024. 2023.
- [33] EVerest. *EVerest Logfiles*. <https://github.com/EVerest/logfiles>. Accessed: 2024-06-30. 2024.
- [34] Infineon. *OPTIGA™ TPM - Trusted Platform Module*. 2024. URL: <https://www.infineon.com/cms/en/product/security-smart-card-solutions/optiga-embedded-security-solutions/optiga-tpm/>.
- [35] Marc Mültin. *The new features and timeline for ISO 15118-20*. 2020. URL: <https://www.switch-ev.com/blog/new-features-and-timeline-for-iso15118-20>.
- [36] Open Charge Alliance. *Ocpp ON FAST TRACK TO AN IEC INTERNATIONAL STANDARD*. 2024. URL: <https://openchargealliance.org/ocpp-on-fast-track-to-an-iec-international-standard/>.
- [37] Rasmus Meier Knudsen and Valdemar Cornelio Foss. “Guidance on OCPP Compliance For An Electric Vehicle Smart Charger”. English. 2022.
- [38] Open Charge Alliance. *Open Charge Point Protocol 1.6 second edition*. 2017. URL: <https://www.openchargealliance.org/protocols/ocpp-16/>.
- [39] Open Charge Alliance. *Using ISO 15118 Plug & Charge with OCPP 1.6*. 2020. URL: https://openchargealliance.org/wp-content/uploads/2023/11/ocpp_1_6_ISO_15118_v10.pdf.
- [40] Alpitronic Srl. *Load management manual - Hypercharger HYC50/HYC200/HYC400 (50kW – 400kW) ultra-fast charging system for electric vehicles*. 2024.
- [41] Open Charge Alliance. *Open Charge Point Protocol 2.0.1 third edition*. 2024. URL: <https://openchargealliance.org/protocols/open-charge-point-protocol/#OCPP2.0.1>.
- [42] Open Charge Alliance. *What is new in OCPP 2.0.1*. 2023. URL: https://openchargealliance.org/wp-content/uploads/2024/01/new_in_ocpp_201-v10.pdf.
- [43] Open Charge Alliance. *Open Charge Point Protocol 2.1 Preliminary Draft 3 v0.48*. 2024.
- [44] Open Charge Alliance. *OCPP & IEC 61850: A Winning Team*. 2023. URL: <https://openchargealliance.org/wp-content/uploads/2024/01/Whitepaper-OCPP-IEC-61850-a-winning-team-Report-No.-23-3107-08-09-2023-Version.-1.0.pdf> (visited on 06/24/2024).
- [45] *IEEE Standard for Smart Energy Profile Application Protocol*. IEEE, 2018. URL: https://standards.ieee.org/standard/2030_5-2018.html (visited on 06/24/2024).

- [46] GE Digital Tech blog. *IEEE 2030.5 – Connect to the Wide World of Distributed Energy Resources*. 2023. URL: <https://www.ge.com/digital/tech/ieee-20305-connect-wide-world-distributed-energy-resources> (visited on 06/24/2024).
- [47] Watt&Well. *EVI datasheet (revAJ)*. 2023. URL: <https://emobility.wattandwell.com/wp-content/uploads/EVI-Cx-Ax-datasheet.pdf>.
- [48] Watt&Well. *BMPU-R2 11 kW datasheet (revAR)*. 2023. URL: <https://emobility.wattandwell.com/wp-content/uploads/BMPU-R2-datasheet.pdf>.
- [49] Rasmus Meier Knudsen and Valdemar Cornelio Foss. “Development of Harmonized Electric Vehicle Smart Charging Tests”. English. 2022.
- [50] Watt&Well. *11 kW Bidirectional Power Unit, DC/DC*. 2024. URL: <https://emobility.wattandwell.com/dc-charging-modules/11kw-bidirectional-module-bmpu-r2-dc/>.
- [51] Watt&Well. *Power Modules*. 2024. URL: <https://emobility.wattandwell.com/dc-charging-modules/>.
- [52] Watt&Well. *Bidirectionnal CCS+CHA charging station prototype user manual*. 2024.
- [53] TechTarget. *DHCP (Dynamic Host Configuration Protocol)*. 2024. URL: <https://www.techtarget.com/searchnetworking/definition/DHCP>.
- [54] Rasmus Meier Knudsen and Valdemar Cornelio Foss. “Smart from Start: Experimental Validation of Dynamic Charging Limits via EVSE”. English. 2021.
- [55] Keysight Technologies. “1146B AC / DC Current Probe, 100 kHz, 100 A”. In: (2024). URL: <https://www.keysight.com/dk/en/product/1146B/ac-dc-current-probe-100-khz-100-a.html>.
- [56] Ben Croston. “RPi.GPIO 0.7.1”. In: (2022). URL: <https://pypi.org/project/RPi.GPIO/>.
- [57] Keysight. *SL1047A Scienlab Charging Discovery System – High-Power Series*. 2024. URL: <https://www.keysight.com/dk/en/product/SL1047A/sl1047a-sciencab-charging-discovery-system-high-power-series.html>.
- [58] Comemso. *EV Charging Analyzer Generation 5 / FLEX*. 2024. URL: https://comemso.com/wp-content/uploads/2024/05/EVCA-EN_web.pdf.
- [59] Trialog. *ComboCS the CCS Test System*. 2024. URL: <https://www.trialog.com/en/combocs-2/>.
- [60] Keysight. *SL1550A EV – EVSE Charging Communication Interface Tester*. 2024. URL: <https://www.keysight.com/dk/en/product/SL1550A/ev-evse-charging-communication-interface-tester.html>.
- [61] Keysight. *SL1556A CCS Charging Protocol Tracer*. 2024. URL: <https://www.keysight.com/dk/en/product/SL1556A/ccs-charging-protocol-tracer.html>.
- [62] Comemso. *EVCA ComOnly Flex*. 2024. URL: https://comemso.com/wp-content/uploads/2024/06/comemso_EVCA-ComOnly-Flex.pdf.
- [63] IoTecha. *IoTecha’s HomePlug GreenPHY+V2G Analyzer for ISO/IEC 15118-2 & 15118-20 V2G*. 2024. URL: <https://www.iotecha.com/pilot-shark/>.
- [64] Vertexcom. *MST216D-D01D Vertexcom GreenPHY Sniffer*. 2024. URL: <http://www.hwtools.net/Adapter/MST216D-D01D.html>.
- [65] Applus IDIADA. *CCS V2G Decoder*. 2024. URL: <https://www.digitalsolutions.applusidiada.com/products/ccs-v2g-decoder>.
- [66] Watt&Well. *EVI - GUI user manual Revision AC*. 2023.
- [67] Watt&Well. *EVI - Technical Reference Manual rev AE*. 2023.
- [68] Watt&Well. *EVI Getting Started manual rev AA*. 2023.
- [69] Trialog. *YaCCS SECC - CCS Stack*. 2023.
- [70] Watt&Well. *EVIS - OCPP documentation*. 2023.

- [71] “Experimental validation of onboard electric vehicle chargers to improve the efficiency of smart charging operation”. English. In: *Sustainable Energy Technologies and Assessments* 60 (2023). ISSN: 2213-1388. DOI: 10.1016/j.seta.2023.103512.
- [72] Beev. *Electric Car Battery: Why an 8-Year Warranty?* 2024. URL: <https://www.beev.co/en/blog/borne-de-recharge/garantie-batterie-voiture-electrique/>.
- [73] Monta. *Powerbank Features*. 2024. URL: <https://monta.com/dk/features/powerbank/>.
- [74] International Electrotechnical Commission. *Electric vehicle conductive charging system – Part 1: General requirements*. en. Standard EN/IEC 61851-23:2014. Geneva, CH: International Electrotechnical Commission, 2014. URL: <https://webshop.ds.dk/standard/M267739/ds-en-61851-23-2014>.

A Appendix

A.1 Watt&Well documentation

A.1.1 B MPU electrical characteristics

Parameter	Condition	Value			Units
		Min	Typ	Max	
AC side					
Voltage (phase-phase)	V2G or G2V	147	400 or 480	530	V _{RMS}
Voltage (phase to neutral)	V2G or G2V	85	230 or 277	305	V _{RMS}
Current (per phase)		0		16	A _{RMS}
AC Inrush current				42.4	A _{pk}
Input frequency	V2G or G2V	42.5	50	69	Hz
Current measurement accuracy	@16A _{RMS}			5	%
Voltage measurement accuracy	@480V _{LL}			2.3	%
Power factor	Reactive power control	-0.4	0.99	+0.4	-
DC side					
Voltage	G2V (charge) V2G (discharge)	150 250		500	V _{DC}
Power	G2V (charge) V2G (discharge)			10.5 -11	kW
Maximum power variation (SW programmable)	Active power			30	kW/s
	Reactive power			5	kW/s
Current	G2V (charge) V2G (discharge)			30 -32	A
Voltage measurement accuracy	@500V			0.5	%
Current measurement accuracy	@ 32A _{dc}			1	%

Figure A.1: Table with B MPU-R2 electrical characteristics. Source: Watt&Well [48].

A.1.2 B MPU ripple

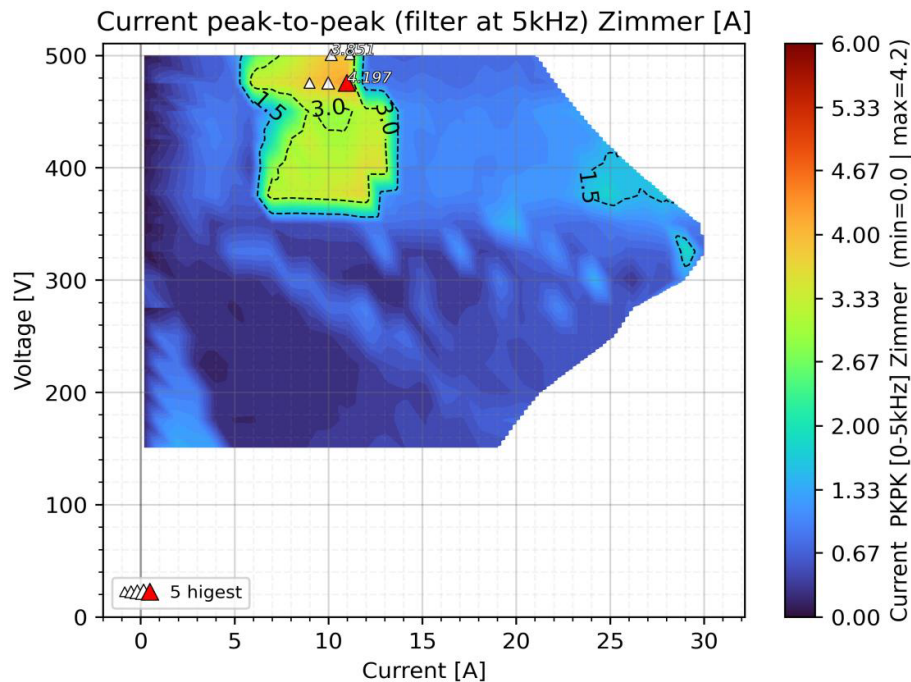


Figure A.2: Peak-to-peak current ripple at the battery side filtered at 5kHz given for grid conditions three-phase with neutral 400V/50Hz and SW version 2.5.4r (build 19020). Source: Watt&Well [48].

A.1.3 B MPU efficiency

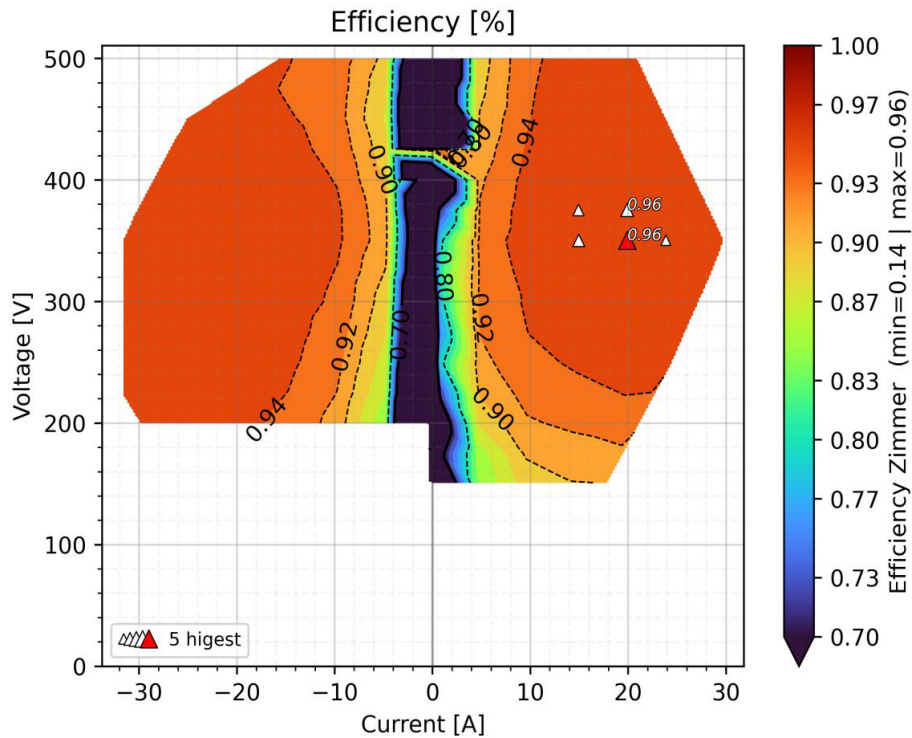


Figure A.3: Typical B MPU-R2 efficiency in three-phase mode without neutral under grid conditions 400V/50Hz at 25°C. Source: Watt&Well [48].

A.1.4 B MPU Safe Operating Area

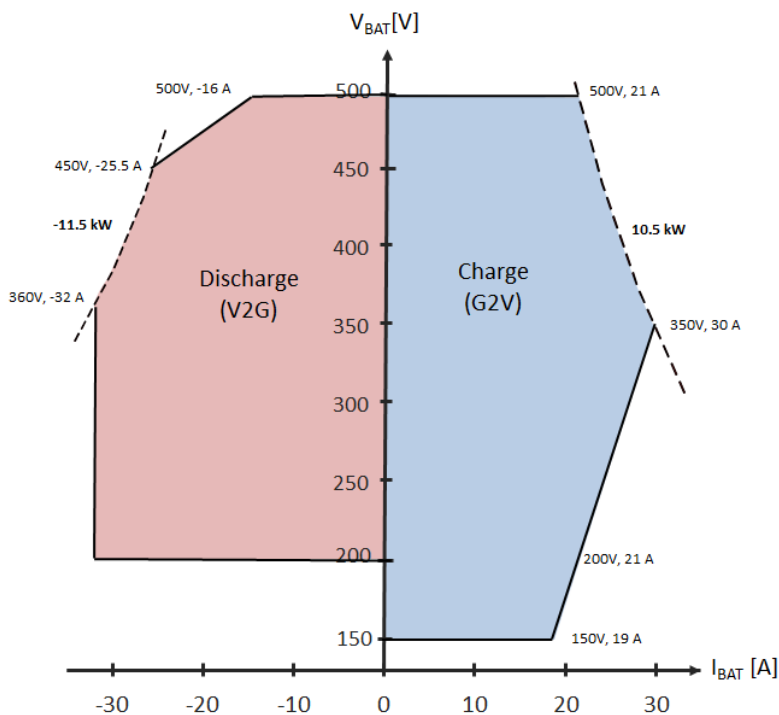


Figure A.4: Battery Side Safe Operating Area under grid conditions 400V/50Hz at 25°C. Source: Watt&Well [48].

A.1.5 B MPU Regulation block diagrams

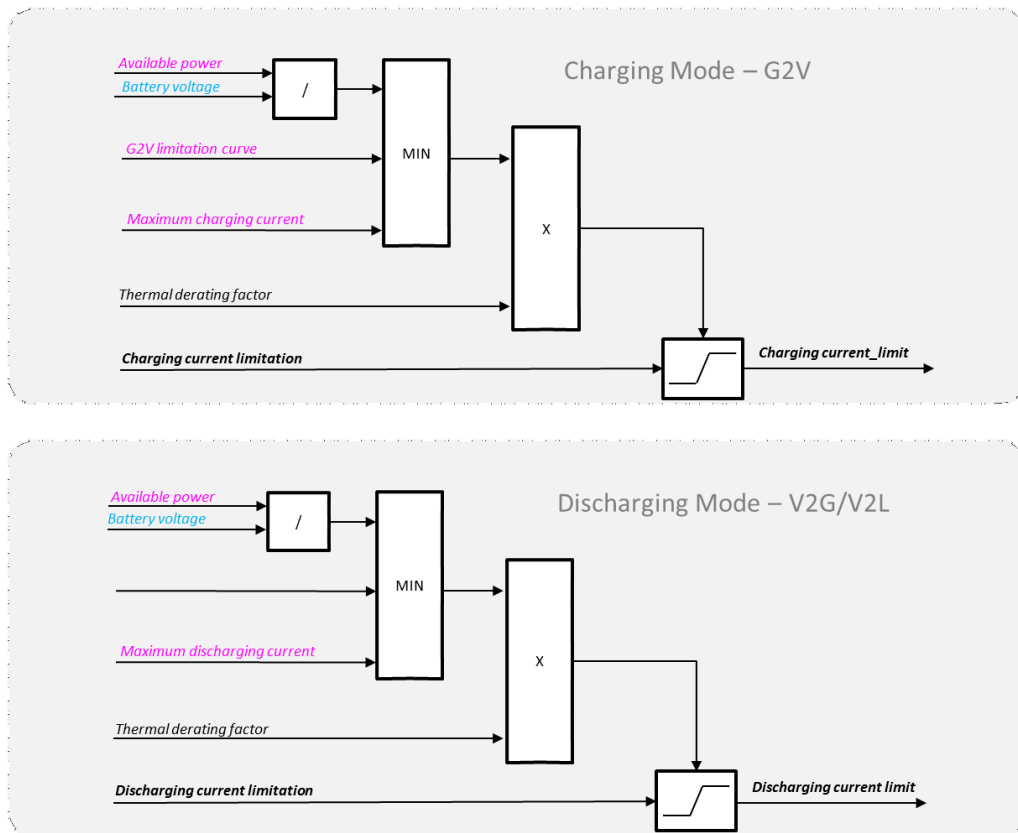


Figure A.5: B MPU Charging and discharging current limitations block diagram. Source: Watt&Well [48].

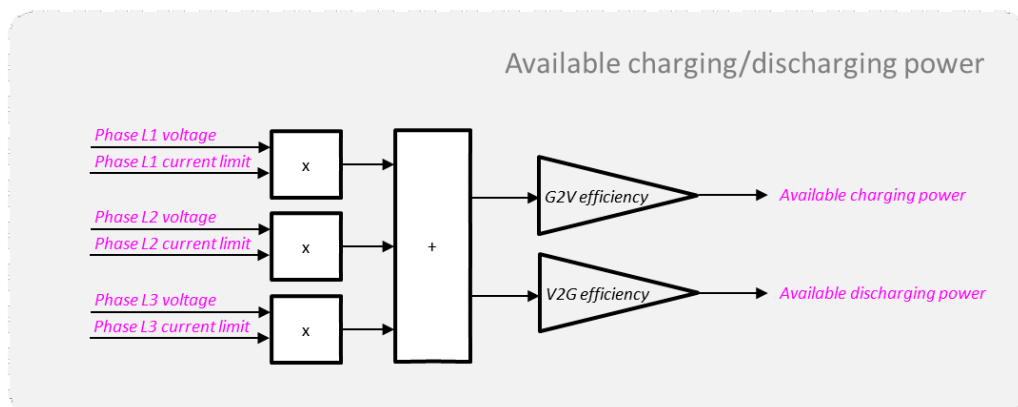


Figure A.6: B MPU Charging and discharging AC side current limitations block diagram. Source: Watt&Well [48].

A.1.6 EVIX-IO contactors

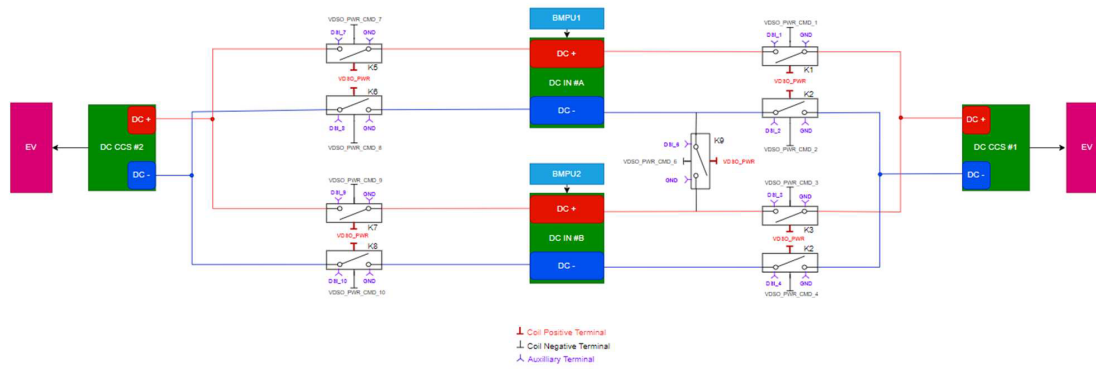


Figure A.7: Schematic diagram of the contactor configuration in the EVIX. Image source: Watt&Well [52]

A.2 ISO 15118 material

A.2.1 ISO 15118-1 Annex D Typical RPT system

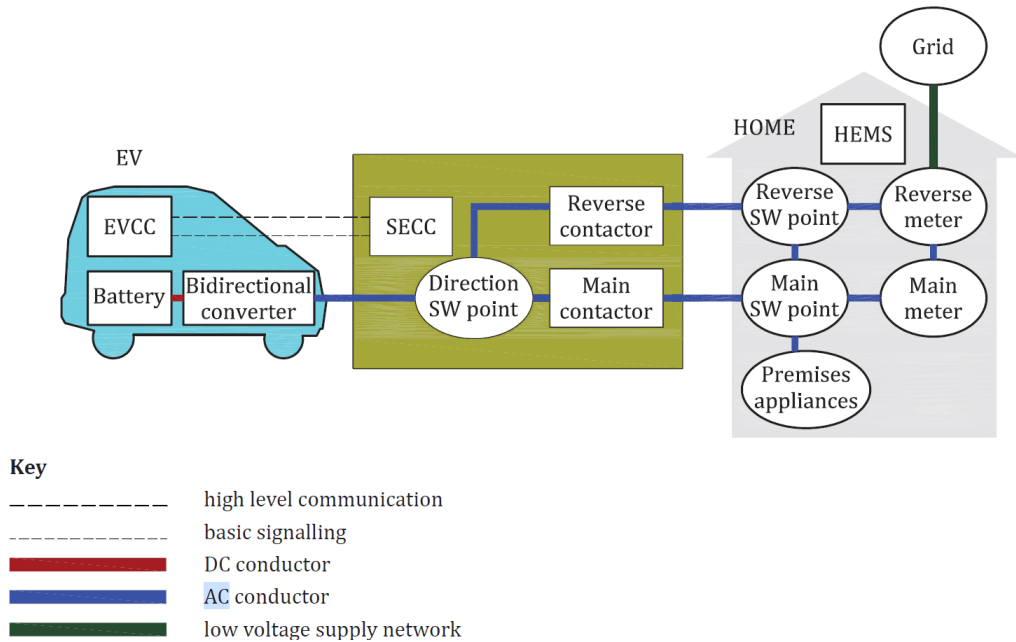


Figure A.8: Block diagram of a typical AC forward and reverse power transfer system. Source: ISO Central Secretary [10].

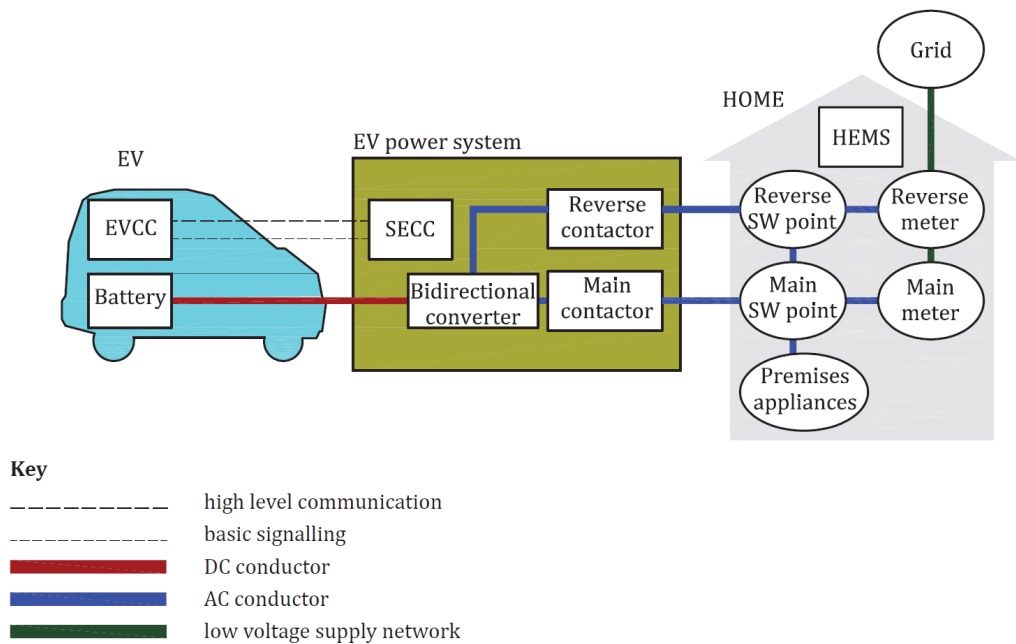


Figure A.9: Block diagram of a typical DC forward and reverse power transfer system. Source: ISO Central Secretary [10].

A.2.2 Message sequence for a DC charging session in 15118-2

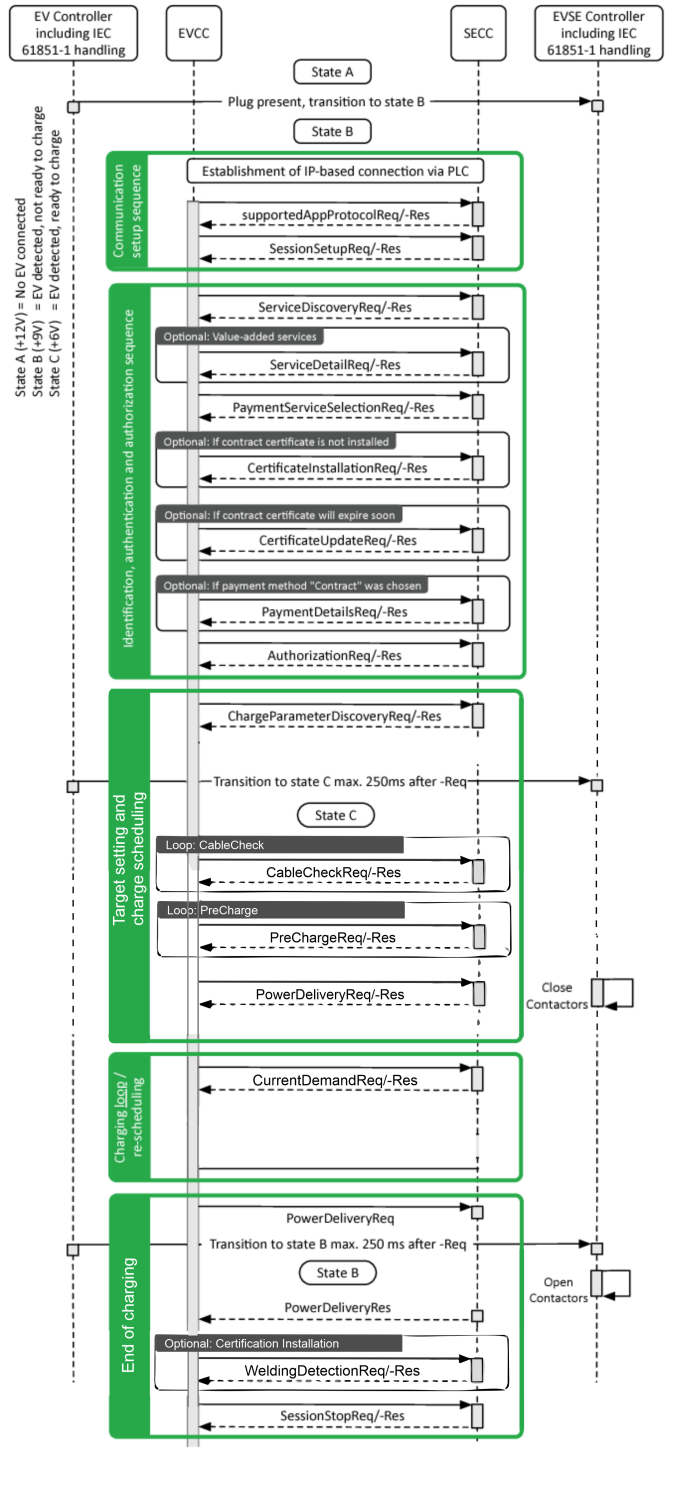


Figure A.10: Diagram illustrating the message sequence for an ISO 15118-2 DC charge. Image source: [31]. Note that an AC version of this diagram is available as a vector image in appendix A.11.

A.2.3 Message sequence for an AC charging session in 15118-2

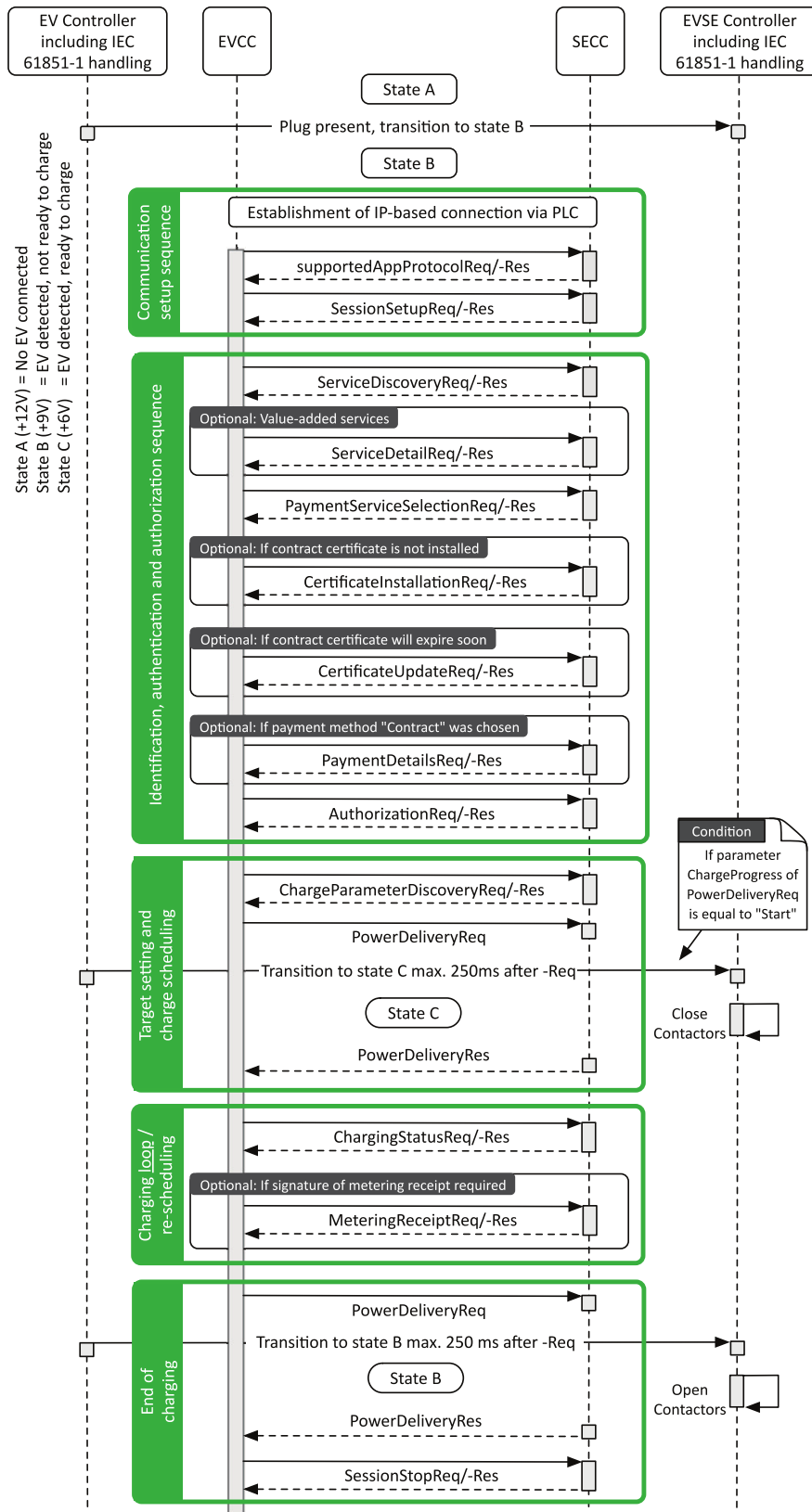


Figure A.11: Diagram illustrating the message sequence for an ISO 15118-2 AC charge. Image source: [27].

A.2.4 Message sequence for a DC session in 15118-20

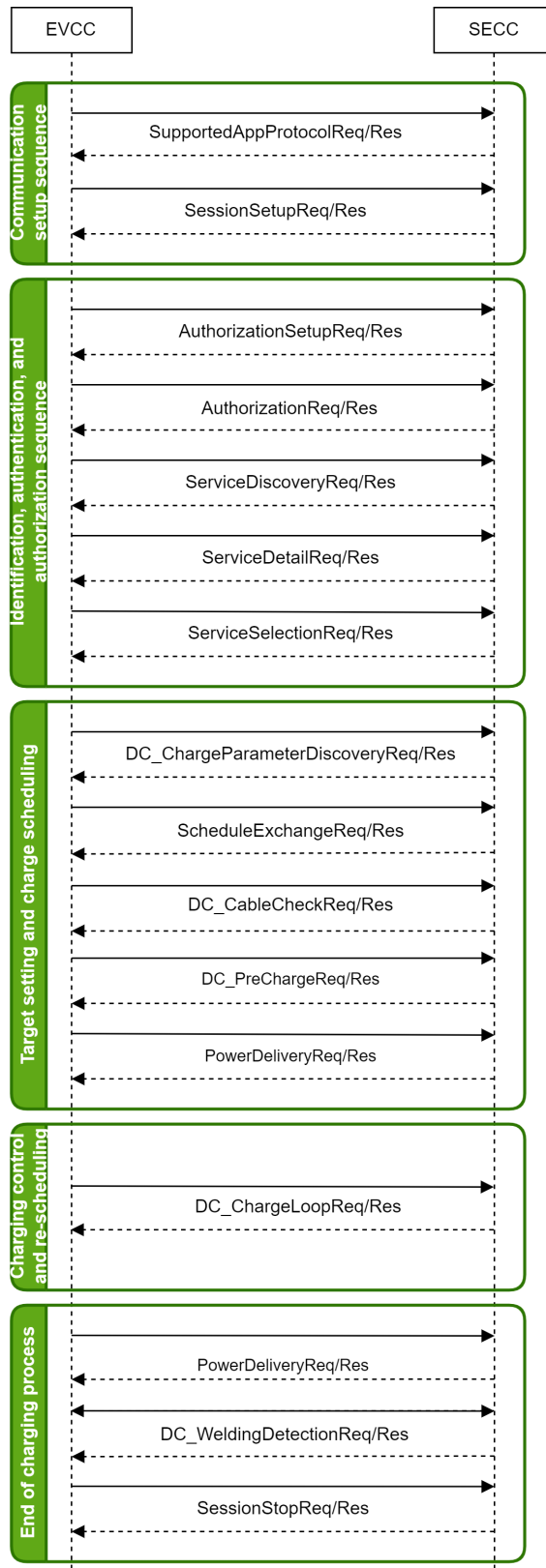


Figure A.12: Diagram illustrating the message sequence for an ISO 15118-20 DC charge. Image source: [31].

A.2.5 15118-20 configuration parameters for AC BPT

ParameterName	ParameterType	Values	Description
Connector	intValue	1: SinglePhase 2: ThreePhase	Usage of the connector.
ControlMode	intValue	1: Scheduled 2: Dynamic	Selection of which party (SECC or EVCC) is responsible to fulfill the mobility needs of this service session.
EVSENominalVoltage	intValue	0 to 500	Line voltage supported by the EVSE. This is the voltage measured between one phase and neutral. If the EVSE supports multiple phase energy transfer the EV might easily calculate the voltage between phases. This parameter is also used as reference for calculating the corresponding maximum charging current out of the power values in the schedule entities.
MobilityNeedsMode	intValue	1: Mobility needs provided by EVCC 2: Mobility needs provided by SECC allowed	Indicate who can provide mobility needs information. Value 2 indicates that not only EVCC but also SECC can provide mobility-needs information (however, the EVCC shall always provide an initial mobility-needs information including DepartureTime). Value 2 can be selected only if DynamicControlMode was selected.
Pricing	intValue	0: No pricing 1: Absolute Pricing 2: Price Levels	Providing information about which pricing structure will be used in the offered schedules.
BPTChannel	intValue	1: Unified 2: Separated	Type of installed power transfer channel. Unified: Single channel Separated: Dual channel
GeneratorMode	intValue	1: GridFollowing 2: GridForming	Power converter behavior. For details see the IEC/TS 62898 series.
GridCodeIslanding DetectionMethod	intValue	1: ActiveDetection 2: PassiveDetection	Parameter to determine what method is used to detect landing.

Table A.1: ISO 15118-20 configuration parameters for AC BPT service. Adapted from [16].

A.3 EV emulators and sniffers

No.	Brand	Name	Model no.	Protocols	Features	Powered testing support	TLS decrypt
1	Trialog	ComboCS4M		All	EV emulation	No native power support. Third-party integration possible	N/A
2	Trialog	Sniffer		All	Sniffing	N/A	No
3	Keysight	EV – EVSE Charging Communication Interface Tester	SL1550A(HW) SL1470A (SW)	All	EV emulation EVSE emulation	Native support for Keysight Charging Discovery System	N/A
4	Keysight	CCS Charging Protocol Tracer	SL1556A (HW) SL1487A (SW)	All	Sniffing	N/A	Yes
5	Keysight	Charging Discovery System	SL1047A (HW) SL1093A (SW)	All	EV emulation EVSE emulation MitM	AC emulation: SL1200A DC emulation: SL1800A	No
6	Comemso	EVCA Flex		All	EV emulation EVSE emulation MitM	No native power support. Third-party integration possible	Presumed
7	Comemso	EVCA Multi Mobile		All	EV emulation EVSE emulation MitM	No native power support. Third-party integration possible	Yes
8	Comemso	EVCA ComOnly		All	EV emulation EVSE emulation Sniffing	No	Presumed
9	IoTecha	PilotShark		All	Sniffing	N/A	Claimed
10	VertexCom	GreenPHY Sniffer	MST216D-D01D	No ISO-20	Sniffing	N/A	No
11	Applus	CCS V2G Decoder		No ISO-20	Sniffing	N/A	No

Table A.2: Extended overview of EV and EVSE emulation and High Level Communication sniffing products. In this table, *All* in the protocols column refers to support for DIN SPEC 70121, ISO 15118-2 and ISO 15118-20. *TLS decrypt* refers to whether the system in question claims to be able to decrypt TLS-encrypted communication.

A.4 Code

A.4.1 Python supervisor

A.4.1.1 Watt&Well example

```
1 import canopen
2 import logging
3 from watt_node_v2.node.supervisor import (
4     GlobalSupervisor,
5     ChargePointType,
6     SupervisorInterface,
7     AllocationWord,
8     AllocationMode,
9 )
10 from watt_node_v2.node.base import ControllerException
11 from watt_node_v2.node.supervisor.supervisor import disable_securities
12 import time
13
14 logging.basicConfig(level=logging.INFO)
15 logger = logging.getLogger(__name__)
16
17
18 def main():
19     # Connect to CAN bus, to adapt (socketcan on linux, etc)
20     network = canopen.Network()
21     network.connect(interface="kvaser", channel=0, bitrate=500_000)
22
23     # Create the global supervisor and add the desired SECCs
24     supervisor = GlobalSupervisor(
25         network=network,
26         chargepoints=[ChargePointType.EVIS_A_CCS],
27         interface=SupervisorInterface.EXTENDED,
28     )
29     # Initialize CANopen specifics
30     supervisor.start()
31     # force start of heartbeat with 1s period
32     supervisor.node.nmt.start_heartbeat(1000)
33
34     # Get a specific charge point (SECC) supervisor
35     secc_evis_a = supervisor.SECCSupervisors[ChargePointType.EVIS_A_CCS]
36     # ----- #
37     #                               Update the limitations                               #
38     # ----- #
39     secc_evis_a.SUP_MaxDcChargePower = 150_000
40     secc_evis_a.SUP_MaxDcChargeVoltage = 500
41     secc_evis_a.SUP_MaxDcChargeCurrent = 200
42     secc_evis_a.SUP_MaxAcChargeCurrent = 100
43
44     # ----- #
45     #                               Update allocations                               #
46     # ----- #
47     allocation = AllocationWord()
48     allocation.bmpu_list = [1,2] # <-- Change with the desired allocations
49     # allocation.mpu_list = [1]
50
51     # To use with caution, this can be used to disable securities on EVI
52     # Should not be used in normal operation
53     evis_node = network.add_node(0x10)
54     # disable_securities(evis_node) # <-- Can be used if simulating a charge,
55     # do not use during a normal charge as it cancels safeties
56
57     try:
```

```

57     secc_evis_a.launch_charge(allocation)
58 except ControllerException as e:
59     logger.error(e)
60     logger.error(f"failed to start the charge. SECC status : {secc_evis_a.
61         get_information()}")
62     return
63
64
65 while True:
66     time.sleep(1)
67
68
69 if __name__ == "__main__":
70     main()

```

Listing A.1: Python supervisor example as provided by Watt Well

A.4.1.2 Final ChaDeMo attempt

```

1  import canopen
2  import logging
3  from watt_node_v2.node.supervisor import (
4      GlobalSupervisor ,
5      ChargePointType ,
6      SupervisorInterface ,
7      AllocationWord ,
8      SupervisorRequestCode ,
9  )
10 from watt_node_v2.node.base import ControllerException
11 from watt_node_v2.node.supervisor.supervisor import disable_securities
12 import time
13
14 logging.basicConfig(level=logging.INFO)
15 logger = logging.getLogger(__name__)
16
17
18 def main():
19     # Connect to CAN bus, to adapt (socketcan on linux, etc)
20     network = canopen.Network()
21     network.connect(interface="socketcan", channel='can0', bitrate=500_000)
22
23     # Create the global supervisor and add the desired SECCs
24     supervisor = GlobalSupervisor(
25         network=network ,
26         chargepoints=[ChargePointType.EVIS_B_CHA] ,
27         interface=SupervisorInterface.V2G,
28     )
29     # Initialize CANopen specifics
30     supervisor.start()
31     supervisor.node.nmt.start_heartbeat(1000) # force start of heartbeat with
32         1s period
33
34     # Get a specific charge point (SECC) supervisor
35     secc_evis_b = supervisor.SECCSupervisors[ChargePointType.EVIS_B_CHA]
36     # ----- #
37     # Update the limitations #
38     # ----- #
39     secc_evis_b.SUP_MaxDcChargePower = 5_000
40     secc_evis_b.SUP_MaxDcChargeVoltage = 500
41     secc_evis_b.SUP_MaxDcChargeCurrent = 200
42     secc_evis_b.SUP_MaxAcChargeCurrent = 100

```

```

42 secc_evis_b.SUP_MaxDcDischargePower = 7_000
43 secc_evis_b.SUP_MaxDcDischargeVoltage = 500
44 secc_evis_b.SUP_MaxDcDischargeCurrent = 200
45 secc_evis_b.SUP_MaxAcDischargeCurrent = 100
46
47 # ----- #
48 #           Update settings (direction)           #
49 # ----- #
50 try:
51     secc_evis_b.update_charge_settings(discharge_compatible=1, dynamic_mode
52                                       =1, discharge_mode=0)
53     print("updating settings to charge, discharge compatible")
54     print("Discharge compatible is " + str(secc_evis_b.discharge_compatible
55     ))
56     print("Dynamic mode is " + str(secc_evis_b.dynamic_mode))
57     print("Discharge mode is " + str(secc_evis_b.discharge_mode))
58 except ControllerException as e:
59     logger.error(e)
60     logger.error(f"failed. SECC status : {secc_evis_b.get_information()}")
61     return
62
63 time.sleep(2)
64
65 # ----- #
66 #           Update allocations                       #
67 # ----- #
68 allocation = AllocationWord()
69 allocation.bmpu_list = [1,2] # <-- Change with the desired allocations
70 # allocation.mpu_list = [1]
71
72 # To use with caution, this can be used to disable securities on EVI
73 # Should not be used in normal operation
74 evis_node = network.add_node(0x10)
75 # disable_securities(evis_node) # <-- Can be used if simulating a charge,
76 # do not use during a normal charge as it cancels safeties
77
78 print(allocation)
79 print("Dynamic mode is " + str(secc_evis_b.dynamic_mode))
80
81 # ----- #
82 #           Start charge                           #
83 # ----- #
84
85 try:
86     secc_evis_b.launch_charge(allocation)
87     print("Started charge!")
88     print(allocation)
89 except ControllerException as e:
90     logger.error(e)
91     logger.error(f"failed to start the charge. SECC status : {secc_evis_b.
92     get_information()}")
93     return
94
95 time.sleep(5)
96
97 # ----- #
98 #           Update limitations                       #
99 # ----- #
100
101 try:
102     secc_evis_b.update_limitations(

```

```

100     max_dc_charge_power=2_000,
101     max_dc_charge_voltage=500,
102     max_dc_charge_current=200,
103     max_ac_charge_current=100,
104 )
105     print("updating limit")
106     print("Charge power is " + str(secc_evis_b.SUP_MaxDcChargePower))
107 except ControllerException as e:
108     logger.error(e)
109     logger.error(f"failed to update limits. SECC status : {secc_evis_b.
110         get_information()}")
111     return
112
113 time.sleep(5)
114
115 # ----- #
116 #           Update settings (direction)           #
117 # ----- #
118 try:
119     secc_evis_b.update_charge_settings(discharge_compatible=1, dynamic_mode
120         =1, discharge_mode=1)
121     print("updating settings to discharge")
122     print("Discharge power is " + str(secc_evis_b.SUP_MaxDcDischargePower))
123 except ControllerException as e:
124     logger.error(e)
125     logger.error(f"failed. SECC status : {secc_evis_b.get_information()}")
126     return
127
128 try:
129     secc_evis_b.SUP_RequestCode = SupervisorRequestCode.SUP3_AllocationDone
130     print("SUP3_AllocationDone set")
131     print("Discharge compatible is " + str(secc_evis_b.discharge_compatible
132         ))
133     print("Dynamic mode is " + str(secc_evis_b.dynamic_mode))
134     print("Discharge mode is " + str(secc_evis_b.discharge_mode))
135 except ControllerException as e:
136     logger.error(e)
137     logger.error(f"failed to update direction. SECC status : {secc_evis_b.
138         get_information()}")
139     return
140
141 while True:
142     time.sleep(10)
143
144 if __name__ == "__main__":
145     main()

```

Listing A.2: Unfinished Python supervisor for dynamic control of a ChaDeMo session

A.4.2 OCPP supervisor

A.4.2.1 CCS supervisor

```

1 [charging_station]
2 ;interface used by the supervisor (this should never change)
3 ;one of 'LEGACY'; 'EXTENDED' or 'V2G'
4 interface = EXTENDED
5
6
7 [hosts]
8 ; host address of QOcpp service
9 qocpp_host = tcp://127.0.0.1

```

```

10 ; local address of charging station , should not change
11 ; '*' means zeromq will bind on any local ip adress
12 csm_host = tcp://*
13
14 [EVIS_A_CCS]
15 ;EVSE id that will be used by CSMS when communicating with multiple EVSE
    inside charging station
16 evse_id = 1
17 ;These are the settings to use for a single charge point.
18 ;This is used for setting up EVIS A (id 0x10) and combo CCS chargepoint
19 ;mode can be "parallel" or "series", and defines if power units will be in
    series or parallel
20 mode = parallel
21 ;List of MPUs to use, "1" is address 0x50, "2", 0x51 etc.
22 ;Up to 14 MPUs can be allocated
23 ;The following list defines the MPUs that can be allocated to this chargepoint
24 ;Not all MPUs need to be allocated
25 mpus = []
26 ;List of bmpus to allocate "1" is address 0x5D, etc
27 ;Up to 16 BMPUs can be allocated
28 bmpus = [1,2]
29 ;These are the charge point limitations that are sent to the EV
30 max_dc_charge_voltage = 500
31 max_dc_charge_current = 100
32 max_dc_charge_power = 22_000
33 max_ac_charge_power = 120_000
34 ; the next parameters are only needed in V2G interface mode
35 ; max_dc_discharge_voltage = 900
36 ; max_dc_discharge_current = 120
37 ; max_dc_discharge_power = 110_000
38 ; max_ac_discharge_power = 120_000

```

Listing A.3: Initialization file for an OCPP CCS supervisor

A.4.3 GUI supervisor API scripts

A.4.3.1 Toggling between charging and discharging

```

1  import requests
2  import json
3  import time
4  import RPi.GPIO as GPIO
5
6  GPIO.setmode(GPIO.BOARD)
7  GPIO.setup(7, GPIO.OUT)
8  GPIO.output(7, 0)
9  print("Setting GPIO low")
10 time.sleep(5)
11
12
13 url = "http://192.168.200.12:8333/supervisor/secc/EVIS_B_CHA/update/command"
14
15 payloadCharge = {
16     "interface": 2,
17     "request_code": 3,
18     "discharge_compatible": True,
19     "discharge_mode": False,
20     "dynamic_mode": True,
21     "imd_external": False,
22     "imd_state": 0
23 }
24
25 payloadDischarge = {

```

```

26     "interface": 2,
27     "request_code": 3,
28     "discharge_compatible": True,
29     "discharge_mode": True,
30     "dynamic_mode": True,
31     "imd_external": False,
32     "imd_state": 0
33 }
34
35 username = "user"
36 password = "pass"
37 auth = (username, password)
38
39 try:
40     response = requests.put(url, json=payloadCharge, auth=auth)
41     if response.status_code == 200:
42         print("Request successful! Set charging mode")
43         GPIO.output(7, 1)
44         print("Setting GPIO low")
45     else:
46         print(f"Request failed with status code {response.status_code}")
47 except requests.RequestException as e:
48     print(f"Error: {e}")
49
50 time.sleep(2)
51 GPIO.output(7, 0)
52 print("Setting GPIO low")
53 print("Waiting 30 seconds")
54 print()
55 time.sleep(30)
56
57 try:
58     response = requests.put(url, json=payloadDischarge, auth=auth)
59     if response.status_code == 200:
60         print("Request successful! Set discharging mode")
61         GPIO.output(7, 1)
62     else:
63         print(f"Request failed with status code {response.status_code}")
64 except requests.RequestException as e:
65     print(f"Error: {e}")
66
67 time.sleep(2)
68 GPIO.output(7, 0)
69 print("Setting GPIO low")
70 print("Waiting 30 seconds")
71 print()
72 time.sleep(30)
73
74 try:
75     response = requests.put(url, json=payloadCharge, auth=auth)
76     if response.status_code == 200:
77         print("Request successful! Set charging mode")
78         GPIO.output(7, 1)
79     else:
80         print(f"Request failed with status code {response.status_code}")
81 except requests.RequestException as e:
82     print(f"Error: {e}")
83
84 time.sleep(2)
85 GPIO.output(7, 0)
86 print("Setting GPIO low")
87 print("Waiting 30 seconds")

```

```

88 print()
89 time.sleep(30)
90
91 try:
92     response = requests.put(url, json=payloadDischarge, auth=auth)
93     if response.status_code == 200:
94         print("Request successful! Set discharging mode")
95         GPIO.output(7, 1)
96     else:
97         print(f"Request failed with status code {response.status_code}")
98 except requests.RequestException as e:
99     print(f"Error: {e}")
100
101 time.sleep(2)
102 GPIO.output(7, 0)
103 print("Setting GPIO low")
104 GPIO.cleanup()

```

Listing A.4: Python script for toggling between charging and discharging via EVI GUI API while also changing the GPIO low high

A.4.3.2 Ramping power down and up

```

1 import requests
2 import json
3 import time
4
5 # Define the base URLs and payloads
6 limitations_url = "http://192.168.200.12:8333/supervisor/secc/EVIS_B_CHA/
7 update/limitations"
8 command_url = "http://192.168.200.12:8333/supervisor/secc/EVIS_B_CHA/update/
9 command"
10
11 sleep_time = 5 # Global sleep time between ramp steps
12 step_size = 500 # Step size in Watt for ramps
13
14 base_payload_discharge = {
15     "max_dc_discharge_voltage": 500,
16     "max_dc_charge_current": 100,
17     "max_ac_charge_current": 100,
18     "max_dc_charge_power": 1000,
19     "max_dc_discharge_current": 100,
20     "max_dc_charge_voltage": 500,
21     "max_ac_discharge_current": 100
22 }
23
24 base_payload_charge = {
25     "max_dc_discharge_voltage": 500,
26     "max_dc_charge_current": 100,
27     "max_dc_discharge_power": 100,
28     "max_dc_charge_power": 1000,
29     "max_dc_discharge_current": 100,
30     "max_dc_charge_voltage": 500,
31     "max_ac_discharge_current": 100,
32     "max_ac_charge_current": 100,
33 }
34
35 command_payload_discharge = {
36     "interface": 2,
37     "request_code": 3,
38     "discharge_compatible": True,
39     "discharge_mode": True,
40     "dynamic_mode": True,

```

```

38     "imd_external": False,
39     "imd_state": 0
40 }
41
42 command_payload_charge = {
43     "interface": 2,
44     "request_code": 3,
45     "discharge_compatible": True,
46     "discharge_mode": False,
47     "dynamic_mode": True,
48     "imd_external": False,
49     "imd_state": 0
50 }
51
52 # Set up basic authentication (replace with your actual credentials)
53 username = "user"
54 password = "pass"
55 auth = (username, password)
56
57 ##### RAMP DOWN TO -22 KW #####
58 current_power = 1
59 target_power = 22500
60
61 while current_power <= target_power:
62     payload = base_payload_discharge.copy()
63     payload["max_dc_discharge_power"] = current_power
64
65     try:
66         # Update limitations
67         response_limitations = requests.put(limitations_url, json=payload,
68             auth=auth)
69         if response_limitations.status_code == 200:
70             print(f"Updated max_dc_discharge_power to {current_power}")
71         else:
72             print(f"Limitations request failed with status code {
73                 response_limitations.status_code}")
74
75         # Send command payload
76         response_command = requests.put(command_url, json=
77             command_payload_discharge, auth=auth)
78         if response_command.status_code == 200:
79             print("Command request successful!")
80         else:
81             print(f"Command request failed with status code {response_command.
82                 status_code}")
83
84     except requests.RequestException as e:
85         print(f"Error: {e}")
86
87     current_power += step_size
88     time.sleep(sleep_time) # Sleep before the next iteration
89
90 ##### RAMP UP to 0 #####
91 current_power = 22500
92 target_power_down = 1
93
94 while current_power >= target_power_down:
95     payload = base_payload_discharge.copy()
96     payload["max_dc_discharge_power"] = current_power
97
98     try:

```

```

96     # Update limitations
97     response_limitations = requests.put(limitations_url, json=payload,
98         auth=auth)
99     if response_limitations.status_code == 200:
100         print(f"Updated max_dc_discharge_power to {current_power}")
101     else:
102         print(f"Limitations request failed with status code {
103             response_limitations.status_code}")
104
105     # Send command payload
106     response_command = requests.put(command_url, json=
107         command_payload_discharge, auth=auth)
108     if response_command.status_code == 200:
109         print("Command request successful!")
110     else:
111         print(f"Command request failed with status code {response_command.
112             status_code}")
113
114     except requests.RequestException as e:
115         print(f"Error: {e}")
116
117     current_power -= step_size
118     time.sleep(sleep_time) # Sleep before the next iteration
119
120     ##### RAMP UP CHARGE POWER #####
121     current_power = 1
122     target_power = 22500
123
124     time.sleep(sleep_time) # Give it a few ekstra seconds to change current
125     direction
126
127     while current_power <= target_power:
128         payload = base_payload_charge.copy()
129         payload["max_dc_charge_power"] = current_power
130
131         try:
132             # Update limitations
133             response_limitations = requests.put(limitations_url, json=payload,
134                 auth=auth)
135             if response_limitations.status_code == 200:
136                 print(f"Updated max_dc_charge_power to {current_power}")
137             else:
138                 print(f"Limitations request failed with status code {
139                     response_limitations.status_code}")
140
141             # Send command payload
142             response_command = requests.put(command_url, json=
143                 command_payload_charge, auth=auth)
144             if response_command.status_code == 200:
145                 print("Command request successful!")
146             else:
147                 print(f"Command request failed with status code {response_command.
148                     status_code}")
149
150         except requests.RequestException as e:
151             print(f"Error: {e}")
152
153         current_power += step_size
154         time.sleep(sleep_time) # Sleep before the next iteration
155
156

```

```

149
150
151 ##### RAMP DOWN CHARGE POWER #####
152
153 current_power = 22500
154 target_power_down = 1
155
156 while current_power >= target_power_down:
157     payload = base_payload_charge.copy()
158     payload["max_dc_charge_power"] = current_power
159
160     try:
161         # Update limitations
162         response_limitations = requests.put(limitations_url , json=payload ,
163             auth=auth)
164         if response_limitations.status_code == 200:
165             print(f"Updated max_dc_charge_power to {current_power}")
166         else:
167             print(f"Limitations request failed with status code {
168                 response_limitations.status_code}")
169
170         # Send command payload
171         response_command = requests.put(command_url , json=
172             command_payload_charge , auth=auth)
173         if response_command.status_code == 200:
174             print("Command request successful!")
175         else:
176             print(f"Command request failed with status code {response_command.
177                 status_code}")
178
179     except requests.RequestException as e:
180         print(f"Error: {e}")
181
182     current_power -= step_size
183     time.sleep(sleep_time) # Sleep before the next iteration

```

Listing A.5: Python script for ramping power down and up via EVI GUI API

A.5 Miscellaneous

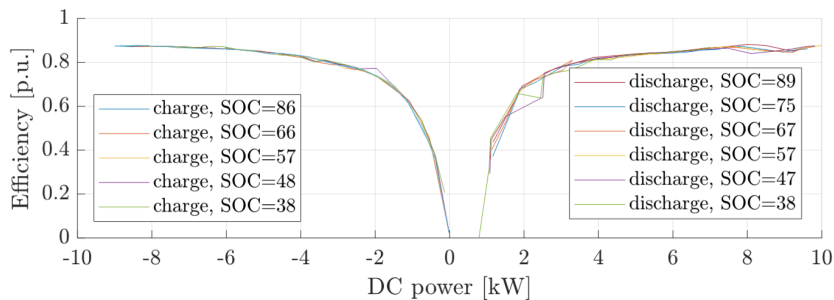


Figure A.13: CHAdeMO V2G charger efficiency map for charging/discharging DC set-points from -10 kW to +10 kW with steps of 400W. Image source: [1].

Technical
University of
Denmark

Frederiksborgvej 399
4000 Roskilde
Tlf. 4525 1700

www.wind.dtu.dk